Universität Rostock Traditio et Innovatio

Leibniz Institute for Baltic Sea Research Warnemünde

Ecological role of Thaumarchaeota in pelagic redox gradients of the Baltic Sea

Dissertation

zur Erlangung des akademischen Grades
doctor rerum naturalium (Dr. rer. nat.)
der Mathematisch-Naturwissenschaftlichen Fakultät
der Universität Rostock

vorgelegt von

Carlo Berg

geb. am 6. Dez. 1984 in Magdeburg
aus Rostock
Rostock, den 24. Okt. 2014

urn:nbn:de:gbv:28-diss2015-0150-4

Gutachter:

Prof. Dr. Klaus Jürgens

Leibniz-Institut für Ostseeforschung Warnemünde

Prof. Dr. Gerhard J. Herndl

Universität Wien

Datum der öffentlichen Verteidigung: 19. Dezember 2014

CONTENTS

INTRODUCTION 1
Globally expanding oxygen-depleted zones . . . 1
Oxygen-depleted waters in the Baltic Sea . . . 2
Microbially mediated biogeochemical cycles . . . 4
Chemoautotrophic prokaryotes of the Baltic Sea redox gradients . . . 6
Ecology of the Thaumarchaeota . . . 8
Aerobic ammonia oxidation and chemoautotrophy . . . 9
Open questions . . . 11
Thesis outline . . . 12
1 SIGNIFICANCE OF ARCHAEAL NITRIFICATION 17
1.1 Introduction . . . 18
1.2 Material and Methods . . . 21
1.2.1 Sampling and physicochemical analyses . . . 21
1.2.2 Quantification of Thaumarchaeota and *Sulfurimonas* sp. subgroup GD17 . . . 22
1.2.3 Potential nitrification rates . . . 22
1.2.4 Sulfide spiking experiment . . . 24
1.2.5 Dark CO_2 fixation . . . 24
1.2.6 Domain-specific inhibition of archaea and bacteria . . . 25
1.2.7 Statistical analyses . . . 26
1.3 Results . . . 27
1.3.1 Redox zone structure in the Gotland Deep, Landsort Deep, and Bornholm Deep . . . 27
1.3.2 Potential nitrification rates in Baltic Sea redox zones . . . 28
1.3.3 Impact of domain-specific inhibitors on nitrification activity . . . 31
1.3.4 Sulfide spiking experiment . . . 32
1.4 Discussion . . . 32
1.4.1 Nitrification activity, CO_2 fixation, and the distribution of Thaumarchaeota . . . 33
1.4.2 Thaumarchaeota contribute substantially to nitrification . . . 34
1.4.3 Impact of sulfide on ammonia-oxidizing Thaumarchaeota . . . 35
1.5 Conclusions . . . 37
1.6 Acknowledgments . . . 37
2 CHEMOAUTOTROPHIC GROWTH OF THAUMARCHAEOTA 41
2.1 Introduction . . . 41
2.2 Material and Methods . . . 44
2.2.1 Retrieval of environmental samples, enrichment and cultivation . . . 44
2.2.2 Cell quantification . . . 44
2.2.3 CO_2 fixation rates . . . 45
2.2.4 Uptake of ^{13}C-bicarbonate and ^{15}N-ammonium and NanoSIMS imaging . . . 46

2.2.5 DNA-extraction and phylogenetic analysis of the 16S rRNA and *amoA* genes . . . 47
2.3 Results . . . 48
2.3.1 Enrichment of ammonia-oxidizing archaea . . . 48
2.3.2 CO_2 fixation . . . 52
2.3.3 Cellular uptake of ^{13}C-bicarbonate and $^{15}NH_4Cl$ . . . 52
2.3.4 Phylogenetic affiliation . . . 54
2.4 Discussion . . . 55
2.4.1 Autotrophy and calculated carbon content per cell . . . 55
2.4.2 Coupling between ammonia oxidation and CO_2 fixation . . . 57
2.4.3 Phylogenetic affiliation with a putative low-salinity group . . . 57
2.5 Acknowledgment . . . 58
3 METATRANSCRIPTOMICS OF CHEMOAUTOTROPHS 61
3.1 Introduction . . . 62
3.2 Material and Methods . . . 64
3.2.1 Sampling and physicochemical analyses . . . 64
3.2.2 Quantification of specific phylogenetic groups by catalyzed reporter deposition fluorescence *in situ* hybridization (CARD-FISH) . . . 64
3.2.3 RNA extraction and sequencing . . . 65
3.2.4 MG-RAST . . . 65
3.2.5 Sequence recruitment using reference genomes . . . 65
3.2.6 Alignments of specific genes via TBLASTN . . . 66
3.2.7 Normalization of read counts . . . 67
3.3 Results and Discussion . . . 68
3.3.1 Redox gradient stratification and metatranscriptome properties . . . 68
3.3.2 "Comfort zones" of key chemoautotrophs . . . 72
3.3.3 Adaptations outside the comfort zones . . . 74
3.3.4 Transcriptional proxies for biogeochemical activities . . . 78
3.4 Conclusions and implications . . . 87
SYNTHESIS AND FUTURE PERSPECTIVES 89
Accomplishments . . . 91
Future perspectives . . . 94
BIBLIOGRAPHY I
APPENDIX XI
Chapter 1 . . . XI
Chapter 2 . . . XIX
Chapter 3 . . . XX
LIST OF PUBLICATIONS XXV
CURRICULUM VITAE XXVII
ACKNOWLEDGMENTS XXIX
DECLARATION XXXI

LIST OF FIGURES

Figure 1	Oxygen concentrations worldwide in a depth at 300 m	1
Figure 2	Map of the Baltic Sea	3
Figure 3	The nitrogen cycle with reactions relevant to the Baltic Sea	5
Figure 4	Schematic of physicochemistry, microbial abundance and processes in Baltic Sea pelagic redox gradients	6
Figure 1.1	Locations of the sampled sites in the Baltic Sea	21
Figure 1.2	Evaluation of different concentrations of GC_7 and erythromycin on CO_2 fixation rates	26
Figure 1.3	Detailed profile of the Gotland Deep redox-zone in July 2011	27
Figure 1.4	Profile within the hypoxic waters of the Landsort Deep redox gradient in June 2012	29
Figure 1.5	Physicochemical profile of the Gotland Deep hypoxic zone in June 2012 during a sulfidic intrusion	30
Figure 1.6	Cell abundances of Cren679-probe hybridized Thaumarchaeota at different grouped oxygen and sulfidic conditions	31
Figure 2.1	Epifluorescence microscopy of representative cells from the enrichment culture	48
Figure 2.2	Growth parameters of triplicate thaumarchaeotal enrichment cultures	49
Figure 2.3	Growth curve of enrichment culture G	51
Figure 2.4	Cell-specific CO_2 fixation rates	52
Figure 2.5	Nano-scale secondary ion mass spectrometry (NanoSIMS) images of ^{13}C-enriched cells sampled 11 days after inoculation	53
Figure 2.6	NanoSIMS images of ^{13}C- and ^{15}N-enriched cells	53
Figure 2.7	Neighbor-joining trees showing the phylogenetic placement of the enrichment	54
Figure 3.1	Approach of the metatranscriptome analysis	66
Figure 3.2	Chemical profile at the Landsort Deep in September 2009	69
Figure 3.3	Relative and absolute cell counts of the three chemoautotrophic key microorganisms	70
Figure 3.4	Relative contributions of the chemoautotrophic key microorganisms to read abundances and cellular abundances	71
Figure 3.5	Relative gene transcript levels of the three key chemoautotrophs as mapped via MUMmer	72
Figure 3.6	Relative gene transcript levels of *Ca.* N. maritimus, *Sulfurimonas gotlandica* or SUP05	73
Figure 3.7	Transcript levels of genes coding for transcription factors in the genome of *Ca.* Nitrosopumilus maritimus	75
Figure 3.8	S-layer gene transcript levels relative to total transcript levels of *Ca.* N. maritimus throughout the redox gradient.	77
Figure 3.9	Number of *cheA* reads per 10,000 *Sulfurimonas gotlandica* reads	78
Figure 3.10	Levels of gene transcripts of the different *amo* subunits *A, B, C* and *X* of *Ca.* Nitrosopumilus maritimus	79

Figure 3.11 Number of *amoA* gene transcripts along the pelagic redox gradient including information on the e-value or % identity 80
Figure 3.12 Concentrations of nutrients and transcript levels of *amt1* and *amt2* throughout the redox gradient 81
Figure 3.13 Transcript levels of genes coding for biogeochemically relevant pathways of the SUP05 metagenome 83
Figure 3.14 Transcript levels of genes coding for biogeochemically relevant pathways of the genome of *Sulfurimonas gotlandica* 84
Figure 3.15 Transcript levels of genes coding for biogeochemically relevant pathways of the genome of *Ca.* Nitrosopumilus maritimus 85
Figure 3.16 Transcript levels of CO_2 fixation associated genes of the three chemoautotrophs. 86
Figure 5 Lateral intrusion of oxygenated water at station TF260 96
Figure A.1 CO_2 fixation activities of ammonia-oxidizing archaea treated with specific inhibitors XV
Figure A.2 Relationship between Thaumarchaeota cell abundances and potential nitrification rates XV
Figure A.3 Concentrations of excess $^{29}N_2$ and $^{30}N_2$ during incubations targeting anaerobic ammonia oxidation (anammox) XVI
Figure A.4 H_2S concentrations at different time points after spiking with different amounts of H_2S XVII
Figure A.5 Absolute cell numbers and relative cell enrichment factor of *Sulfurimonas* sp. subgroup GD17 before and after spiking with H_2S . XVII
Figure A.6 CO_2 fixation activities in H_2S-spiked samples XVIII
Figure A.7 Amount of carbon fixed in three parallel batch cultures XIX
Figure A.8 Ammonium consumption and total cell counts (DAPI) during the batch growth XIX
Figure A.9 Number of flagella associated reads per 10,000 *Sulfurimonas gotlandica* reads XXIII
Figure A.10 Number of chemotaxis associated reads per 10,000 *Sulfurimonas gotlandica* reads XXIII

LIST OF TABLES

Table 1.1 Effect of H_2S addition on nitrification activity 32
Table 2.1 Growth characteristics and balances during the exponential phase of enrichment cultures 50
Table 3.1 Overview of the different types of normalization 67
Table 3.2 Parameters of the Landsort Deep metatranscriptomes 71
Table A.1 Inorganic nutrient data, cell abundances, CO_2 fixation and nitrification rates XIII
Table A.1 Inorganic nutrient data, cell abundances, CO_2 fixation and nitrification rates XIV
Table A.2 List of investigated biogeochemically relevant genes XX
Table A.3 Annotations for genes involved in autotrophic carbon fixation pathways XXI
Table A.4 List of genes, which are relevant to the assembly of the flagella according to the genome of *S. gotlandica* XXII

LIST OF ACRONYMS AND ABBREVIATIONS

3-HP/4-HB	3-hydroxypropionate/4-hydroxybutyrate
AFIS	automatic flow injection sampler
AMO	ammonia monooxygenase
amoA	ammonia monooxygenase gene subunit A
anammox	anaerobic ammonia oxidation
ANOVA	Analysis of variance
ANCOVA	Analysis of covariance
AOA	ammonia-oxidizing archaea
AOB	ammonia-oxidizing bacteria
ATP	adenosine triphosphate
BLAST	Basic local alignment search tool
C	carbon
Ca.	*Candidatus*
CARD	catalyzed reporter deposition
CDS	coding sequence
CTD	conductivity, temperature and depth
DAPI	4',6-diamidin-2-phenylindol
DFG	Deutsche Forschungsgemeinschaft
DIC	dissolved inorganic carbon
DNA	Deoxyribonucleic acid
DON	dissolved organic nitrogen
e-value	expect value
FISH	fluorescence *in situ* hybridization
GC	gas chromatography
GC_7	N^1-guanyl-1,7-diaminoheptane
GSO	gammaproteobacterial sulfur-oxidizer
HAO	Hydroxylamine oxidoreductase
IOW	Institut für Ostseeforschung Warnemünde (Institute for Baltic Sea Research Warnemünde)

IRMS	isotopic ratio mass spectrometry
MBq	Mega Becquerel
MeV	Multi Experiment Viewer
MG-RAST	Metagenomic Rapid Annotations using Subsystems Technology
MOCA	Microbial Oceanography of ChemolithoAutotrophic planktonic communities
mRNA	messenger RNA
MUM	maximum unique matches
N	nitrogen
NanoSIMS	nano-scale secondary ion mass spectrometry
ND	not determined
NOB	nitrite-oxidizing bacteria
nt	nucleotide
ODV	Ocean Data View
OMZ	oxygen minimum zone
PEPCK	Phosphoenolpyruvate carboxykinase
RNA	ribonucleic acid
rRNA	ribosomal RNA
RuBisCO	Ribulose bisphosphate carboxylase/oxygenase
R/V	research vessel
S	sulfur
SD	standard deviation
SE	standard error
SUP05	gammaproteobacterial group named after the Suiyo Seamount Hydrothermal Plume
S-layer	surface layer
TBLASTN	BLAST of a protein query against a translated nucleotide subject

ABSTRACT

The recognition of the feature of ammonia oxidation among the *Archaea* led to a revision of the microbial drivers and processes within the nitrogen cycle. Affiliated with the novel phylum *Thaumarchaeota*, the globally distributed ammonia-oxidizing archaea (AOA) inhabit a magnitude of ecosystems in substantial numbers, suggesting a prominent role in biogeochemical cycles through their predominantly chemolithoautotrophic lifestyle. Thaumarchaeota also occur in the deep, oxygen-depleted basins of the Baltic Sea. This system, which is characterized by eutrophication, infrequent ventilation and expanding anoxic zones, is substantially governed by the activities of nitrogen cycling microorganisms. Within the pelagic redox gradients, Thaumarchaeota, being represented by one dominating subcluster occur in company with chemoautotrophs related to sulfur-oxidizing epsilon- and gammaproteobacteria of the *Sulfurimonas* sp. subgroup GD17 and the SUP05 cluster, respectively. Together, these three key chemolithoautotrophs act in concert by catalyzing nitrification, denitrification and sulfur oxidation. The present thesis sheds light on the ecology of the thaumarchaeotal assemblages in the Baltic Sea and their contributions to nitrification, CO_2 fixation as well as their adaptations to periodic exposure to sulfide. A suite of molecular, microbial, bioinformatic and biogeochemical approaches combined with extensive field-samplings, experiments with natural samples or enrichment cultures as well as metatranscriptomic analyses was employed. ^{15}N rate measurements and group-specific cell counts using catalyzed reporter deposition fluorescence *in situ* hybridization showed that maximum potential nitrification rates of up to 122–884 nmol N L^{-1} d^{-1} coincided with peaks of thaumarchaeotal abundances of up to 2.5–6.9 $\times$ 10^5 cells mL^{-1} throughout several sites and times. Archaeal-specific inhibition revealed that AOA were responsible for up to 86–100% of the nitrification rates. A sulfide-spiking experiment suggested that Baltic Sea Thaumarchaeota are well-adapted to the close proximity of the sulfidic zone as nitrification was maintained after pulses of *in-situ*-like levels of sulfide. The establishment of an enrichment culture served to examine chemoautotrophy by a member of *Nitrosoarchaeum* sp., which performed growth largely via CO_2 fixation at the expense of ammonia oxidation. Metatranscriptomic analyses of a representative redox gradient revealed group-specific and distinct "comfort zones" of elevated activities by Thaumarchaeota, *Sulfurimonas* sp. and SUP05, with thaumarchaeotal activities being highest in the putative nitrification zone.

Differential expression patterns of genes for ammonium transporters, S-layer proteins and transcription factors indicate adaptations to different chemical niches. Altogether, the investigations performed in the present thesis revealed that in the Baltic Sea, Thaumarchaeota are enduring microorganisms and substantial drivers of ammonia oxidation with a potential adaptation to periodic exposure to sulfide. Thus, important ecosystem functions rely on the activities of archaeal ammonia oxidizers being the major suppliers of oxidized nitrogen compounds, which are important substrates for the subsequent removal of fixed nitrogen or the detoxification of sulfur compounds in the Baltic Sea.

ZUSAMMENFASSUNG

Die Entdeckung der Ammoniumoxidation bei Vertretern der *Archaea* führte zu einer Revision der beteiligten Mikroorganismen und Prozesse im Stickstoffkreislauf. Ammoniumoxidierende Archaeen (AOA) sind global weit verbreitet und werden in das neue Phylum der *Thaumarchaeota* eingeordnet. Sie sind in vielen Ökosystemen in einer hohen Anzahl vorhanden, sodass von einer bedeutenden Beteiligung an biogeochemischen Kreisläufen durch ihre vorwiegend chemolithoautotrophe Lebensweise ausgegangen werden kann. Thaumarchaeota sind auch in den tiefen, sauerstoffarmen Becken der Ostsee vorzufinden. Dieses mit Eutrophierung, unzureichender Durchmischung und sich ausdehnenden anoxischen Gebieten konfrontierte Ökosystem ist zu großen Teilen durch Stickstoff umsetzende Mikroorganismen beeinflusst. Die Thaumarchaeota sind entlang der pelagischen Redox-Gradienten Teil einer chemoautotrophen mikrobiellen Gemeinschaft, die ebenso Vertreter von schwefeloxidierenden Epsilon- und Gammaproteobakterien (*Sulfurimonas* sp. subgroup GD17 und SUP05) beinhaltet. Diese drei chemolithoautotrophen Schlüsselorganismen katalysieren ineinander greifende Prozesse wie Nitrifikation, Denitrifikation und die Oxidation von Schwefelverbindungen. Die vorliegende Arbeit beleuchtet die Rolle der Thaumarchaeota in der Ostsee im Hinblick auf ihre Beteiligung an der Nitrifikation und CO_2-Fixierung sowie ihre Anpassungen an gelegentliche Sulfidexposition. Die Untersuchungen erfolgten mithilfe von molekularbiologischen, mikrobiologischen, bioinformatischen und biogeochemischen Methoden, zahlreicher Probenahmen im Freiland, Experimenten mit Umwelt- und Anreicherungsproben sowie Metatranskriptomanalysen. Ratenmessungen mittels ^{15}N Markierung und gruppenspezifische Zellquantifizierung über signalverstärkte Fluoreszenz *in situ* Hybridisierung (CARD-FISH) ergaben, dass über mehrere Standorte und Zeitpunkte verteilt, die höchsten potentiellen Nitrifikationsraten

von bis zu 122–884 nmol N L^{-1} Tag^{-1} mit den Abundanzmaxima für Thaumarchaeota (2.5–6.9 $\times$ 10^5 Zellen mL^{-1}) assoziiert waren. *Archaea*-spezifische Inhibierungsexperimente zeigten, dass die AOA für bis zu 86–100% der Nitrifikationsraten verantwortlich waren. Ein Experiment mit kontrollierter Sulfid-Zugabe deutete darauf hin, dass die Thaumarchaeota in der Ostsee an die Nähe zu sulfidhaltigen Wasserschichten angepasst sind, da auch nach Zugabe von natürlichen Sulfid-Konzentrationen die Nitrifikationsaktivität noch nachweisbar war. Die Etablierung einer Anreicherungskultur diente für Untersuchungen der Chemoautotrophie eines Vertreters von *Nitrosoarchaeum* sp., welche zeigten, dass dessen Wachstum hauptsächlich mittels CO_2-Fixierung und Ammoniumoxidation erfolgte. Metatranskriptomanalysen von Proben eines repräsentativen Redox-Gradienten zeigten gruppenspezifische und distinkte "Komfortzonen" von erhöhter Transkriptionsaktivität für Thaumarchaeota, *Sulfurimonas* sp. und SUP05, wobei die Aktivität der Thaumarchaeota in der potentiellen Nitrifikationszone am höchsten war. Unterschiedliche Verläufe von Transkripten von Genen für Ammoniumtransporter, S-Layer Proteine und Transkriptionsfaktoren deuteten auf potentielle Anpassungen an die variierenden chemischen Bedingungen im Habitat hin. Zusammengefasst zeigen die im Rahmen dieser Arbeit durchgeführten Analysen, dass die Thaumarchaeota in der Ostsee beständige Mikroorganismen sind, welche wesentlich an der Ammoniumoxidation beteiligt sind. Dies ist möglicherweise auf spezifische Anpassungen an periodische Sulfideinschübe in die Nitrifikationszone zurückzuführen. Wichtige Ökosystemfunktionen sind abhängig von den Aktivitäten archaeeller Ammoniumoxidierer als Produzenten von oxidierten Stickstoffverbindungen, welche wichtige Substrate für die Entfernung von fixiertem Stickstoff oder die Detoxifikation von Schwefelverbindungen in der Ostsee darstellen.

Introduction

Globally expanding oxygen-depleted zones

In aquatic environments worldwide, oxygen is not distributed equally but instead extended oxygen-deficient areas exist in coastal regions, marginal and inland seas, fjords, or in the oxygen minimum zones (OMZ) of the open oceans (Wright *et al.*, 2012*b*). Major aquatic ecosystems, that display permanent or periodic oxygen-depletion are the Cariaco Basin off the coast of Venezuela, the Namibian and Peruvian OMZs, areas of the eastern tropical North and South Pacific, the northeast subarctic Pacific, the Arabian Sea, the Black Sea and the Baltic Sea (Figure 1).

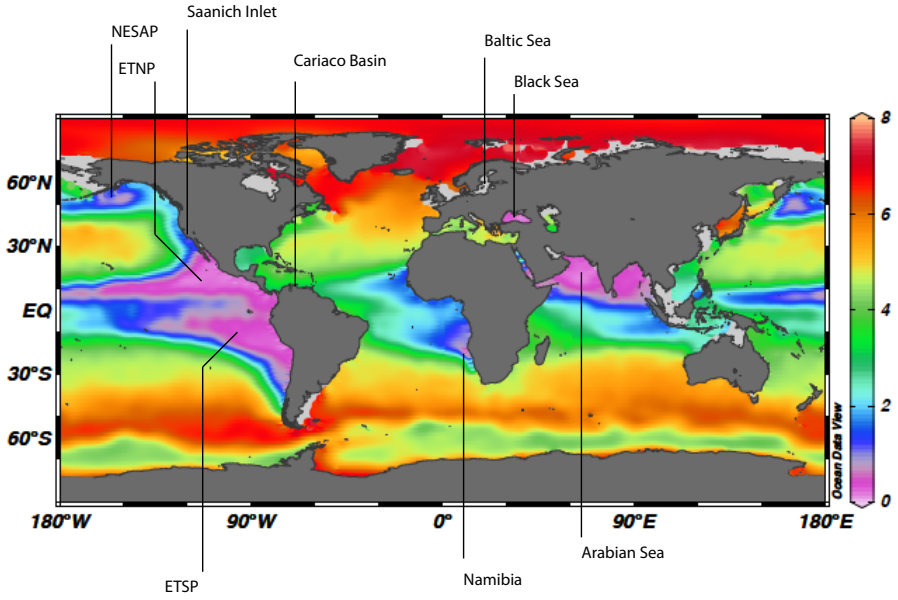

Figure 1.: Oxygen concentrations worldwide in a depth at 300 m. Oxygen-depleted areas are marked. The data was obtained from the World Ocean Atlas (WOA) 2009 (Garcia *et al.*, 2010) and plotted in Ocean Data View (ODV) v4.6.2, 2014 (http://odv.awi.de). The scale bar shows oxygen levels in mL L^{-1}. Map composed after Wright *et al.* (2012*b*). NESAP, northeast subarctic Pacific; ETNP, eastern tropical north Pacific; ETSP, eastern tropical south Pacific.

Because molecular oxygen (O_2) is life-determining for aerobic organisms its availability has direct consequences for the presence of higher-organized forms of life (Stramma *et al.*, 2010, 2012). However, beyond this obvious relationship lies also a magnitude of complex implications for the prokaryotic life: With less oxygen available, microorganisms,

which can utilize alternative electron acceptors instead of O_2, promote increased cycling of a variety of inorganic nutrients in their environment. Thus, in oxygen-depleted systems, the cycling of e.g. nitrogen is enhanced because for example nitrite (NO_2^-), nitrate (NO_3^-), and ammonium (NH_4^+) are used as alternative electron acceptors and donors, respectively. According to Wright *et al.* (2012*b*), 1–7% of the global ocean volume can be defined as oxygen minimum zones, where the levels of oxygen are below 20 µmol per kg water, resulting in enhanced cycling of alternative electron acceptors. Yet, the significance of oxygen-depleted waters for the nitrogen cycle is prominent as 30–50% of the oceanic fixed nitrogen-loss occurs in OMZ waters (Kuypers *et al.*, 2005; Lam and Kuypers, 2011; Wright *et al.*, 2012*b*).

The formation of oxygen-depleted waters is driven by a net over-consumption of dissolved oxygen, which is not replenished at the same rate by mixing with O_2-rich surface waters, leading to chemical stratification of the water-column. In coastal areas and inland seas, intensified anthropogenic nutrient inputs from surrounding land masses promote enhanced cyanobacterial growth. When the accumulated cyanobacteria die, the system is confronted with a substantial amount of biomass. Subsequently, a rain of organic material sinks into deeper water layers where it is respired by aerobic, O_2-consuming microorganisms. Insufficient circulation may further hamper the re-oxygenation of anoxic waters.

Oxygen-depleted waters in the Baltic Sea

The Baltic Sea is a marginal sea, surrounded by a catchment area that accounts four times the size of the sea itself and which is populated by around 85 million people (HELCOM, 2003). During the last century and until present the Baltic Sea has been facing eutrophication (Voss *et al.*, 2011; Carstensen *et al.*, 2014*a*) due to increased nutrient deposition. It constitutes the "largest anthropogenically induced hypoxic area in the world" as stated by Carstensen *et al.* (2014*a*). The authors point out that this system has been confronted with a 10-fold increased extent of hypoxia during the last century, which implies extensive consequences for ecosystem functioning and requires physiological versatility of the organismic components to thrive. In the major deep basins of the central Baltic Sea (Figure 2), which are the Gotland Deep (249 m) and the Landsort Deep (459 m), anoxic bottom waters extend over large areas. A vertical salinity gradient that promotes the establishment

of a stable halocline prevents thorough mixing of deeper anoxic waters with oxygen-rich surface waters.

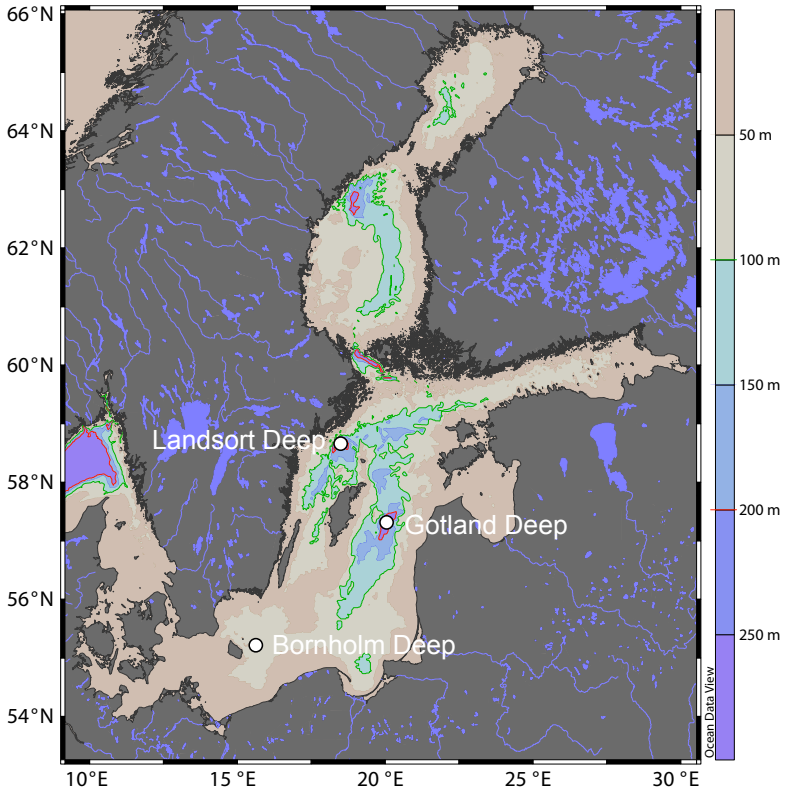

Figure 2.: Map of the Baltic Sea plotted with ODV. The isobars of 200 m, 150 m and 100 m are shown in red, blue and green, respectively.

The only connection to the North Sea is represented by the Danish Straits, and the shallow depths near the Darß Sill allow only limited exchange with oxygen-rich, saline water coming from the North Sea (Jakobsen and Castejon, 1995). Restricted to specific, prolonged meteorologic conditions that foster sufficiently strong winds from the west, major inflow-events that reach the central Baltic Sea, occur in time frames of decades (Matthäus and Franck, 1992). As a consequence, the areas of anoxic water spread in vertical and horizontal space and remain for several years.

The water layers, where oxygen-depleted and anoxic water masses meet represent an oxic-anoxic interface consisting of a hypoxic zone and an underlying anoxic zone, which is characterized by sulfide accumulation. The depth of the first appearance of sulfide is often referred to as *chemocline* whereas the term *redoxcline* is mostly used for the the transition zone covering both oxygen-depleted and sulfidic waters. As a *cline* usually refers to a single depth, rather than an interval of depths, the term *redox gradient* is used in the present thesis to include both the depths of decreasing oxidized and increasing reduced inorganic compounds.

Microbially mediated biogeochemical cycling of nitrogen

The chemically stratified redox gradients extend several meters vertically and cover a large area. Consequently, the biologically mediated element transformations have a considerable impact on the element cycles of nitrogen, carbon and sulfur in this ecosystem.

Due to the depletion of molecular oxygen, lithotrophic prokaryotes utilize alternative inorganic electron acceptors for energy conservation according to the highest energetic exploitation of the redox couples (Ulloa *et al.*, 2012*a*). Since the energy released by reactions using alternative electron acceptors instead of O_2 is comparably low, the turnover of inorganic substrates is accordingly high. Additionally, the carbon source is often inorganic carbon dioxide (CO_2), thus chemolithoautotrophy. The activities of chemolithoautotrophs connect and shape the budgets of multiple element cycles such as the nitrogen, carbon or sulfur cycles depending on the electron donors and acceptors utilized.

The various extents of oxygen-depletion have been subject to different definitions. A common characteristic is that oxygen-depletion reaches levels, which lead to increased utilization of alternative electron acceptors. For the Baltic Sea, operational definitions have been made such as that the suboxic layer represents concentrations of less than 5 µmol L^{-1} of O_2 and other inorganic nutrients (Labrenz *et al.*, 2010). In the scope of this thesis hypoxia is operationally defined as oxygen levels of 0–10 µmol L^{-1}. Hypoxia was recognized to regulate the biogeochemical cycling of nitrogen (Carstensen *et al.*, 2014*b*) and water layers exhibiting low oxygen concentrations are sites of nitrate accumulation by active nitrification (Figure 3). Potential nitrification rates were reported to account for 85–160 nmol N L^{-1} d^{-1} (Hietanen *et al.*, 2012). In close proximity to the nitrification zone, denitrification takes place under anaerobic or microaerobic conditions and reduces nitrate or nitrite via several intermediate steps to molecular dinitrogen (N_2). Rate measurements in the Baltic Sea reported denitrification at the intersection of nitrate and hydrogen sulfide (Brettar and Rheinheimer, 1991; Hietanen *et al.*, 2012), reaching up to 2.7 µmol N_2 L^{-1} d^{-1} (Hannig *et al.*, 2007). Within the nitrogen cycle, nitrification and denitrification are important interacting processes that impact the nitrogen budgets. Chemoautotrophic denitrification constitutes the most important nitrogen loss process in the pelagic waters of the Baltic Sea but also in other euxinic systems with sulfide accumulation such as the Mariager Fjord where maximum potential denitrification rates accounted for 18.6 µmol N_2 L^{-1} d^{-1} (Jensen *et al.*, 2009).

Nitrification is a two-step process governed by different guilds of prokaryotes, the archaeal or bacterial ammonia oxidizers and the bacterial nitrite oxidizers. Ammonia-oxidizing prokaryotes catalyze the first and rate-limiting step and provide nitrite to the nitrite-oxidizing bacteria, which further oxidize it to nitrate. Ammonia oxidation may be catalyzed aerobically with O_2 or anaerobically using NO_2^- as terminal electron acceptor, whereas the latter process plays a minor role in the Baltic (Hannig *et al.*, 2007). It occurs only after major inflows of oxygen-rich North Sea water reaching the anoxic deeps; following ventilation and re-establishment of the redox-gradients, a non-sulfidic, oxygen-free zone can establish, thereby facilitating the chemical requirements for anaerobic ammonia oxidation (anammox) to take place (Hannig *et al.*, 2007). In contrast, the Black Sea water-column exhibits an extended anoxic zone free of both O_2 and H_2S allowing for anammox to occur (Kuypers *et al.*, 2003). In the Black Sea, anaerobic ammonia oxidation is therefore an alternative sink of fixed inorganic nitrogen and also an alternative process for the oxidation of ammonia.

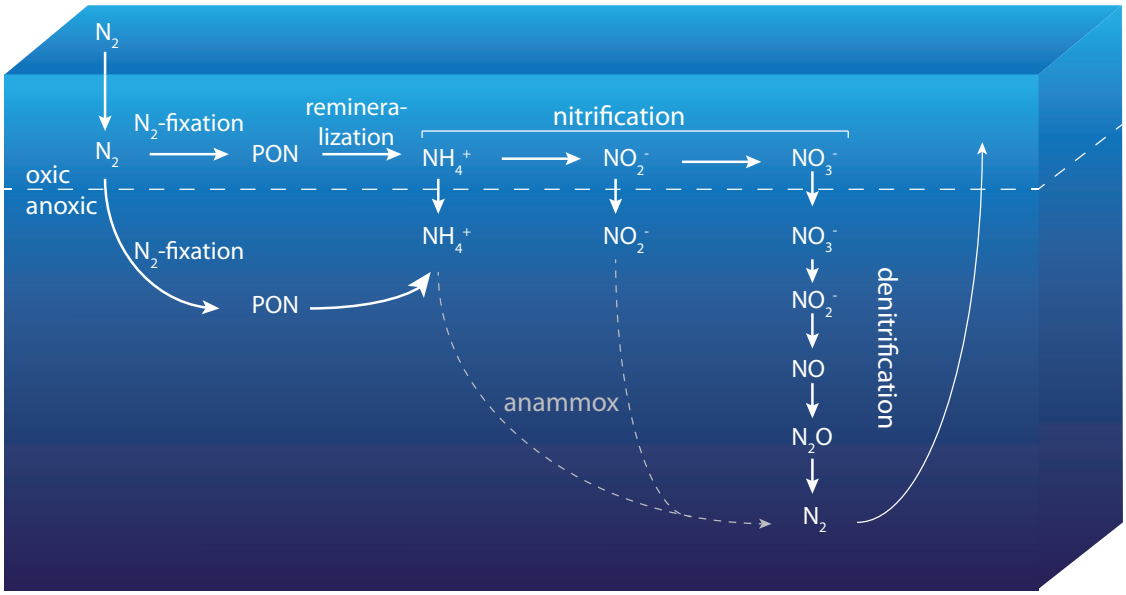

Figure 3.: The nitrogen cycle with reactions relevant to the Baltic Sea pelagic redox gradients. Synthesis of schematics as presented in Francis *et al.* (2007), Lam *et al.* (2009) and Offre *et al.* (2013).

The hydrodynamic nature of Baltic Sea waters is expressed at small and large spatial scales by local mixing events and lateral intrusions of different water bodies, respectively (Wieczorek *et al.*, 2008; Friedrich *et al.*, 2014). Small-scale mixing, in particular at the oxic-anoxic interface may facilitate the temporal co-occurrence of both electron donors and acceptors. As a consequence, these areas may experience on the one hand higher microbial activities by e.g. denitrifiers. On the other hand, intrusions of sulfide into the overlying oxic waters may inhibit the activities of aerobic microorganisms like the nitrifying

assemblages. These variations in the physico-chemical parameters likely have an impact on the performance of biogeochemically active microorganisms and consequently influence the rates of element transformations.

Chemoautotrophic prokaryotes of the Baltic Sea redox gradients

The described processes are catalyzed in biological reactions carried out mainly by chemolithoautotrophic prokaryotes, which occur at elevated abundances along the Baltic Sea pelagic redox gradients (see Figure 4; Labrenz *et al.*, 2007; Grote *et al.*, 2007; Labrenz *et al.*, 2010; Glaubitz *et al.*, 2013). The presence of chemolithoautotrophs determines the properties at which biogeochemical processes are taking place. Within the water-column, these prokaryotes form a peak in cellular abundances and represent an additional source of non-photosynthetic primary production. They exhibit a diverse genetic potential for functions associated with biogeochemical cycles (Thureborn *et al.*, 2013), i.e. nitrification, denitrification, sulfur oxidation and fixation of inorganic carbon. Previous studies revealed the occurrence of three major chemoautotrophs, which show distinct distribution patterns ranging from the hypoxic zone, the oxic-anoxic interface layer and into the sulfidic zone.

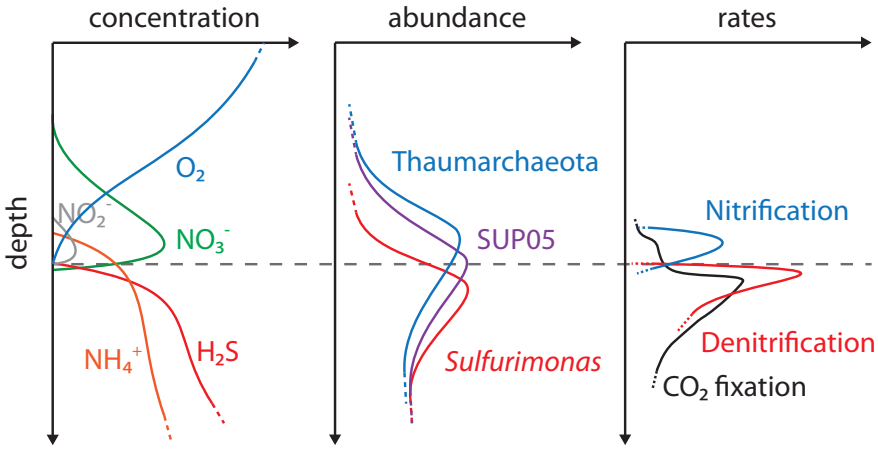

Figure 4.: Simplified schematic with approximate locations of physicochemical properties, microbial distributions and processes with emphasis along a typical Baltic Sea pelagic redox gradient as based on observations by Labrenz *et al.* (2007); Jost *et al.* (2008); Grote *et al.* (2008); Labrenz *et al.* (2010); Hietanen *et al.* (2012) and Glaubitz *et al.* (2013). The dashed line marks the interface between the hypoxic and sulfidic zones.

In the sulfidic zone, epsilonproteobacteria of the *Sulfurimonas* sp. subgroup GD17 (Grote *et al.*, 2007), which are closely affiliated with the cultivated model organism *Sulfurimonas gotlandica* str. GD1 (Grote *et al.*, 2012; Labrenz *et al.*, 2013) comprise high cell numbers, up to 15% of the bacterial cells (Grote *et al.*, 2007). They contribute substan-

tially to CO_2 fixation in the sulfidic zone, driven by denitrification via sulfur oxidation with nitrate. Physiological studies with *S. gotlandica* str. GD1 and its genomic capacity show that nitrate is of major importance as an electron acceptor. Utilization of oxygen could not be detected but growth was not inhibited until 10% oxygen saturation (Grote *et al.*, 2012). *S. gotlandica* str. GD1 possesses monopolar flagella and genes for chemotaxis are present in its genome. Accordingly, chemotactical behaviour towards nitrate was demonstrated in capillary assays (Grote *et al.*, 2012) and could be a strategy in environmental micro- and macro-gradients of nitrate to acquire compounds relevant for energy conservation.

The SUP05 cluster is a gammaproteobacterial group that has been associated with nitrate respiration, sulfur oxidation and chemoautotrophy based on its genomic features (Walsh *et al.*, 2009) and has a global distribution in OMZ waters (Wright *et al.*, 2012*b*) and at hydrothermal vent sites (Sunamura *et al.*, 2004). In the OMZ off Namibia, related gammaproteobacterial sulfur oxidizers were abundant and co-occurred with substantial denitrification rates (Lavik *et al.*, 2009). In Baltic pelagic redox gradients, the SUP05 cluster comprises high cellular abundances that account for 10-30% of the total cell counts (Glaubitz *et al.*, 2013). Baltic Sea SUP05 cells were found to predominate especially around the oxic-anoxic interface layer at depths with minimal sulfide concentrations (Glaubitz *et al.*, 2013), which is in line with the genomic feature of sulfur oxidation detected in the SUP05 metagenome (Walsh *et al.*, 2009). Yet, direct proofs of biogeochemical activities by SUP05 in the Baltic remain to be made. First indications for active CO_2 fixation by SUP05 were inferred from recovered *cbbM* transcripts, which affiliated with the SUP05 cluster (Glaubitz *et al.*, 2013) as well as from an RNA stable isotope probing study that demonstrated bicarbonate uptake by a related gammaproteobacterial member (Glaubitz *et al.*, 2009).

Both described groups of sulfur oxidizers require oxidized nitrogen in the form of nitrite or nitrate to oxidize sulfur compounds. Nitrite may be supplied by ammonia oxidizers of which archaeal representatives were detected at high cell numbers in the Gotland Deep (Labrenz *et al.*, 2010), while ammonia-oxidizing bacteria (AOB) accounted for less than 1% of the total cell numbers (Bauer, 2003) or are below the detection limit of molecular surveys (Labrenz *et al.*, 2010). The closest cultivated relative of the putative archaeal ammonia oxidizers in the Baltic Sea is *Candidatus* Nitrosopumilus maritimus that grows autotrophically and on the expense of ammonia oxidation (Könneke *et al.*, 2005). Therefore, it was suggested that the Baltic Sea thaumarchaeotal subcluster is an active

ammonia oxidizer, as inferred from its expression of *amoA* and high abundance in the putative nitrification zone of overlapping oxygen and ammonium gradients (Labrenz *et al.*, 2010). Whether the previously detected nitrification activities in the Baltic deeps (Bauer, 2003; Hietanen *et al.*, 2012) are associated with these archaea remains to be clarified.

Ecology of the Thaumarchaeota

Until a decade ago, aerobic ammonia oxidation was assumed to be performed exclusively by members of the *Betaproteobacteria* and *Gammaproteobacteria*. Since the discoveries of the key gene *amoA* coding for subunit A of ammonia monooxygenase on an archaeal-associated scaffold by Venter *et al.* (2004) and on an archaeal fosmid by Treusch *et al.* (2005) ammonia-oxidizing archaea (AOA) are increasingly recognized as ubiquitous, globally abundant and relevant catalysts within the nitrogen cycle (Francis *et al.*, 2005; Offre *et al.*, 2013). Their occurrence at low ammonium concentrations as they prevail in the oligotrophic ocean suggests adaptations, which are more efficient than those of their bacterial counterparts. A strong involvement of AOA in the nitrogen cycle as suppliers of nitrite entailed a revision of the processes and drivers within the nitrogen cycle (Francis *et al.*, 2007; Lam *et al.*, 2009). The isolation of the first marine AOA, *Ca.* Nitrosopumilus maritimus (Könneke *et al.*, 2005), from an aquarium biofilter at the Seattle Aquarium (Washington, USA) provided further details on the physiology and genetic capacities of AOA (Walker *et al.*, 2010). The phylogenetic placement of the ammonia-oxidizing archaea, previously assigned to the *Crenarchaeota*, in an own phylum, the *Thaumarchaeota* (Brochier-Armanet *et al.*, 2008), is reflected in distinctive features in information processing like transcription, translation and replication (Spang *et al.*, 2010) or the cell cycle as based on studies with *Ca.* Nitrosopumilus maritimus (Pelve *et al.*, 2011, 2013). Furthermore, the thaumarchaeotal variant of the 3-hydroxypropionate/4-hydroxybutyrate cycle points to an early divergent evolution different from the *Crenarchaeota* and is more efficient than the crenarchaeotal variant, presumably an adaptation to low-energy environments (Könneke *et al.*, 2014).

Thaumarchaeota are found in a broad variety of habitats. Their largest numbers are probably among the 1.3×10^{28} archaeal cells in the oceans, as estimated by Karner *et al.* (2001). *Nitrososphaera viennensis*, which is the first formally described Thaumarchaeon (Stieglmeier *et al.*, 2014) was isolated from garden soil in Vienna, Austria (Tourna *et al.*, 2011). Further habitats populated by Thaumarchaeota are hot springs (Hatzenpichler *et al.*, 2008), lakes (Auguet *et al.*, 2012; Auguet and Casamayor, 2013), the oligotrophic

ocean (Francis *et al.*, 2005), subglacial antarctic lakes (Christner *et al.*, 2014) or the human skin (Probst *et al.*, 2013). This broad spectrum of environments goes beyond the ecological range of known AOB (Stahl and de la Torre, 2012) and points towards a magnitude of strategies to thrive in various environments. Thaumarchaeota are also abundant in the Baltic Sea where they may be significantly involved in the nitrogen and carbon cycles.

Labrenz *et al.* (2010) showed that in pelagic waters of the Baltic Sea, Thaumarchaeota are present with up to 2.3×10^5 cells mL^{-1}, exhibiting a remarkably low diversity, inferred from the dominance of only one phylogenetic subcluster that is related to *Ca.* Nitrosopumilus maritimus. The expression of the *amoA* gene in the zone of overlapping oxygen and ammonium gradients is a strong indication for their activity in ammonia oxidation. Their occurrence in close proximity to the sulfidic zone and stable abundances in anoxic, sulfidic waters attests a good adaptation to this environment. As hypothesized by Labrenz *et al.* (2010), tolerance against sulfide may be one reason, why in the Baltic AOA represent a large population in contrast to the low-abundant AOB (Bauer, 2003). This hypothesis arises also from a study on sulfidic sediments where archaeal *amoA* genes and nitrification activity were detected (Caffrey *et al.*, 2007). Thus, the presence of hydrogen sulfide in environments populated by Thaumarchaeota may shape their physiological adaptations and could also mean an advantage of archaeal over bacterial ammonia oxidizers (Erguder *et al.*, 2009).

Aerobic ammonia oxidation and chemoautotrophy

Aerobic oxidation of ammonia (NH_3) or its protonated form ammonium (NH_4^+) to nitrite (NO_2^-) (Equation 1) to fuel growth by incorporation of CO_2 is found in most Thaumarchaeota. The stoichiometry of ammonia oxidation by AOA and AOB is the same (Equation 1, Martens-Habbena *et al.*, 2009) and the reaction yields $\Delta G^{\circ\prime} = 235$ kJ $mole^{-1}$ (Thamdrup, 2012). As CO_2 fixation is costly and requires significant amounts of energy (see e.g. Könneke *et al.*, 2014), AOA growth influences the pools of ammonium and nitrite in their habitats even though the biomass of the typically small Thaumarchaeota (Könneke *et al.*, 2005) can be expected to be at the lower range of planktonic cells (Lee *et al.*, 1987; Herndl *et al.*, 2005).

$$2NH_3 + 3O_2 \longrightarrow 2NO_2^- + 4H^+ + 2H_2O \quad (1)$$

Among ammonia-oxidizing bacteria, the oxidation of ammonia (Equation 2) is catalyzed by the enzyme ammonia monooxygenase (AMO) and produces hydroxylamine (NH_2OH) as an intermediate, which is then further oxidized to nitrite by hydroxylamine oxidoreductase (HAO). The reaction of the oxidation of ammonia to nitrite in the bacterial ammonia oxidizer *Nitrosomonas europaea* occurs as follows (Arp *et al.*, 2002):

$$NH_3 + O_2 + 2H^+ \xrightarrow[AMO]{} H_2O + NH_2OH \xrightarrow[HAO]{} {NO_2}^- + 5\,H^+ \tag{2}$$

Among ammonia-oxidizing archaea, the initial step of ammonia oxidation occurs likewise via an AMO homologue. Stable isotope tracer analyses with *Ca.* Nitrosopumilus maritimus have shown that hydroxylamine is produced also during archaeal ammonia oxidation (Vajrala *et al.*, 2012) but the enzyme, which catalyzes the oxidation of hydroxylamine remains to be identified. The fact that no homologue of the HAO was identified in current AOA genomes indicates that the bacterial HAO and the archaeal enzyme for hydroxylamine oxidation differ substantially. Therefore, hydroxylamine-oxidation may be one of the features distinguishing the archaeal from the bacterial ammonia oxidizers. Additionally, studies with *Ca.* Nitrosopumilus maritimus revealed an exceptionally high affinity for ammonia (K_m = 133 nmol L^{-1}), which is about 200-fold higher than that of AOB (Martens-Habbena *et al.*, 2009). Thus, the presence of AOA at low ammonium concentrations may be caused by the AOA themselves which exploit the ammonium pools more efficiently than the AOB.

In contrast to the AOB, which fix CO_2 via the Calvin-Benson-Bassham (CBB) cycle, AOA exhibit a variant of the 3-hydroxypropionate/4-hydroxybutyrate (3-HP/4-HB) cycle (Könneke *et al.*, 2014), which is also used by *Crenarchaeota* (Berg *et al.*, 2007, 2010). However, the thaumarchaeotal variant is energetically more efficient because of ADP- rather than AMP-producing enzymes, enzymes capable of catalyzing multiple reactions and a better aerobic stability, which altogether make it the most energy-efficient aerobic CO_2 fixation pathway known to date (Könneke *et al.*, 2014).

Environmental field studies with focus on the activities of Thaumarchaeota indicated that these are actively participating in the cycling of nitrogen and carbon. In the California Current, archaeal *amoA* gene copies were located near the maxima of nitrification rates while bacterial copies of the *amoA* gene were close to the detection limit suggesting active contributions to nitrification by Thaumarchaeota (Santoro *et al.*, 2010). In waters of the Central Mediterranean Sea, inorganic carbon incorporation was largely attributed to

Thaumarchaeota (Yakimov *et al.*, 2011). Incorporation of ^{13}C-labeled dissolved inorganic carbon into thaumarchaeotal lipids in coastal North Sea waters declined pronouncedly in the presence of nitrification inhibitors, thereby establishing a link between autotrophy and nitrification by Thaumarchaeota (Veuger *et al.*, 2013). In the subtropical North Pacific Gyre, natural radiocarbon properties in the archaeal membrane lipids suggested that Thaumarchaeota live mainly autotrophically (Ingalls *et al.*, 2006). Investigations in polar Arctic waters suggested that Thaumarchaeota may also utilize alternative carbon and energy sources such as urea for growth and energy conservation, respectively (Alonso-Sáez *et al.*, 2012), which would be an advantageous adaptation to the low-energy conditions in such habitats. Various environmental factors may shape the adaptations of Thaumarchaeota to their environments such as the concentrations of ammonium or the exposure to sulfide (reviewed by Erguder *et al.*, 2009). The effect of these potentially niche-determining properties remains however to be investigated in terms of thaumarchaeotal activities and adaptations throughout the water-column.

Open questions

In a time in which human mankind proceeds to alter ecosystems through e.g. increased nutrient inputs, it is crucial to acquire a deep, profound understanding of affected ecosystems, including their microbiota (Stahl and de la Torre, 2012). Especially within the nitrogen cycle, which plays a major role in ecosystem-productivity and regulation, the recent discoveries indicate the necessity of identifying microbial catalysts of important processes and their regulation. The ammonia-oxidizing archaea of the phylum *Thaumarchaeota* inhabit also Baltic Sea water-columns and presumably play an important role for this ecosystem. Thaumarchaeota have been found at high abundances in the Baltic Sea (Labrenz *et al.*, 2010), at sites where nitrification was detected (Hietanen *et al.*, 2012). However, the presence of Thaumarchaeota and nitrification rates were so far not investigated simultaneously so that their quantitative contribution to this process remains elusive. Sulfide has been discussed as a potential factor to impact the activities of AOA and AOB in different ways (Erguder *et al.*, 2009) and is known to regulate nitrification activity (Joye and Hollibaugh, 1995). The role of temporal exposures of sulfide into the nitrification zone for the nitrification process and the viability of the ammonia oxidizers, is unknown. The distribution of Thaumarchaeota within sulfidic waters was recognized by Labrenz *et al.* (2010) but at present, nothing is known about their activities in these sulfidic, anoxic waters, which do

not permit aerobic ammonia oxidation and represent a toxic environment for most aerobic organisms, including nitrifiers.

Thesis outline

The aim of the present thesis was, to elucidate the ecological role of Thaumarchaeota in pelagic Baltic Sea redox gradients. First, their contribution to nitrification was quantified and the effect of hydrogen sulfide on nitrification activities and potential adaptations of Thaumarchaeota to sulfide exposure was investigated. The second focus was on the relevance of autotrophic carbon assimilation and the extent to which CO_2 fixation may contribute to biomass in a representative of the *Thaumarchaeota*, which was enriched from a Baltic redox gradient. And third, as the Baltic Sea Thaumarchaeota are a constituent part among other chemoautotrophic prokaryotes, light is shed on their niche-partitioning, regulation and adaptations within the context of these associated chemoautotrophs with special focus on the features of Thaumarchaeota.

To address the aforementioned topics, a diverse suite of molecular, microbial, biogeochemical and bioinformatics tools was applied in combination with field samplings, cultivation of enrichments and metatranscriptomic analyses.

- Chapter 1 examines the distribution of Thaumarchaeota at several sites and times in Baltic Sea pelagic redox gradients as well as their quantitative contributions to the process of nitrification. Furthermore, a potential tolerance of the nitrifying assemblages against hydrogen sulfide was assessed. These questions were addressed in the scope of multiple research cruises and extensive field samplings in three different Baltic deep basins, the Bornholm Deep, Gotland Deep and the Landsort Deep throughout 2011–2012. Quantitative analyses using CARD-FISH were combined with rate measurements of nitrification via ^{15}N stable isotope incubations and gas chromatographic isotopic ratio mass spectrometry. The respective contributions of bacterial and archaeal activities to nitrification were dissected by amendment of domain-specific inhibitors. Additions of sulfide to environmental samples from the nitrification maximum were followed by nitrification rate measurements to examine the inhibitory effect of sulfide on this process.
- Chapter 2 focuses on the chemoautotrophic capacities of a member of the *Thaumarchaeota*, enriched from a Landsort Deep redox gradient. It presents a novel en-

richment culture of ammonia-oxidizing Thaumarchaeota from brackish waters and elucidates the proportional coupling between ammonia oxidation and CO_2 fixation. Calculations on carbon and nitrogen balances were made throughout a batch growth experiment and the uptake of ^{13}C labeled inorganic carbon and ^{15}N labeled ammonium followed on the single-cell level. Additionally, this enrichment culture served to assess the efficiency of domain-specific inhibitors, which were used on environmental samples in the study of Chapter 1.

- Chapter 3 sheds light on the activities of Thaumarchaeota in a natural redox gradient of the Landsort Deep, employing metatranscriptomics. Special focus was set on the differences in thaumarchaeotal activities between the oxic and the sulfidic milieu. The activities of both biogeochemically and physiologically relevant genes as proxies for the corresonding processes and adaptations, respectively, were examined with respect to different chemical niches, among Thaumarchaeota as well as chemoautotrophs of the *Sulfurimonas* sp. subgroup GD17 and the SUP05 cluster. Using reference genomes of close relatives, organism-specific sequence recruitment in combination with a subsequent cluster analysis served to determine group-specific activity zones and to identify genes that play an important role outside these zones, such as in the sulfidic zone.

Chapter one

Significance of archaeal nitrification in hypoxic waters of the Baltic Sea

1

SIGNIFICANCE OF ARCHAEAL NITRIFICATION IN HYPOXIC WATERS OF THE BALTIC SEA

Abstract

Ammonia-oxidizing archaea (AOA) of the phylum *Thaumarchaeota* are widespread, and their abundance in many terrestrial and aquatic ecosystems suggests a prominent role in nitrification. AOA also occur in high numbers in oxygen-deficient marine environments, such as the pelagic redox gradients of the central Baltic Sea; however, data on archaeal nitrification rates are scarce and little is known about the factors, e.g. sulfide, that regulate nitrification in this system. In the present work, we assessed the contribution of AOA to ammonia oxidation rates in Baltic deep basins and elucidated the impact of sulfide on this process. Rate measurements with ^{15}N-labeled ammonium, CO_2 dark fixation measurements and quantification of AOA by catalyzed reporter deposition fluorescence *in situ* hybridization (CARD-FISH) revealed that among the three investigated sites the highest potential nitrification rates (122–884 nmol L^{-1} d^{-1}) were measured within gradients of decreasing oxygen, where thaumarchaeotal abundance was maximal (2.5–6.9 $\times$ 10^5 cells mL^{-1}) and CO_2 fixation elevated. In the presence of the archaeal-specific inhibitor GC_7, nitrification was reduced by 86–100%, confirming the assumed dominance of AOA in this process. In samples spiked with sulfide at concentrations similar to those of *in situ* conditions, nitrification activity was inhibited but persisted at reduced rates. This result together with the substantial nitrification potential detected in sulfidic waters suggests the tolerance of AOA to periodic mixing of anoxic and sulfidic waters. It begs the question whether the globally distributed Thaumarchaeota respond similarly in other stratified water-columns or if the observed robustness against sulfide is a specific feature of the thaumarchaeotal subcluster present in the Baltic Deeps.

1.1 Introduction

Since the discovery that autotrophic ammonia oxidation is not restricted to the *Bacteria* but is also performed by members of the *Archaea* (Venter *et al.*, 2004; Treusch *et al.*, 2005; Könneke *et al.*, 2005), mesophilic ammonia-oxidizing archaea (AOA) have been recognized as one of the most successful and ubiquitous groups of microorganisms on Earth (Francis *et al.*, 2005; Offre *et al.*, 2013). Phylogenetically affiliated with the novel phylum *Thaumarchaeota* (Brochier-Armanet *et al.*, 2008; Spang *et al.*, 2010), AOA occur in high abundances in both terrestrial (Zhang *et al.*, 2010; Pratscher *et al.*, 2011) and aquatic (Yakimov *et al.*, 2011; Biller *et al.*, 2012; Amano-Sato *et al.*, 2013) ecosystems, often outnumbering bacterial ammonia oxidizers (Schleper, 2010). As a consequence, questions arise regarding the ecological niche of AOA, their roles in nitrification and primary production, and the environmental factors that regulate their contribution to these processes.

The conversion of ammonia (NH_3) or its protonated form ammonium (NH_4^+) to nitrite (NO_2^-) is the first and generally rate-limiting step in nitrification (except to some extent in the primary nitrite maximum in the oceans; Lomas and Lipschultz, 2006). The relative contributions to ammonia oxidation by autotrophic AOA and ammonia-oxidizing bacteria (AOB) have been inferred using the archaeal and bacterial *amoA* genes, which encode subunit A of the key enzyme ammonia monooxygenase (e.g. Rotthauwe *et al.*, 1997; De Corte *et al.*, 2009; Sauder *et al.*, 2011; Auguet *et al.*, 2012). These studies often revealed the dominance of archaeal over bacterial ammonia oxidizers (Francis *et al.*, 2005; Wuchter *et al.*, 2006; Mincer *et al.*, 2007; Agogué *et al.*, 2008; Newell *et al.*, 2013). Further support for the strong role for AOA in nitrification comes from observations of the co-occurrence of archaeal *amoA* in areas of nitrification activity (Caffrey *et al.*, 2007; Beman *et al.*, 2008; Alves *et al.*, 2013) and from metatranscriptomic studies (Baker *et al.*, 2012; Lesniewski *et al.*, 2012). However, to determine the actual contribution and impact of AOA on the nitrogen cycle it requires measurements of ammonium oxidation rates, as they cannot be deduced from transcript abundance alone (Mußmann *et al.*, 2011) given that quantification is influenced by e.g. mRNA degradation during sampling (Feike *et al.*, 2012) and, additionally, may not inevitably reflect environmental activity.

In the globally expanding marine oxygen minimum zones (OMZ) and in other oxygen-deficient systems, archaea are prominently embedded in the cycles of carbon (C) and nitrogen (N) (Löscher *et al.*, 2012; Stewart *et al.*, 2012), consistent with the recognition of these systems as hotspots for chemolithoautotrophs (Ulloa *et al.*, 2012*b*). Concerted

dissimilatory microbial processes successively transform fixed nitrogen species into dinitrogen gas (Lam and Kuypers, 2011) and autotrophy promotes the fixation of inorganic carbon into biomass (Herndl *et al.*, 2005). Accordingly, AOA have been shown to play an important role within the N (Francis *et al.*, 2007; Stewart *et al.*, 2012) and C cycles (Ingalls *et al.*, 2006). Since AOA may contribute strongly to nitrification and primary production, knowledge of their ecology and regulation are crucial for the understanding of ecosystem-relevant N- and C-cycling in oxygen-deficient zones.

Nitrogen transformations and the responsible microorganisms have also been investigated in the oxic-anoxic transition zones of the water column of the central Baltic Sea (Hannig *et al.*, 2007; Schneider *et al.*, 2010; Hietanen *et al.*, 2012). Oxygen depletion in deep basins is accompanied by gradients of NO_3^-, NO_2^-, H_2S, and NH_4^+, which are exploited by different guilds of chemolithoautotrophic prokaryotes (Grote *et al.*, 2008; Glaubitz *et al.*, 2013; Labrenz *et al.*, 2010). Autotrophic ammonia oxidation is an essential ecological function for the N and C cycle in the Baltic Sea, which receives high loads of nutrient input from its catchment area (Voss *et al.*, 2011). Nitrification fuels subsequent denitrification, which in the water column is mainly carried out by chemolithoautotrophic prokaryotes that link the latter process to the oxidation of reduced sulfur compounds (Brettar and Rheinheimer, 1991; Hannig *et al.*, 2007; Dalsgaard *et al.*, 2013). Anaerobic ammonia oxidation (anammox) has been shown to occur periodically upon major inflow events of oxygen-rich water, causing temporary non-sulfidic conditions (Hannig *et al.*, 2007) in Baltic deep basins. Since an extended oxygen- and sulfide-free zone is lacking most of the time (in contrast to the Black Sea; Lam *et al.*, 2007), ammonia oxidation is carried out mostly aerobically due to the sensitivity of anammox bacteria towards oxygen and potentially sulfide (Jin *et al.*, 2012; Carvajal-Arroyo *et al.*, 2013). Where ammonium and oxygen gradients overlap, potential nitrification rates as high as 85–160 nmol L^{-1} d^{-1} have been measured (Hietanen *et al.*, 2012). Labrenz *et al.* (2010) reported the dominance of a single thaumarchaeotal subcluster, termed GD2, related to the autotrophic *Candidatus* Nitrosopumilus maritimus (Könneke *et al.*, 2005), that accounted for up to 26% of all prokaryotes in hypoxic waters. The high-level transcription of archaeal *amoA* further indicates a substantial contribution of AOA to ammonia oxidation (Labrenz *et al.*, 2010; Feike *et al.*, 2012). Moreover, the dominance of archaea is in contrast to AOB abundance, as very low cell numbers ($< 1\%$ of total cell numbers; Bauer, 2003) and *amoA* transcript levels below the detection limit (Labrenz *et al.*, 2010) point to their minor role in ammonia oxidation in Baltic Sea redox gradients. However, cell abundance does not necessarily reflect the respective organism's contribution to a specific process (Musat *et al.*, 2008). AOA and AOB belong to different

domains with specific physiologies, and levels of functional gene expression may not be equally extrapolated to the process rates, so that alternative experimental approaches are required to confirm this hypothesis. In the case of ammonia oxidation, rate measurements can be linked with archaeal vs. bacterial contributions by the use of inhibitors specific for either *Bacteria* or *Archaea* (Yokokawa *et al.*, 2012; Löscher *et al.*, 2012).

Sulfide (H_2S) directly impairs metabolism and is therefore toxic to most aerobic microorganisms, including nitrifiers (Joye and Hollibaugh, 1995); thus, its mixing into hypoxic waters (0-10 µmol O_2 L^{-1}) such as those of Baltic redox gradients affects microbial activities (Hoppe *et al.*, 1990) and likely also nitrification. The presence of AOA in sulfidic environments (Coolen *et al.*, 2007; Caffrey *et al.*, 2007) suggests that they are able to cope with sulfide, unlike highly H_2S-sensitive AOB (Sears *et al.*, 2004). Among the oxygen-depleted systems worldwide, the Baltic Sea presents not only an ideal habitat to investigate archaeal nitrification but also its response to sulfidic conditions. The high abundance of Thaumarchaeota reported by Labrenz *et al.* (2010) in a sulfidic basin of the Baltic Sea suggested that they are the predominating ammonia oxidizers, potentially because they are better adapted than their bacterial counterparts to periodically sulfidic conditions. Erguder *et al.* (2008) reported a shift towards archaeal *amoA* enrichment in a sequential batch reactor when pulsed with sulfide. In the pelagic redox gradient of the Baltic Sea, sulfide is used as an electron donor by chemoautotrophic sulfide-oxidizing bacteria, e.g., the autotrophic *Sulfurimonas* sp. subgroup GD17 (Grote *et al.*, 2008) and perhaps by *Gammaproteobacteria* of the SUP05 group (Glaubitz *et al.*, 2013), but short-term mixing events would also expose sulfide-sensitive microbes such as nitrifiers to low and potentially toxic sulfide concentrations. In fact, lateral intrusions and small-scale mixing have been shown to influence microbially mediated transformations in pelagic redox gradients (Fuchsman *et al.*, 2012) and are also frequent in the Baltic Sea (Kuzmina *et al.*, 2005; Wieczorek *et al.*, 2008; Friedrich *et al.*, 2014).

In this study we quantified Thaumarchaeota and potential nitrification at different times and locations, assessing the contribution of AOA to this process by using archaea-specific inhibitors. In addition, we sought to elucidate the effect of sulfide on nitrification activity in Baltic Sea redox gradients. Our results provide compelling evidence that Thaumarchaeota are indeed responsible for the major portion of ammonia oxidation in hypoxic waters of the Baltic Sea and that they are likely adapted to its periodically occurring anoxic and sulfidic conditions.

1.2 Material and Methods

1.2.1 Sampling and physicochemical analyses

Sampling was conducted in the eastern and western Gotland Basin and the Bornholm Basin (locations and coordinates in Figure 1.1), specifically at Gotland Deep station 271, Landsort Deep station 284, and Bornholm Deep station 213 during cruises with the research vessels *Alkor* (Feb 2011), *Elisabeth-Mann-Borgese* (July 2011), and *Meteor* (Nov 2011 and June 2012).

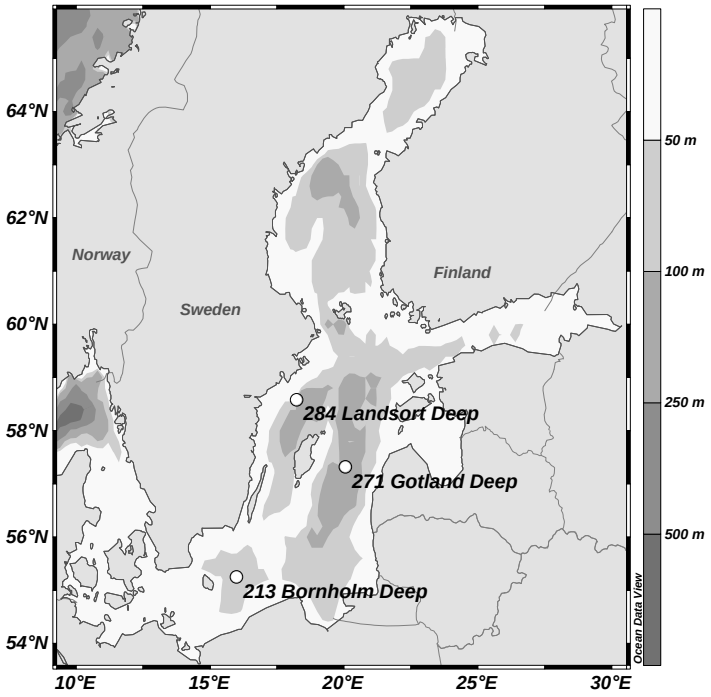

Figure 1.1.: Overview of the locations of the three sampled sites in the Baltic Sea: station 213 at the Bornholm Deep (55°15.0300N, 015°59.1400E), station 271 at the Gotland Deep (57°19.2041N, 020°02.9291E), and station 284 at the Landsort Deep (58°35.0056N, 018°14.0344E).

During all cruises, water was collected, with emphasis on oxic-anoxic transition zones, in free-flow water bottles attached to a conductivity, temperature, and depth (CTD) probe. For each depth, sampling was conducted with two 5-L Niskin-bottles. Water was taken from one bottle for nitrification and CO_2 fixation rate measurements, followed by sampling for cell counts. At the same time, samples from the second bottle were immediately analyzed on board for O_2, H_2S, NH_4^+, NO_3^-, and NO_2^- concentrations (detection limits L^{-1}: 1 µmol for O_2; 0.2 µmol for H_2S; 0.2-0.5 µmol for NH_4^+ and NO_3^-, 0.05 µmol L^{-1} for NO_2^-) according to the method of Grasshoff *et al.* (1983) or Cline (1969) (for H_2S). O_2

was determined via automatic titration (Titrino 702, Metrohm); the titer of the thiosulfate solution was determined daily and the solution renewed if deviating more than 0.1 from the reference value of 1.0. Standards for H_2S were run ranging from 0.1–3 mg L^{-1} with an r^2 between 0.9882 to 0.9997. Calibration for NH_4^+ and NO_3^- was done using standards of 10 µmol L^{-1} or 2 µmol L^{-1} for NO_2^-. At Gotland Deep in 2011, water was retrieved in two consecutive CTD-casts. Samples for the sulfide spiking experiment and dissolved inorganic carbon (DIC) determination were obtained in subsequent separate CTD-casts.

1.2.2 Quantification of Thaumarchaeota and *Sulfurimonas* sp. subgroup GD17

From each depth, samples of 100 mL were fixed for 6–12 h with 0.2-µm-filtered formaldehyde (2% final concentration) at 4 °C. From these, volumes of 20–40 mL (profiles) or 4 mL (spiking experiment) were filtered onto 0.2-µm polycarbonate filters (Nuclepore track-etched, Whatman). The filters were dried and stored at -20 or -80 °C until analysis. Catalyzed reporter deposition fluorescence *in situ* hybridization (CARD-FISH) was performed according to Pernthaler *et al.* (2002) with a few modifications. Briefly, the filters were embedded in 0.1% agarose prior to digestion with lysozyme and achromopeptidase at 37 °C for 60 and 15 min, respectively. Hybridization with the horseradish-peroxidase-labeled Cren679 probe, specifically targeting thaumarchaeotal subcluster GD2 (Labrenz *et al.*, 2010), was carried out overnight at 35 °C in the presence of 35% formamide, followed by tyramide signal amplification with Alexa Fluor 488 (Invitrogen). Hybridization and quantification targeting cells of *Sulfurimonas* sp. subgroup GD17 was conducted with probe SUL90 and 55% formamide according to Grote *et al.* (2007). Dried filter sections were embedded in Vectashield mounting medium (Vector Labs, California, USA) containing 4',6-diamidin-2-phenylindol (DAPI). For enumeration by epifluorescence microscopy, 600–1,400 DAPI-stained cells from randomly selected microscopic fields were inspected using a Zeiss Axioskop 2 mot plus (Zeiss, Oberkochen, Germany).

1.2.3 Potential nitrification rates

Incubations with amended 5 µmol $^{15}NH_4Cl$ L^{-1} (99% ^{15}N, Cambridge Isotope Laboratories, Massachusetts, USA) were conducted as described in Holtappels *et al.* (2011) with minor modifications. We consider the measured nitrification rates as potential rates because the

addition of $^{15}NH_4Cl$ resulted in ammonium concentrations significantly exceeding the *in situ* concentrations (Table S1). The details of the procedure are as follows: sample water was transferred from the CTD into 0.5-L or 1-L glass bottles with a three-fold overflow and then closed without headspace with PTFE-taped butyl rubber stoppers. The bottles were transferred to a cooling room (6–11 °C) where a gas-tight syringe (Hamilton, Switzerland) was used to inject them with 5 µmol of an anoxic $^{15}NH_4Cl$ solution L^{-1}. Before and after tracer amendment, the total NH_4^+ concentration in the samples was determined in order to calculate the percentage of $^{15}NH_4^+$-labeling, which ranged between 21-100% (Table S1). The water was distributed from the bottle into aliquots of 12-mL in Exetainer glass vials (Labco Ltd., UK). For this, the bottle was placed upside down, gently discharging the seawater by replacement with N_2 through a glass tube into Exetainer vials with three-fold overflow one after another. Then, the Exetainers were immediately capped without headspace. Incubations took place in the dark at approximately the *in situ* temperature. Two or three vials were removed approximately every 6 h over a period of 30 h from the beginning of the experiment. Headspace was added to each vial then they were frozen at -20 °C.

For mass-spectrometric analysis, the frozen samples were thawed, and the NO_3^- in a 4.5-mL aliquot reduced to NO_2^-, adding approximately 0.3 g spongy cadmium per sample, as described by Jones (1984). After horizontal shaking overnight, the tubes were centrifuged and 4 mL of the supernatant was transferred into new 6-mL Exetainer vials. These vials were then closed with caps and flushed with helium (grade 5.0) for 10 min. The NO_2^- pool was reduced to N_2 as described in Füssel *et al.* (2011), by adding 50 µL of 4% sulfamic acid and shaking the samples overnight. With only a small fraction of the bulk NO_2^- labelled, $^{15}NO_2^-$ was converted to $^{15}N^{14}N$. The vials were stored upside down until gas chromatographic isotopic ratio mass spectrometry analysis (GC-IRMS), carried out within a few days. The accumulation of $^{15}N^{14}N$ was determined by GC-IRMS (Delta V plus Isotope Ratio MS, Thermo Finnigan Conflo III, Thermo Fisher Scientific) analysis of a 500-µL sample of the headspace N_2. Potential nitrification rates were derived from the excess in the $^{29}N_2/^{28}N_2$ ratio, measured over time during the incubation period, above the initial ratio and from the percentage of ^{15}N-labeling of ammonia (see Supplementary Information; Thamdrup and Dalsgaard, 2000).

1.2.4 Sulfide spiking experiment

At the Gotland Deep site in 2011, water from the zone with the highest potential nitrification rates (122 nmol N L^{-1} d^{-1} at a depth of 110 m) was retrieved and transferred to 0.5-L or 1-L bottles as described above but, because of limitations in the sample volume, without overflow. The bottles were randomly assigned to one of four H_2S treatment groups, generated by adding H_2S as spikes from a stock solution of 188 mmol H_2S L^{-1} to final concentrations of 0 (control), 4.1, 8.3, and 16.6 µmol L^{-1}. To detect a potential impact of sulfide addition on nitrification activity after spiking, potential nitrification rates were measured as described above, i.e., by subsampling from one bottle of each group into Exetainer vials at 0, 24, and 48 h after spiking, such that nitrification rate determinations covered the intervals 0–24, 24–48, and 48–72 h. The Exetainer incubations were similarly stopped for parallel vials of the control and each sulfide amendment four to nine times during the following 24 h, in order to determine potential nitrification rates. In addition, samples from the bottles and Exetainers were fixed with $ZnCl_2$ to measure sulfide concentrations according to Cline (1969).

1.2.5 Dark CO_2 fixation

Rates of dark CO_2 fixation were determined, slightly modified, as described in Jost *et al.* (2010). Seawater was transferred directly from the CTD bottles into 12-mL Exetainer glass vials with three-fold overflow. The vials were closed without headspace after which a gas-tight syringe was used to add approximately 1.85 MBq of $NaH^{14}CO_3$ (Hartmann Analytic GmbH, Germany) from an anoxic stock solution. Three parallels plus a killed-control, in which the sample was fixed with formaldehyde (2% final concentration), were incubated at approximately the *in situ* temperature for 24 h; the exact times were noted. The incubations were stopped by filtering the contents of the vials onto 0.2-µm cellulose acetate (Sartorius, Göttingen, Germany) or polycarbonate (Nuclepore track-etched, Whatman) filters (25 mm diameter). Before filtration, 50 µL of the sample was withdrawn to determine the total radioactivity added to each vial. The filters were exposed to HCl fumes for 0.5–2 h and then transferred into 4 mL of LumaSafe scintillation cocktail (PerkinElmer). Total- and filter-^{14}C disintegrations per minute were analyzed in a PerkinElmer Tri-Carb 2800R liquid scintillation analyzer. CO_2 fixation rates were derived (see Supplementary

Information) from the fraction of ^{14}C incorporated in relation to the total activity added and the background concentration of DIC, ranging between 2003 and 2037 µmol kg^{-1} (Gotland Deep, July 2011). The determination of C_T was performed by coulometry using the SOMMA system designed by Johnson *et al.* (1993). The system was calibrated with certified carbon reference material (Dr. A. Dickson, Universtity of California, San Diego) and allowed for a precision/accuracy of about ± 2 µmol kg^{-1}. Counts of the killed controls were subtracted before the rates were calculated.

1.2.6 Domain-specific inhibition of archaea and bacteria

Taking advantage of the fundamental differences in the translation machinery of *Archaea* and *Bacteria*, we chose inhibitors targeting archaeal or bacterial protein biosynthesis and tested them prior to *in situ* application. To do so, the chemoautotrophic activity (dark CO_2 fixation rates) of a thaumarchaeotal AOA enrichment culture was used to determine the extent of inhibition. This culture, originally obtained from the redox gradient of the Landsort Deep and enriched over a period of 1.5 years in the presence of streptomycin and NH_4Cl, contained 89–97% archaea (according to CARD-FISH (probe Arc915); Berg *et al.* (submitted), see Chapter 2). The archaeal inhibitors, N^1-guanyl-1,7-diaminoheptane (GC_7; Biosearch Technologies, California, USA; Jansson *et al.*, 2000) and diphtheria toxin (Sigma-Aldrich, Germany; Mußmann *et al.*, 2011; Yokokawa *et al.*, 2012), at concentrations of 0.25–2.0 mmol L^{-1} and 0.5–10 µg mL^{-1}, respectively, and the bacterial inhibitor erythromycin (VWR, Germany), at concentrations between 10 and 50 µg mL^{-1} (Yokokawa *et al.*, 2012) were assessed. GC_7 shuts down biosynthesis via cell cycle arrest and specifically targets archaea (Jansson *et al.*, 2000), including *Ca.* N. maritimus SCM1, but it has no effect on AOB (Löscher *et al.*, 2012).

While diphtheria toxin caused no inhibition, GC_7, at a concentration of 1 mmol L^{-1}, significantly reduced dark CO_2 fixation activity by 81% (one-way ANOVA $p < 0.0004$; Figure 1.2) within 24 h and was therefore chosen as the archaeal inhibitor for environmental samples. The GC_7 solvent (acetic acid) was likewise tested and had no significant inhibitory effect on AOA (Figure A.1). For the environmental samples, GC_7 dissolved in 5 mmol acetic acid L^{-1} to a concentration of 100 mmol L^{-1} was prepared as a stock solution and stored at -20 °C until use. For inhibitor experiments, sample water from the Gotland Deep and the Landsort Deep was amended with $^{15}NH_4Cl$ and then distributed into 6-mL or 12-mL vials as described above. Immediately afterwards, GC_7 was injected (1 mmol

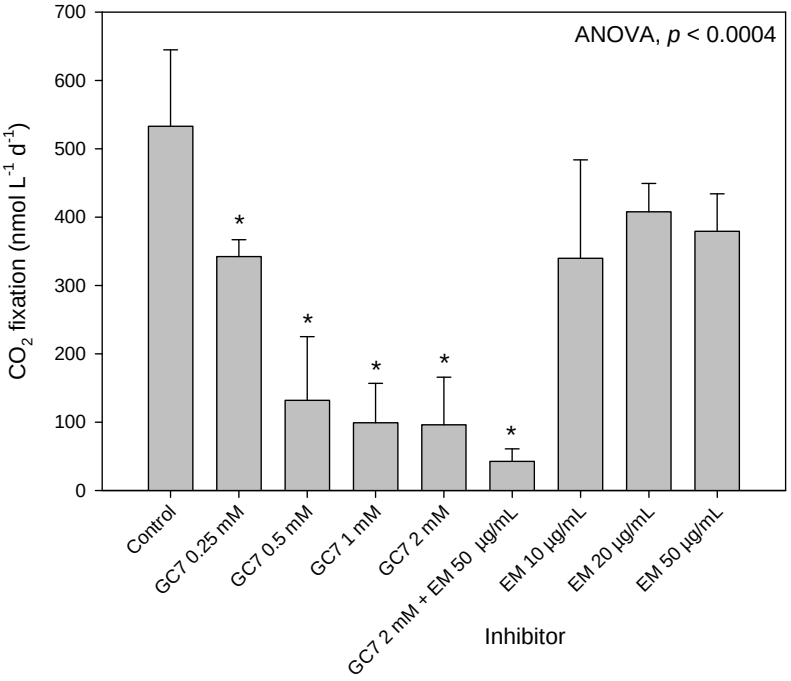

Figure 1.2.: Evaluation of different concentrations of GC_7 and erythromycin (EM) on CO_2 fixation rates in a thaumarchaeotal enrichment culture. Measurements were conducted in triplicate subsamples taken from the culture; error bars show the standard deviation. An asterisk indicates a significant ($p < 0.0004$) difference of the treatment compared to the control (one-way ANOVA and Tukey's pairwise comparison).

L^{-1} final concentration) into the vials, which were then incubated alongside the controls (without inhibitor) for 6, 12, or 24 h. Activity was arrested by freezing the samples at -20 °C.

1.2.7 Statistical analyses

All statistical analyses were performed with the PAST software package v 3.0 (Hammer *et al.*, 2001). Correlation between potential nitrification rates and the abundance of Thaumarchaeota was tested, via linear bivariate regression of measured potential nitrification rates and thaumarchaeotal cell counts. Domain-specific inhibition of CO_2 fixation activity in an AOA enrichment culture with inhibitors at several concentrations was compared using one-way analysis of variance (one-way ANOVA) followed by Tukey's pairwise comparison. A generalized linear model (GLS) was used to test for significant difference of regression slopes from zero. Difference in regression slopes of potential nitrification rates with and without GC_7 or erythromycin was tested using analysis of covariance (one-way ANCOVA).

1.3 Results

1.3.1 Redox zone structure in the Gotland Deep, Landsort Deep, and Bornholm Deep

At the Gotland Deep in July 2011, the water column was oxygenated in the upper 119 m, including a hypoxic zone with low oxygen concentrations (< 10 µmol L^{-1}) between 109 and 119 m (Figure 1.3). An overlap of oxygen with small amounts of sulfide was detected between 114 and 119 m. Below this depth, sulfide concentrations increased. The sampling depths, which spanned from 74 to 119 m, covered a broad peak of nitrate, with a maximum concentration of 8.4 µmol L^{-1} at 104 m. Nitrite ranged between 0.1 and 0.4 µmol L^{-1}. Ammonium was detectable in the hypoxic zone at concentrations of 0.1–0.2 µmol L^{-1} and increased progressively with depth. Total prokaryotic cell numbers ranged between 3.2 and 7.5 × 10^5 cells mL^{-1}, with a peak in the hypoxic zone at 110 m. The Thaumarchaeota subcluster GD2 accounted for 2–24% of total cell numbers, reaching a maximal abundance of 1.8 × 10^5 cells mL^{-1} at 110 m, i.e., within the hypoxic zone.

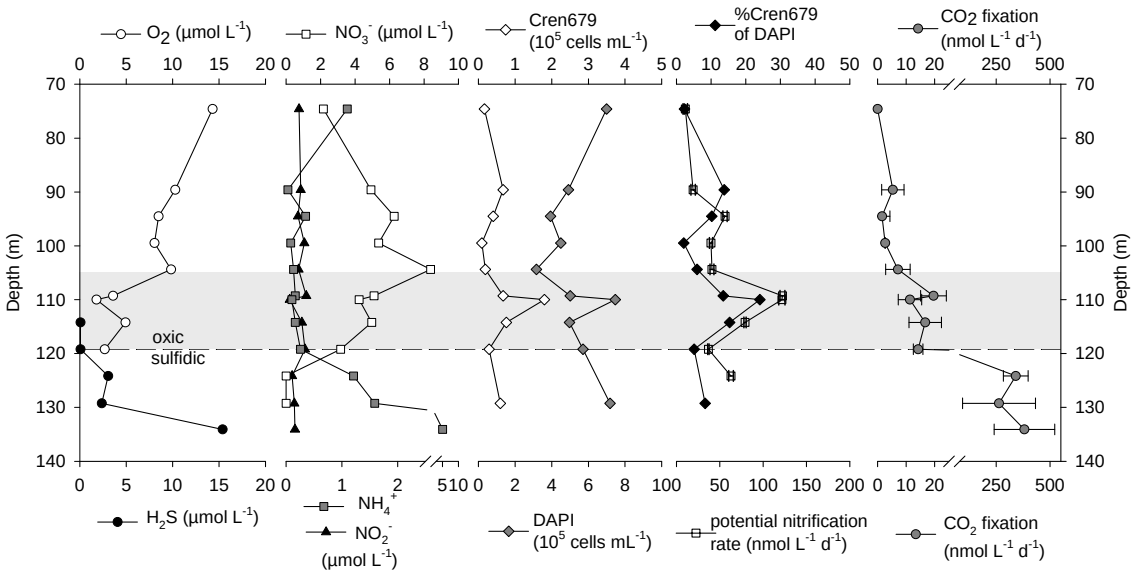

Figure 1.3.: Detailed profile of the Gotland Deep redox-zone in July 2011. Concentrations of NO_3^-, NO_2^-, NH_4^+, H_2S, and O_2, total prokaryotic cell numbers counted by DAPI staining, GD2 thaumarchaeotal cell abundances (CARD-FISH probe Cren679), potential nitrification rates, and CO_2 fixation rates were determined. The hypoxic zone, where oxygen concentrations were below 10 µmol L^{-1}, is shaded gray. Error bars show the standard deviation of triplicate samples (CO_2 fixation rates) or the standard error of the slope of excess ^{29}N (potential nitrification rates).

At the Landsort Deep in June 2012, the hypoxic zone was sampled within a gradient of decreasing nitrate, covering also the nitrite maximum (Figure 1.4). Ammonium

concentrations increased pronouncedly, from 0.1 to 1.4 µmol L^{-1}, while oxygen concentrations decreased from 22 to 2.7 µmol L^{-1}. Sulfide did not exceed 0.1 µmol L^{-1}. At the Gotland Deep in June 2012, the hypoxic zone was sampled at depths between 70 and 104 m (Figure 1.5) above the sulfidic/anoxic zone, which was not covered by the sampling depths. The physicochemical profile deviated from the typical stratification by showing a narrow band of increased H_2S and NH_4^+ concentrations at 94 m. Above this intrusion, sharp peaks in nitrate and nitrite were located at depths of 85 and 89 m, respectively. The Bornholm Deep in 2011 was characterized by a declining oxygen gradient, with concentrations as low as < 10 µmol L^{-1} above the seafloor (Table 9), coinciding with NH_4^+ concentrations of 13.6 (Nov 2011) and 1.8 µmol L^{-1} (July 2011). The highest potential nitrification rates were detected in Nov 2011, when Thaumarchaeota were highly abundant (4.3×10^5 cells mL^{-1}). Also at this site, hydrogen sulfide was detected above the seafloor at a concentration of 23.4 µmol L^{-1}.

Dark CO_2 fixation, as a measure of chemoautotrophic activity in the non-sulfidic, hypoxic zones of the Bornholm Deep, Gotland Deep, and Landsort Deep (Figure 1.3 and Figure 1.4, Table S1), achieved rates of up to 28, 19, and 58 nmol L^{-1} d^{-1}, respectively, coinciding with high potential nitrification rates. This level of carbon fixation was at least 20-fold lower than the rates in the upper sulfidic waters of the Gotland Deep, which were as high as 380 nmol L^{-1} d^{-1} (Figure 1.3).

1.3.2 Potential nitrification rates in Baltic Sea redox zones

Potential nitrification, as evidenced from the increase in ^{15}N-label in the NO_2^- and NO_3^- pools with time after $^{15}NH_4^+$ addition, was detectable on all sampling occasions at varying rates and within depth intervals of several meters. Maximal potential nitrification rates in the redox zones of the Gotland Deep (Figure 1.3) and Landsort Deep (Figure 1.4A) in 2011 and 2012 were in the range of 133–351 nmol L^{-1} d^{-1} (Table S1). In the Bornholm Deep, maximum rates of 189–884 nmol L^{-1} d^{-1} were measured within a narrow zone above the seafloor at 78 m depth (Table S1). In both the Gotland Deep and Landsort Deep, the zone of maximal nitrification was generally located below the nitrate peak and at oxygen concentrations below 10 µmol L^{-1}, coinciding with the nitrite peak (Figure 1.3 and Figure 1.4). Increasing potential rates of nitrification were accompanied by decreasing oxygen concentrations and a high abundance of GD2 Thaumarchaeota cells (Figure 1.6 and Figure A.2). For the combined data from the Gotland Deep, Landsort Deep and

Bornholm Deep, the relationship between potential nitrification rates and thaumarchaeotal abundance varied considerably but the correlation was positive and significant ($p < 0.002$, r^2=0.20, n=46) (Figure A.2). At Gotland Deep, July 2011, anammox activity was not detected in incubations from selected depths (114-124 m) as evidenced from the absence of significant $^{29}N_2$ accumulation over time (Figure A.3).

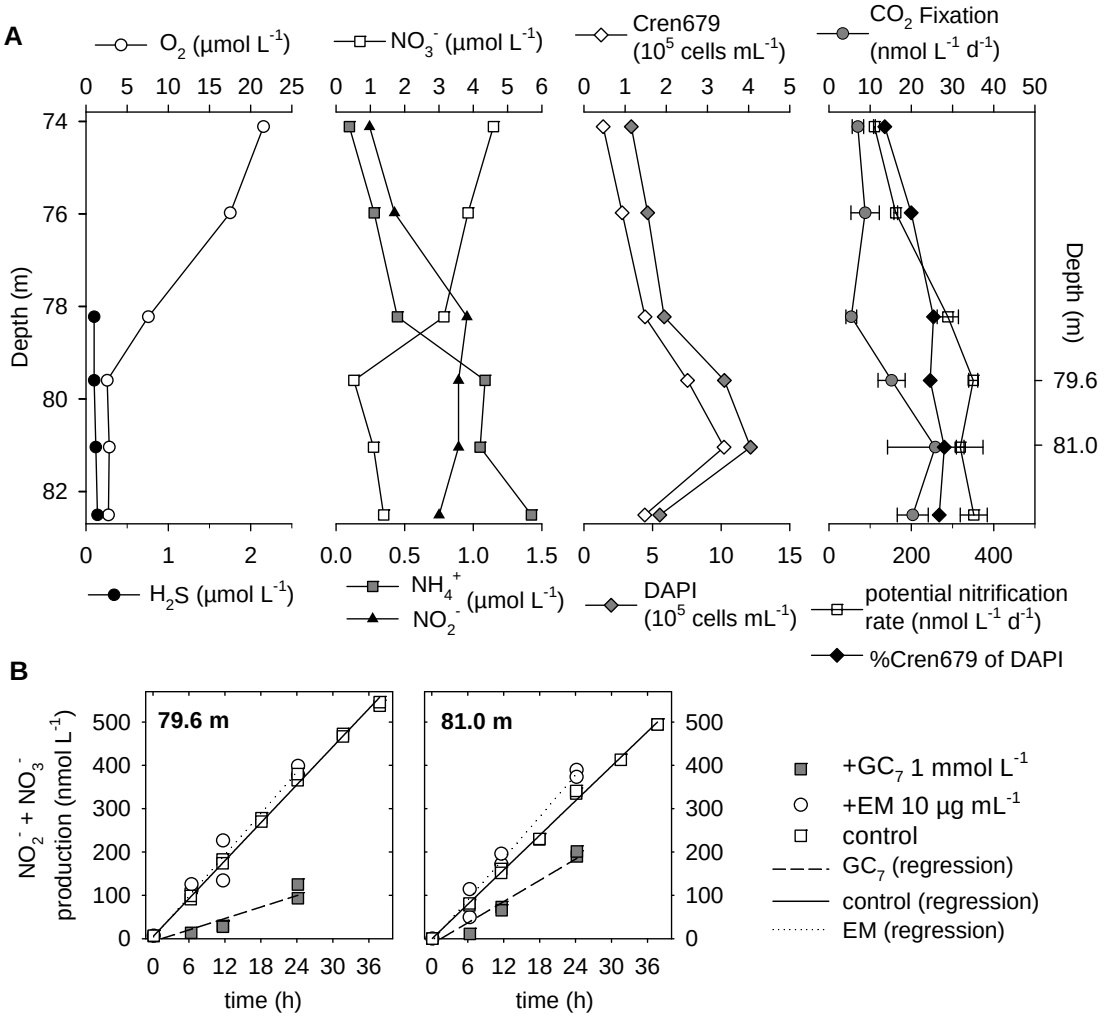

Figure 1.4.: (A) Profile within the hypoxic waters of the Landsort Deep redox gradient in June 2012. Error bars show the standard deviation of triplicate samples (CO_2 fixation rates) or the standard error of the slope of excess ^{29}N (potential nitrification rates). Water from 79.6 and 81 m was used to determine nitrification activity in the presence of specific inhibitors: (B) Time course of $NO_2^- + NO_3^-$ production from NH_4^+, taking into account both the ambient $^{14}NH_4^+$ and added $^{15}NH_4^+$ concentrations during nitrification. Measurements were made in untreated samples (control) and in the presence of archaeal (GC_7) and bacterial (Erythromycin, EM) inhibitors. Regression slopes of $NO_2^- + NO_3^-$ production of GC_7 treated samples differed significantly from the control at $p < 10^{-5}$ while those treated with EM were greater than the control at $p > 0.1$ (79.6 m) and $p > 0.01$ (81 m), respectively (one-way ANCOVA).

A potential nitrification rate of 62 nmol L^{-1} d^{-1} was also measured in samples taken from a moderately sulfidic depth (3 µmol H_2S L^{-1}, 124 m), at the Gotland Deep in July 2011 (Figure 1.3). In the hypoxic zone of the Gotland Deep in June 2012 (Figure 1.5A),

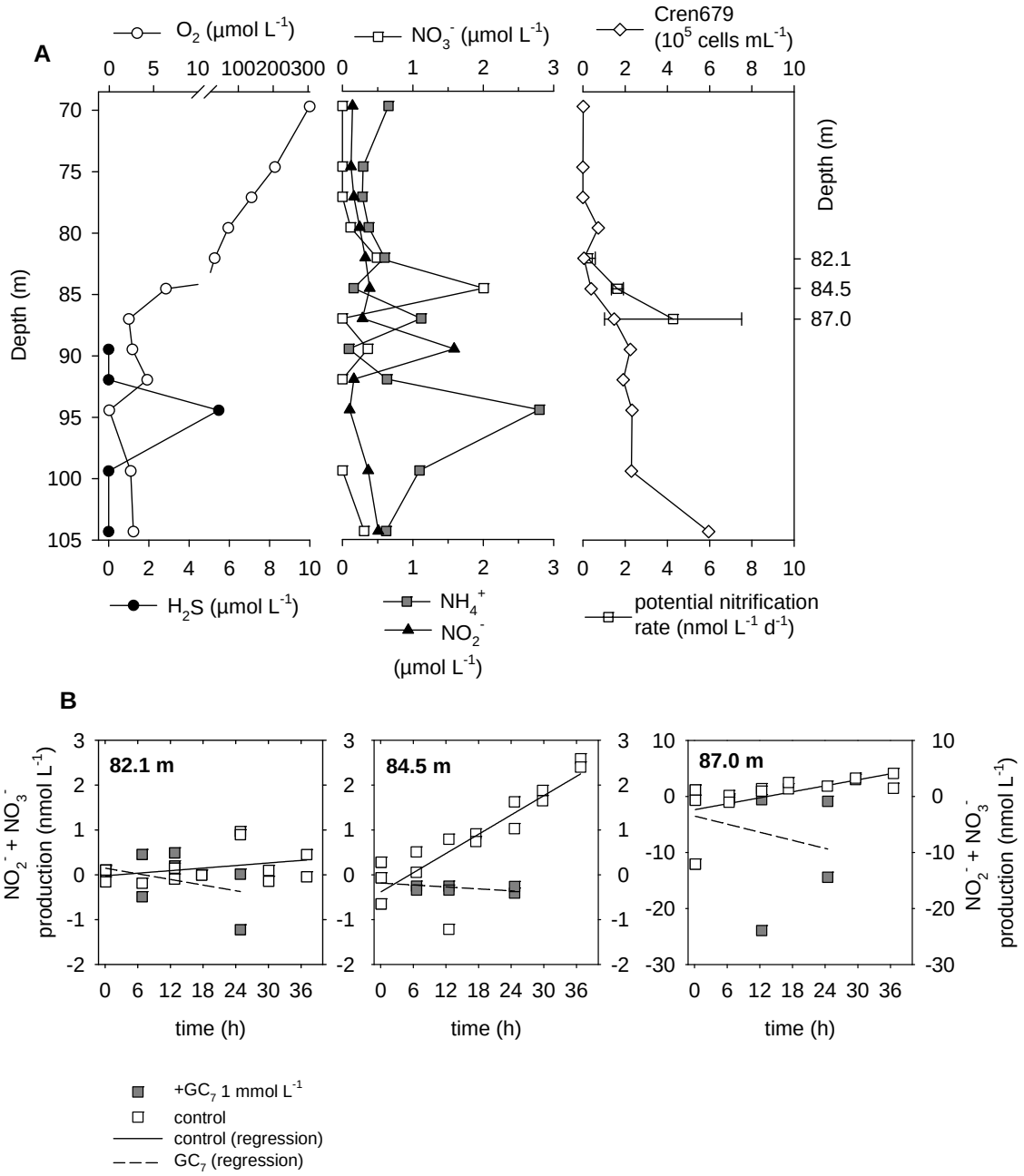

Figure 1.5.: (A) Physicochemical profile of the Gotland Deep hypoxic zone in June 2012 during a sulfidic intrusion. Error bars show the standard error of the slope of excess ^{29}N. Nitrification was measured at three depths above the intrusion and in the presence or absence of the archaeal inhibitor GC_7. (B) Time course of NO_2^- and NO_3^- production during nitrification at three depths in the Gotland Deep in 2012.

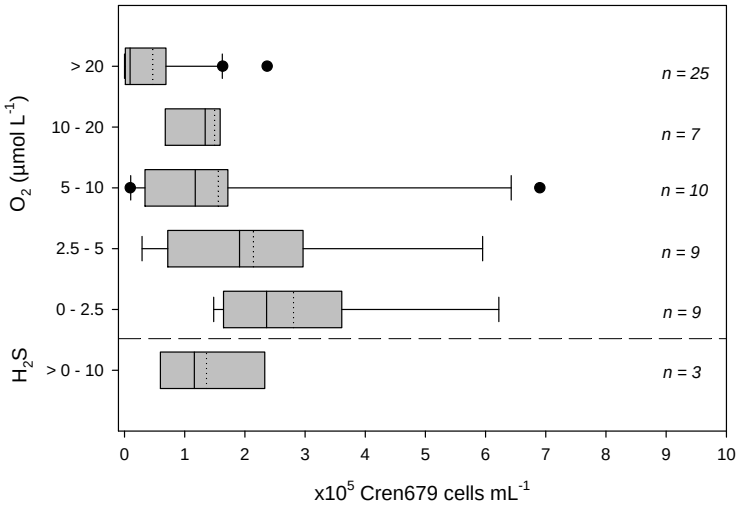

Figure 1.6.: Cell abundances of Cren679-probe hybridized Thaumarchaeota at different grouped oxygen and sulfidic conditions in the hypoxic zones of Gotland Deep, Landsort Deep and Bornholm Deep. Vertical solid lines: mean; vertical dotted lines: median.

potential nitrification rates of 0.2-4.3 nmol L^{-1} d^{-1} were measured in depths from 82-87 m, close to a narrow band of anoxic water enriched in H_2S and NH_4^+ at 94 m.

1.3.3 Impact of domain-specific inhibitors on nitrification activity

In samples from two depths of the Landsort Deep (79.6 and 81 m) collected in June 2012 and treated with the archaeal inhibitor GC_7, the potential nitrification rate was significantly reduced (one-way ANCOVA, $p < 10^{-5}$) compared to the untreated controls (Figure 1.4B). Nitrification was most strongly inhibited within the first 6 h (83–86%) at both depths, with the effect tailing off with longer incubation times. By contrast, nitrification activity in samples treated with the bacterial inhibitor erythromycin either did not decrease or increased slightly (one-way ANCOVA, $p < 0.2$ and $p < 0.02$, respectively) relative to the untreated controls. In water from the Gotland Deep in June 2012, when a sulfidic intrusion was observed and potential nitrification rates were substantially lower overall, the addition of GC_7 resulted in the complete elimination of nitrification (Figure 1.5B) as evidenced from negative regression slopes of NO_2^- + NO_3^- production significantly different from the untreated controls (one-way ANCOVA, 82.1 m: $p < 0.4$; 84.5 m: $p < 10^{-4}$; 87.0 m: $p < 0.05$).

1.3.4 Sulfide spiking experiment

Sulfide was added to water taken from the nitrification maximum (110 m depth) of the Gotland Deep in July 2011 (Figure 1.3) to examine its effect on nitrification. Between sulfide addition and the distribution of samples into the Exetainer vials sulfide losses were minimal (Figure A.4); nonetheless, over time sulfide concentrations decreased in both the bottles and the Exetainers (Figure A.4A vs. B). Nitrification was significantly inhibited (one-way ANOVA, $p < 10^{-5}$) by the addition of 4.1 µmol H_2S L^{-1} (Table 1.1). A higher concentration of H_2S (8.3 µmol H_2S L^{-1}) further decreased potential nitrification rates compared to the untreated control, and 16.6 µmol H_2S L^{-1} completely inactivated nitrification activity. Cell numbers of *Sulfurimonas* sp. subgroup GD17 increased by up to 25-fold during the incubations, especially in those with H_2S addition (Figure A.5), where also CO_2 fixation rates were higher than in the untreated control (Figure A.6).

Table 1.1.: Effect of H_2S addition on nitrification activity (nmol L^{-1} d^{-1}) in water taken from the Gotland Deep nitrification maximum. Values in parentheses are the percentage of activity remaining after H_2S-spiking relative to mean nitrification in the untreated control samples. Results from each of the duplicate incubations are shown. Nitrification was determined within 0–24, 24–48, and 48–72 hours after the addition of sulfide.

	0 (control)		4.1		8.3		16.6	
0-24 h	132	128	2 (1.5%)	15 (11.5%)	0	0	0	0
24-48 h	190	115	54 (35.4%)	13 (8.5%)	0	0	0	0
48-72 h	246	174	28 (13.3%)	24 (11.4%)	8 (3.8%)	0	0	0

1.4 Discussion

Our study shows that Thaumarchaeota are the main catalyzers of ammonia oxidation in Baltic Sea redox gradients as revealed by domain-specific inhibition experiments. This habitat, harbouring one dominating group of Thaumarchaeota (Labrenz *et al.*, 2010) is periodically exposed to sulfidic intrusions from subjacent waters into the nitrification zone. Addressing this ecological feature via a sulfide-spiking experiment, we found that nitrification persisted after sulfide pulses of *in situ*-like concentrations suggesting a tolerance against sulfide by AOA assemblages in the Baltic Deeps.

1.4.1 Nitrification activity, CO_2 fixation, and the distribution of Thaumarchaeota

In hypoxic areas of the Baltic's deep basins, nitrification was detected at varying rates during several seasons, covering more than one year. Low-oxygen waters above the onset of sulfide consistently hosted maximal thaumarchaeotal abundances (Figure 1.6), showing that AOA are a stable component of Baltic Sea redox gradients as presumed by Labrenz *et al.* (2010). The highest potential nitrification rates (max. 884 nmol L^{-1} d^{-1}) along with abundant Thaumarchaeota (4.3×10^5 cells mL^{-1}) were detected at Bornholm Deep in Nov 2011. This site showed an ammonium gradient with concentrations higher than those detected in the other deeps. In general, our data confirm the temporal and spatial variability in potential nitrification rates reported by Hietanen *et al.* (2012) but also underline the persistence of nitrification in the Baltic Sea over time. Anaerobic oxidation of ammonium (anammox), however, was not detected in selected depths of the Gotland Deep (Figure A.3), which is in accordance to detectable anammox activity only after the inflow of oxygen-rich water into the Baltic Sea (Hannig *et al.*, 2007). Thus, ammonia oxidation occurred probably mostly aerobically in Baltic Sea redox gradients.

The abundance of marine group I Thaumarchaeota in the Black Sea hypoxic zone is one order of magnitude lower, at 4.3×10^4 cells mL^{-1} (Lam *et al.*, 2007), than in the Baltic Sea, concurrent with the lower nitrification rates of 5–50 nmol L^{-1} d^{-1} (Ward and Kilpatrick, 1991) although potential nitrification rates – as in our study – may be higher than the actual *in situ* nitrification rates (Horak *et al.*, 2013). Similarly, in the Cariaco Basin, Thaumarchaeota comprise maximally 9% (Cren537 probe) (Lin *et al.*, 2006) to 13% (Cren679 probe, max. 1.5×10^4 cells mL^{-1}; Gordon Taylor, personal communication) of the total cell counts but also prevail around the redox transition zone. These comparisons show that pelagic Baltic redox gradients offer particularly favourable conditions for both high nitrification activities and high AOA abundances. Apparently, AOA are the best-adapted ammonia oxidizers to the predominant sulfidic conditions in this system, since anammox occurs only during sulfide-free periods (Hannig *et al.*, 2007) and AOB may be more susceptible to sulfide (Joye and Hollibaugh, 1995), making AOA the main utilizers of ammonium. In contrast, in the Black Sea, anammox bacteria obtain nitrite from aerobic ammonia oxidizers and compete with them for ammonium (Lam *et al.*, 2007), whereas in Baltic redox gradients ammonium may exclusively be used by AOA to produce the nitrite, which subsequently fuels autotrophic denitrification. The dominance and high cell

numbers of AOA in the Baltic Sea basins might be caused by the close proximity of the nitrification zone to sulfidic waters.

The energy provided by aerobic ammonia oxidation serves to carry out CO_2 fixation for growth in autotrophic Thaumarchaeota. In our measurements, potential nitrification rates usually were one order of magnitude higher than the corresponding CO_2 fixation activities. This is in line with the 10:1 ratio of N oxidized per C incorporated reported for nitrifiers (Tijhuis *et al.*, 1993; Middelburg, 2011) and suggests that CO_2 fixation in Baltic Sea hypoxic zones is coupled mainly to nitrification by AOA. In general, the rates of CO_2 dark fixation in hypoxic waters were notably lower than those in the upper sulfidic zone, a difference attributed to the activity in the latter of high numbers of chemoautotrophic denitrifiers of the *Sulfurimonas* sp. subgroup GD17 (Grote *et al.*, 2007, 2008; Jost *et al.*, 2008).

1.4.2 Thaumarchaeota contribute substantially to nitrification

Our archaea-specific inhibition experiments provide evidence of the major contributions of archaea to nitrification. The Landsort Deep exhibited high potential nitrification rates, which were inhibited up to 83–86% by GC_7 (Figure 1.4); at the Gotland Deep, nitrification rates were comparably low and completely inhibited by the archaea-specific inhibitor (Figure 1.5). The different inhibition levels at the two sites may be due to their different hydrological histories: Landsort Deep showed a stable stratification while at Gotland Deep, a sulfidic intrusion (Figure 1.5) may have impaired activities of ammonia oxidizers prior to sampling, resulting in low potential nitrification rates, and cells being more susceptible to the biosynthesis inhibitor GC_7. Additionally, the tailing off of inhibition by GC_7 at Landsort Deep may relate to the degradation of the inhibitor by amine oxidases (Park *et al.*, 1994), such that inhibition was reversible (Jansson *et al.*, 2000), or by the recovery of incompletely inhibited cells.

Taken together, inhibition of archaeal nitrification by GC_7 and the correlation between thaumarchaeotal abundance and nitrification activity in Baltic Sea depth profiles provide complementary evidence that archaea are the main mediators of ammonium oxidation in these waters. Given the low diversity of the archaeal community (Labrenz *et al.*, 2010), the determined ammonia oxidation activities likely rely on only one well-adapted dominant subcluster, related to *Ca.* N. maritimus.

1.4.3 Impact of sulfide on ammonia-oxidizing Thaumarchaeota

Episodic sulfidic plumes have previously been recognized to occur in OMZs, for example, off Peru (Schunck *et al.*, 2013) and the Namibian Shelf (Lavik *et al.*, 2009). In Baltic Sea redox gradients, periodic intrusions of different water layers result in the juxtapositioning of sulfidic, anoxic, and low-oxygen waters that undergo temporal changes (Hannig *et al.*, 2007; Bruckner *et al.*, 2013). The sulfidic part of the redox gradient does not permit oxygen-driven ammonia oxidation and, correspondingly, *amoA* expression is minimal here (Labrenz *et al.*, 2010). Instead, at these depths Thaumarchaeota may reside inactive. Notably, the detected nitrification potential, likely due to small oxygen additions during sampling (De Brabandere *et al.*, 2012), of 62 nmol L^{-1} d^{-1} at a sulfidic depth (Figure 1.3) suggests that AOA persist during sulfidic conditions and quickly become active as soon as oxygen is again available. Hietanen *et al.* (2012) pointed out that a nitrification potential might extend into deeper layers, even into the sulfidic waters. Physiological adaptations, e.g., in cell membrane composition, may enable Thaumarchaeota to tolerate the sulfide pulses encountered in the nitrification zone or sulfide accumulation in these waters. This would enable sulfide tolerant Thaumarchaeota to persist also in sulfidic waters and carry out ammonia oxidation after ventilation of sulfidic deep waters caused by major inflow events, thereby sustaining an ecologically important N-cycle function under dynamic conditions.

In line with that, our sulfide spiking experiment showed that nitrification activities in Baltic Sea redox gradients, dominated by Thaumarchaeota, are not completely terminated at *in-situ*-like concentrations of hydrogen sulfide (Table 1.1), consistent with the observation from water-column profiles that nitrification is still active at low sulfide concentrations (<4 µmol L^{-1}) (Table S1 and Hietanen *et al.*, 2012). Recovery of nitrification after spiking with time was indicated (Table 1.1) but longer time-intervals between sulfide spike and nitrification measurement may show a significant recovery. Added sulfide persisted up to 24h (Figure A.4) impairing microbial activities directly at addition, and then declined during the incubation, most likely as a result of biotic oxidation by denitrifiers (Grote *et al.*, 2008), rather than chemical. Sulfide-oxidizing chemolithoautotrophic denitrifiers of the *Sulfurimonas* sp. subgroup GD17 comprise stable (Labrenz *et al.*, 2007; Grote *et al.*, 2007) and active (Grote *et al.*, 2008; Glaubitz *et al.*, 2009) populations in Baltic Sea redox gradients and were stimulated during the incubation as indicated by their strongly increased cell numbers (Figure A.5) and elevated CO_2 fixation activities (Figure A.6). Thus,

potential consumption of $^{15}NO_2^-$ or $^{15}NO_3^-$ produced by nitrification may even have led to underestimated or undetectable nitrification at higher sulfide concentrations. Presuming stoichiometry of chemolithoautotrophic denitrification by *Sulfurimonas gotlandica* str. GD1 as calculated by Bruckner *et al.* (2013), added sulfide would have been sufficient to denitrify the NO_3^- pool. Given the impairment of sulfide pulses on nitrification activity, the supply of oxidized nitrogen in redox gradients by nitrification is also indirectly suppressed by intermittent sulfidic water masses being toxic to nitrifiers.

On the ecosystem level, our findings emphasize the effect of sulfide on nitrifiers in regulating nitrogen budgets in the Baltic Sea and they are in line with those of Joye and Hollibaugh (1995), who showed that the inhibition of nitrification in sediments by sulfide limits nitrogen loss processes. Different histories, i.e., lateral intrusions vs. small-scale vertical mixing with sulfidic waters, may therefore explain the varying nitrification rates reported in this and previous (Hietanen *et al.*, 2012) studies. For example, at the Bornholm Deep, sulfidic conditions occur less frequently such that nitrification is more stable, proceeding at higher rates and fostering high AOA abundance. Moreover, the portion of Thaumarchaeota residing in sulfidic waters provides a high potential for nitrification upon oxygenation and may therefore represent a stable and important component within the N cycle in the Baltic Sea, particularly in the light of the dynamic perturbations and lateral intrusions that characterize these waters.

Future studies may investigate how nitrification is potentially initiated in sulfidic water after oxygen spikes or ventilation. Sulfidic pulses may act as a "switch" by pausing nitrification and stimulating denitrification – after reoxygenation, nitrification may quickly re-start again. Such process-fluctuations and the coupling between nitrification and denitrification could be a major force that drives the N-removal in the Baltic and may represent an intriguing mechanism involved in ecosystem functioning. It is furthermore worthwhile to study whether Thaumarchaeota in other oxygen-depleted systems respond similarly to sulfidic mixing. The role of Thaumarchaeota in sulfidic habitats is not extensively clarified at present and asks for elucidation of the physiological mechanisms that allow for tolerance of these conditions.

1.5 Conclusions

Nitrification in Baltic Sea redox gradients was detected as a persistent process together with the presence of Thaumarchaeota. The correlation between potential nitrification rates and thaumarchaeotal abundance and the results of our inhibition experiments support the conclusion that AOA are the main drivers of this process. In a sulfide-spiking experiment with environmental samples, nitrification proved to be robust against lower *in-situ*-like sulfide concentrations, as would occur upon mixing with sulfidic waters. Our study emphasizes the role of Thaumarchaeota for N cycling in the Baltic Sea and shows that the supply of oxidized N compounds from aerobic ammonium oxidation is mainly dependent on Thaumarchaeota, which in the Baltic Sea are represented by one abundant phylogenetic group. Our results suggest that the dominance and high abundance of AOA in this ecosystem results from a tolerance of the cells to periodic exposures to sulfidic waters and the close proximity of the nitrification zone to sulfidic water layers. It appears worthwhile to examine whether this robustness of archaeal nitrification against sulfide can also be detected among other globally distributed AOA or if it is an exclusive feature of the Baltic Sea thaumarchaeotal assemblages.

1.6 Acknowledgments

This study was financed by the German Science Foundation (DFG) and European Science Foundation (ESF) within the EuroEEFG program and the project Microbial Oceanography of ChemolithoAutotrophic planktonic Communities (MOCA) (JU 367/12-1). BT acknowledges support from the Danish Research Council for Independent Research and the Danish National Research Foundation (DNRF53). Katja Becker, Ines Bartl, Anna Hagenmeier, and Sabine Glaubitz are thanked for their technical assistance during sampling. We thank Luisa Listmann for assistance with enrichment cultures, Carolin Löscher for sharing details on GC_7, and Bernd Schneider and Hildegard Kubsch for DIC measurements. Thanks also to Günter Jost, Maren Voß, and Claudia Frey for sharing methods, and to Phyllis Lam and Jessika Füssel, from the Max Planck Institute for Marine Microbiology, for method details in nitrification rate measurements. We thank four anonymous reviewers for their critical comments, which significantly improved the manuscript. The professional support of the chief scientists Klaus Nagel and Christian Stolle and of the cap-

tains, crews, and scientific teams of the research vessels *Alkor*, *Elisabeth-Mann-Borgese*, and *Meteor* is highly appreciated.

Chapter two

Chemoautotrophic growth of ammonia-oxidizing Thaumarchaeota enriched from hypoxic waters of the Baltic Sea

2

CHEMOAUTOTROPHIC GROWTH OF AMMONIA-OXIDIZING THAUMARCHAEOTA ENRICHED FROM HYPOXIC WATERS OF THE BALTIC SEA

Abstract

Ammonia-oxidizing archaea (AOA) are an important component of the planktonic community in aquatic habitats, linking nitrogen and carbon cycles through nitrification and carbon fixation. However, determinations of CO_2 fixation in relation to ammonia oxidation for AOA are limited. In this study, by enriching AOA from a brackish, oxygen-depleted water-column in the Landsort Deep, central Baltic Sea, we were able to investigate ammonium oxidation, chemoautotrophy, and growth in seawater batch experiments. The highly enriched culture consisted of up to 97% archaea, with maximal archaeal numbers of 2.9 × 10^7 cells mL^{-1}. Phylogenetic analysis of the 16S rRNA and ammonia monooxygenase subunit A (*amoA*) gene sequences revealed an affiliation with assemblages from low-salinity and freshwater habitats, with *Candidatus* Nitrosoarchaeum limnia as the closest relative. Growth correlated significantly with nitrite production, ammonium consumption, and CO_2 fixation, which occurred at a ratio of 10 atoms N oxidized per 1 atom C fixed. According to the carbon balance, AOA biomass production can be entirely explained by chemoautotrophy. The cellular carbon content was estimated to be 9 fg C per cell. Single-cell-based ^{13}C and ^{15}N labeling experiments and analysis by nano-scale secondary ion mass spectrometry provided further evidence that cellular carbon was derived from bicarbonate and that ammonium was taken up by the cells. Our study therefore revealed that growth by AOA belonging to the genus *Nitrosoarchaeum* can be sustained largely by chemoautotrophy.

2.1 Introduction

The aerobic oxidation of ammonia (NH_3) or ammonium (NH_4^+) to nitrite (NO_2^-) is an essential step in the cycling of nitrogen and was long assumed to be performed exclusively

by distinct members of Bacteria. This paradigm changed (Francis *et al.*, 2007; Lam *et al.*, 2009) following the discovery of the ammonia monooxygenase subunit A (*amoA*) gene among Archaea (Venter *et al.*, 2004; Treusch *et al.*, 2005) and the subsequent isolation of the first marine representative of the ammonia-oxidizing archaea (AOA), *Candidatus* Nitrosopumilus maritimus (Könneke *et al.*, 2005). Molecular surveys inferring the presence of AOA via the detection of *amoA* recognized their global prevalence in many marine habitats (e.g., Francis *et al.*, 2005). All known archaea possessing the *amoA* gene affiliate within the novel phylum *Thaumarchaeota* (Brochier-Armanet *et al.*, 2008; Spang *et al.*, 2010), formerly assigned to the *Crenarchaeota*. The global distribution and high abundances of AOA (Francis *et al.*, 2005) point to their major impact on biogeochemical cycles. Cell-specific balances of carbon utilization and ammonia oxidation allow estimates of overall fluxes in specific ecosystems. In field studies, a correlation was determined between archaeal *amoA* transcripts and the occurrence of Thaumarchaeota (Caffrey *et al.*, 2007; Beman *et al.*, 2008), while nitrification rate measurements with specific inhibitors (Berg *et al.*, in press) further underlined the environmental significance of AOA.

As deduced from the growth conditions of isolates (Könneke *et al.*, 2005; Tourna *et al.*, 2011), culture enrichments (e.g. Hatzenpichler *et al.*, 2008; Santoro and Casciotti, 2011; Jung *et al.*, 2011; Matsutani *et al.*, 2011; French *et al.*, 2012; Lebedeva *et al.*, 2013), and the gene sets detected in AOA genomes (e.g. Hallam *et al.*, 2006*a*,*b*; Walker *et al.*, 2010; Blainey *et al.*, 2011; Spang *et al.*, 2012), in these Thaumarchaeota ammonia oxidation serves to conserve energy and the fixation of inorganic carbon to generate biomass. Yet, variations have also been described, such as the utilization of urea (Hallam *et al.*, 2006*a*,*b*; Alonso-Sáez *et al.*, 2012) or the absence of ammonia oxidation despite the expression of *amoA* (Mußmann *et al.*, 2011). Additionally, autotrophy as the sole carbon source for growth has been debated for AOA. In a study of wastewater treatment plants, there was no evidence of CO_2 fixation by AOA, despite their abundance and signs of their active growth (Mußmann *et al.*, 2011). Furthermore, the utilization of organic carbon by *Thaumarchaeaota* in marine *in situ* assemblages (Teira *et al.*, 2006) and by AOA isolates was reported. For example, the growth of *Nitrososphaera viennensis* was substantially enhanced when pyruvate was provided as an additional organic carbon source (Tourna *et al.*, 2011; Stieglmeier *et al.*, 2014), and two recent isolates related to *Ca.* N. maritimus showed obligate mixotrophy, since their growth depended on the assimilation of organic carbon compounds (Qin *et al.*, 2014). Due to their chemolithoautotrophic lifestyle, in many ecosystems AOA are part of the organismal backbone involved in element transformations. Studies of the genomes of *Ca.* Nitrosopumilus maritimus, *Nitrososphaera*

viennensis, and *Ca.* Nitrosoarchaeum limnia, revealed carbon fixation via a modified 3-hydroxypropionate/4-hydroxybutyrate cycle (3-HP/4-HB) (Berg *et al.*, 2007; Walker *et al.*, 2010; Blainey *et al.*, 2011; Tourna *et al.*, 2011). The use of this very cost-effective CO_2 fixation pathway (Könneke *et al.*, 2014) by AOA distinguishes them from autotrophic ammonia-oxidizing bacteria, which use the Calvin-Benson-Basham cycle (e.g., Chain *et al.*, 2003; Klotz *et al.*, 2006). AOA capable of using the 3-HP/4-HB-cycle may also metabolize small organic substrates, as suggested by Hatzenpichler (2012). Despite the fact that most enriched or isolated Thaumarchaeota grow chemoautotrophically on inorganic media, the relationship between ammonia oxidation and chemoautotrophy has not been studied. Direct measurements of CO_2 fixation by AOA are scarce and the fraction of AOA that live autotrophically is unknown for most environments. Besides three previously reported marine AOA isolates (Könneke *et al.*, 2005; Qin *et al.*, 2014), AOA enrichment cultures from various sources have been established and investigated, e.g., from freshwater (French *et al.*, 2012), estuarine sediments (Mosier *et al.*, 2012), the ocean (Wuchter *et al.*, 2006; Santoro and Casciotti, 2011), agricultural soil (Jung *et al.*, 2011), and thermal habitats (Hatzenpichler *et al.*, 2008), among others. These studies have contributed new details on the physiology, niche partitioning, and biogeochemistry of Thaumarchaeota. Because data on specific biogeochemical activities of AOA in natural environments are difficult to acquire, activity-based experiments with AOA enrichment cultures offer a suitable alternative approach.

In oxygen-depleted waters of the Baltic Sea, Thaumarchaeota account for up to one third of the total cell counts and thus constitute a substantial fraction of the microbial community (Labrenz *et al.*, 2010; Berg *et al.*, in press). At the overlap of oxygen and ammonium gradients, AOA are the main catalyzers of ammonia oxidation (Berg *et al.*, in press). Moreover, they supply oxidized N for denitrification, a relevant N-loss process in the Baltic Sea nitrogen cycle, that is carried out in pelagic redox gradients mainly by chemoautotrophic epsilonproteobacteria (Grote *et al.*, 2012).

In this study, we investigated the balances of chemoautotrophy and ammonium oxidation in an AOA enrichment culture obtained from the Landsort Deep redox gradient, central Baltic Sea. Our findings provide insights into the coupling between ammonium oxidation and carbon fixation in this enrichment and therefore on the relevance of chemoautotrophy for the generation of biomass by AOA. In addition, by determining the carbon balance for a member of the genus *Nitrosoarchaeum* we shed light on the role played by AOA in both primary production and nitrification in aquatic ecosystems.

2.2 Material and Methods

2.2.1 Retrieval of environmental samples, enrichment and cultivation

Water from the Baltic Sea Landsort Deep station TF284 (58 35.0183N, 018 14.0795E) was retrieved onboard the *R/V Heincke* in November 2010. Samples were taken from the pelagic redox gradient, where a high abundance of Thaumarchaeota can be expected (Labrenz *et al.*, 2010; Berg *et al.*, in press). After sampling and thereafter, the water was kept under oxic conditions and in the dark; 1 mmol NH_4Cl L^{-1} and 50 mg streptomycin L^{-1} were added. The sample bottles were stored at room temperature with headspace and occasionally screened for NO_2^- production according to the method described by Grasshoff *et al.* (1983). To select for the typically small thaumarchaeotal cells (diameter <0.22 µm, Könneke *et al.*, 2005; Labrenz *et al.*, 2010), water from nitrite-positive bottles was filtered through 0.45-µm syringe filters and the filtrate further incubated. Enrichments with continuous NO_2^- production and increased archaeal cell numbers were inoculated into 0.1-µm filtered seawater collected from Baltic Sea redox gradients and supplemented with NH_4Cl and streptomycin, as described above, to further promote the growth of AOA. After approximately 1.5 years, with occasional transfers of 10–15% of the volume into 0.1-µm filtered seawater, archaea numerically dominated the enrichments. A batch growth experiment was carried out at 22 °C in the dark, during which growth was monitored along with chemoautotrophy and ammonium oxidation. Concentrations of ammonium and nitrite were determined after the method of Grasshoff *et al.* (1983). Ammonium was measured directly after sampling; nitrite samples were filtered through 0.2-µm filters and stored at -20 °C until analysis. All batch cultures were inoculated from the same initial enrichment.

2.2.2 Cell quantification

Depending on the cell density, 0.1-4 mL subsamples of the enrichment cultures were fixed for 2–6 h with particle-free formaldehyde (2% final concentration) and subsequently filtered on 0.2-µm polycarbonate filters (Whatman, 25 mm diameter). Archaeal or bacterial cells on the filter slices were specifically hybridized via catalyzed reporter deposition fluorescence *in situ* hybridization (CARD-FISH) according to Pernthaler *et al.*

(2002), using either the Arc915 probe targeting archaea (Stahl and Amann, 1991) or the EUB338/EUB338II-III probe mix targeting bacteria (Amann *et al.*, 1990; Daims *et al.*, 1999). Cells on the hybridized filters were counter-stained with 4',6-diamidino-2-phenylindol (DAPI) in Vectashield mounting medium (Vector Labs, California, USA). Ten microscopic fields were randomly selected and DAPI-stained and specifically hybridized cells were then counted using a Zeiss Axioskop 2 mot plus (Zeiss, Oberkochen, Germany) epifluorescence microscope. For three of the enrichment cultures (A, B, and C), the filters were prepared and analyzed in triplicate; cells that were hybridized during CARD-FISH were counted on slices from one filter.

2.2.3 CO_2 fixation rates

Subsamples of 2–4 mL were taken from the batch cultures and incubated in triplicate together with a killed control (fixed with 2% formaldehyde) for 6–24 h after the addition of 0.56–1.85 MBq of $NaH^{14}CO_3$ (Hartmann Analytic GmbH, Germany), depending on the cell density. The incubations were stopped by filtration onto 0.2-µm polycarbonate (Whatman, 25 mm diameter) filters. Prior to filtration, 50 µL were withdrawn to determine the total radioactivity added to each vial. The filters were exposed to HCl fumes for 0.5–2 h and then transferred into 4 mL of LumaSafe scintillation cocktail (PerkinElmer). Total- and filter-^{14}C disintegrations per minute were analyzed with a PerkinElmer Tri-Carb 2800R liquid scintillation analyzer. CO_2 fixation rates were derived from the fraction of ^{14}C incorporated in relation to the total activity added and taking into account the dissolved inorganic carbon concentration of 2 mmol L^{-1} that is characteristic of Baltic Sea redox gradients (Grote *et al.*, 2008; Berg *et al.*, in press). CO_2 fixation rates were calculated as follows:

$$CO_2\ fixation = \frac{\frac{dpm_f - dpm_d}{dpm_l} \times DIC}{t} \tag{2.1}$$

where t is the incubation time; dpm_f, the filter disintegrations per minute; dpm_d, the dpm counts on filters of the dead control; dpm, the dpm counts in the liquid sample; and DIC, the ambient concentration of dissolved inorganic carbon.

Mean CO_2 fixation rates and the increase in cell numbers during the exponential growth phase (from t_1 to t_2) between days 19 and 32 (enrichments A, B, and C) and days

32 and 54 (enrichment E) were considered in calculating the carbon content of one cell as follows:

$$C_{content} = \frac{\frac{[\mathrm{CO_2}\text{ fixation rate}]_{t_2} + [\mathrm{CO_2}\text{ fixation rate}]_{t_1}}{2} \times (t_2 - t_1)}{[\text{cells mL}^{-1}]_{t_2} - [\text{cells mL}^{-1}]_{t_1}} \tag{2.2}$$

To determine the accumulated amount of fixed CO_2, the fixation rates were multiplied by the number of days until the next CO_2 fixation rate measurement. These intervals were then cumulatively added for the specific time points of the CO_2 fixation rate measurements. A correlation was tested by linear bivariate regression using the PAST software package v3.0 (Hammer *et al.*, 2001).

2.2.4 Uptake of ^{13}C-bicarbonate and ^{15}N-ammonium and NanoSIMS imaging

Enrichment culture G was amended with 2 mmol of additional $NaH^{13}CO_3$ L^{-1} (99% ^{13}C, Cambridge Isotope Laboratories, Massachusetts, USA) directly after inoculation; 58 µmol of $^{15}NH_4Cl$ L^{-1} (99% ^{15}N, Cambridge Isotope Laboratories, Massachusetts, USA) was added during the exponential growth phase (on day 40). During the following 24 h, the conversion of labeled $^{15}NH_4Cl$ to $^{15}NO_2^-$ was determined using gas chromatographic isotopic ratio mass spectrometry (GC-IRMS). Duplicate samples were taken from the enrichment culture over a 24-h period and frozen at -20 °C to stop the reaction. The samples were prepared and analyzed according to Holtappels *et al.* (2011) and Füssel *et al.* (2011) and as described in Berg *et al.* (in press).

For single-cell analysis by nano-scale secondary ion mass spectrometry (NanoSIMS) (e.g. Musat *et al.*, 2011), samples from the enrichment were taken at several time points and processed using the same procedure described for CARD-FISH except that they were filtered onto prepared gold-coated 0.2-µm polycarbonate filters. The filter surface was gold-sputter-coated with an Agar sputter coater (model 108) for 120 s, resulting in a 20- to 40-nm thin layer of gold. Incorporation of the label into single cells was assessed using a Cameca NanoSIMS 50L, by measuring the secondary ions emitted in response to sputtering selected areas of the filter surface by a Cs^+ primary ion beam. The primary ion beam current was 2 pA, with scanning parameters of 256 × 256 pixels for areas of 20 × 20 to 30 × 30 µm, with a dwell time of 1 µs per pixel. The mass resolving power was adjusted to suppress interferences at all masses. Data of the secondary ion counts were analyzed

using the MATLAB R2011b (The MathWorks, USA) based Look@NanoSIMS software (Polerecky *et al.*, 2012). Thus, 30–60 planes were aligned and included in the analysis; regions of interest were defined using the biomass signal based on the $^{12}C^{14}N$ counts. Ratios of $^{13}C/^{12}C$ were derived from the secondary ion counts of $^{13}C^-$ and $^{12}C^-$, respectively, to determine ^{13}C enrichment. Cellular ^{15}N uptake was determined by calculating the ratio $^{15}N^{12}C/^{14}N^{12}C$.

2.2.5 DNA-extraction and phylogenetic analysis of the 16S rRNA and *amoA* genes

Samples were taken on day 54, i.e., during the late exponential phase, from enrichment cultures D–G and filtered on 0.2-µm GVWP filters (Millipore). DNA was extracted as described in Weinbauer *et al.* (2002). DNA of the nearly full-length 16S rRNA gene was PCR-amplified using the Fermentas *taq* polymerase and the primer pairs Arch21f/1492r (Lane, 1991; DeLong, 1992) for *Archaea* and 27f/1492r (Lane, 1991) for *Bacteria*. The archaeal *amoA* primer pairs were Arch-amoAF/Arch-amoAR (Francis *et al.*, 2005); the beta- and gammaproteobacterial *amoA* primers were amoA-1F/2R and amoA-3F/4R, respectively (Purkhold *et al.*, 2000). PCR products were purified using the Agencourt AMPure kit XP (Beckman Coulter, Krefeld, Germany) according to the manufacturer's instructions. Both the 16S rRNA and the *amoA* gene amplicons were cloned with the StrataClone PCR cloning kit (Agilent, Karlsruhe, Germany) as described by the manufacturer and sequenced by LGC Genomics (Berlin, Germany). The sequences were quality-revised with DNAStar SeqMan II v5.06 and forward and reverse sequences were assembled into a contig. Chimeric sequences were detected using DECIPHER (Wright *et al.*, 2012*a*). Phylogenetic analysis was conducted using the ARB 5.1 software package (Ludwig *et al.*, 2004). The 16S rRNA gene sequences were aligned with the online SILVA incremental aligner (SINA) v1.2.11 (Pruesse *et al.*, 2012), then imported into ARB and inspected for alignment errors. Translated *amoA* protein sequences were aligned using the *amoA* ARB database provided by Pester *et al.* (2012). The 16S rRNA phylogenetic tree was constructed with the Phylip neighbor-joining algorithm, Jukes-Cantor correction, and using the ssuref:archaea filter provided in the SILVA SSU Ref NR 99 ARB database (Quast *et al.*, 2013). The *amoA* neighbor-joining tree was generated based on the protein alignment, using Phylip with a Fitch model and *Ca.* N. maritimus SCM1 as a filter. The *amoA* and 16S rRNA gene se-

quences were deposited in the European Nucleotide Archive under the accession numbers LN590601–LN590650 and LN590651–LN590669, respectively.

2.3 Results

2.3.1 Enrichment of ammonia-oxidizing archaea

Samples obtained from oxygen-depleted waters of the Baltic Sea and incubated for 1.5 years under conditions promoting the growth of AOA yielded highly enriched cultures (Figure 2.1). AOA enrichment was evident from nitrite production, the consumption of ammonium, and the concurrent increase in archaeal cell numbers (Figure 2.2). CARD-FISH for archaea revealed that cells similar in size and morphology to *Ca.* N. maritimus (Könneke *et al.*, 2005; Figure 2.1) dominated the cultures.

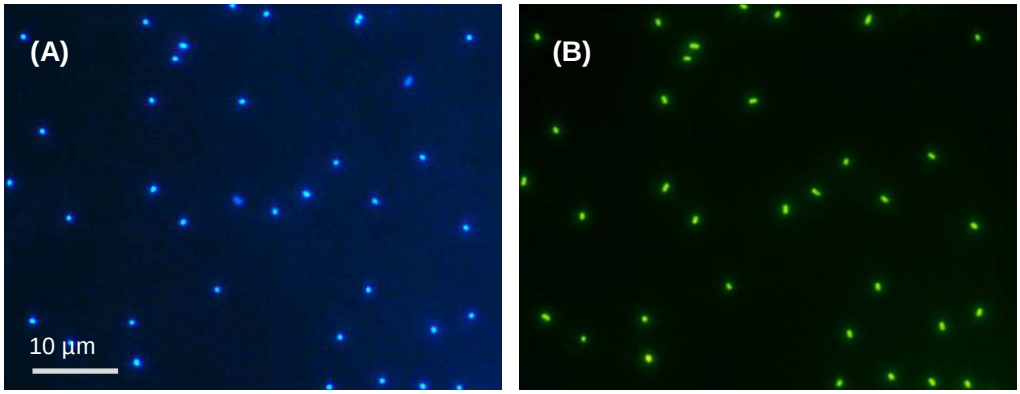

Figure 2.1.: Epifluorescence microscopy of representative cells from enrichment culture B on day 1. The cells were stained with DAPI (A) or hybridized with the archaea-specific probe Arc915 (B) and then analyzed by CARD-FISH. Same field of view; the scale bar represents 10 µm.

In a batch growth experiment (cultures A, B, and C), total cell numbers during exponential growth reached a maximum of 3.1×10^7 cells mL^{-1}, with archaeal cells comprising 93–97%, as determined by CARD-FISH (Figure 2.2), and bacterial cells, identified with the probes EUB338I-III, 5–10%. After a lag phase of 19 days, the archaeal cells grew exponentially, with a generation time of 4.5 days (Table 2.1). Ammonium consumption during exponential growth accounted for an oxidation rate of 12.81 ± 0.80 µmol NH_4^+ L^{-1} d^{-1} and was accompanied by increasing archaeal cell numbers and the accumulation of up to 231 ± 18.1 µmol nitrite L^{-1}. Culture G had similar properties but a longer generation time (Table 2.1): total cell numbers reached 5.2×10^7 cells mL^{-1}, up to 448 µmol

nitrite L^{-1} accumulated, and ammonium was completely consumed at a rate of 11.55 µmol NH_4^+ L^{-1} d^{-1}, comparable to that by cultures A–C (Figure 2.3). Enrichment cultures D and F (Figure A.8) grew more slowly and less continuously, reaching maximum total cell abundances of 1.5×10^7 cells mL^{-1}. The growth of enrichment culture E (Figure A.8) was similar to that of cultures A–C and G.

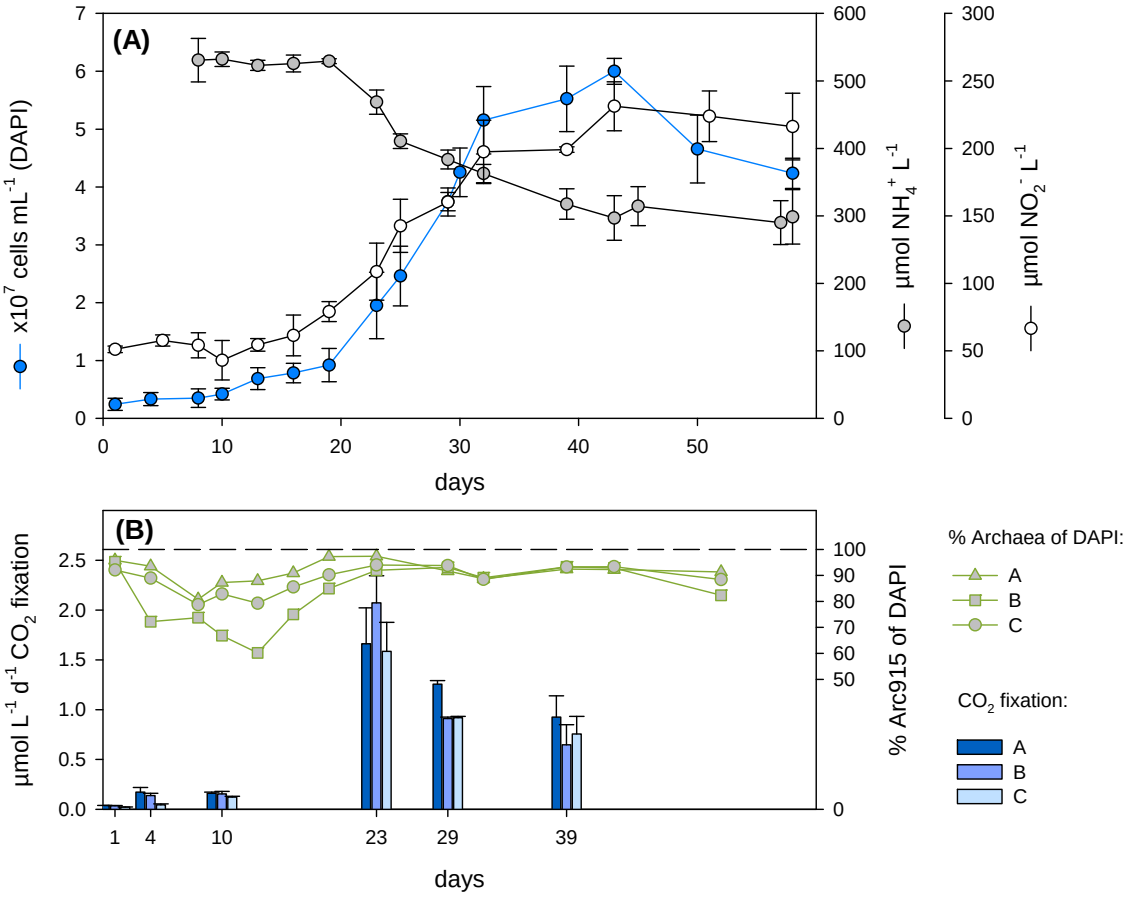

Figure 2.2.: Cell numbers, ammonium concentration, CO_2 fixation rates, and the archaeal fraction in triplicate enrichment cultures (A, B, and C). Error bars show the standard deviations of cell counts and nitrite and ammonium concentrations from cultures grown in triplicate.

Table 2.1.: Growth characteristics and balances during the exponential phase of enrichment cultures grown on natural 0.1-µm filtered seawater. Ammonium oxidation rates were determined by measuring the decrease in NH_4^+ concentrations or by using $^{15}NH_4^+$ and GC-IRMS. -, not determined; SD, standard deviation of triplicate cultures; SE, standard error of the regression slope.

Parameter	A, B, C (mean ± SD)	D	E	F	G (± SE)	Unit
NH_4^+ oxidation	12.81 ± 0.80	5.31	12.32	6.99	11.55	µmol L^{-1} d^{-1}
NH_4^+ oxidation (GC-IRMS)	-	-	-	-	12.53 ± 0.33	µmol L^{-1} d^{-1}
CO_2 fixation (bulk)	1.28 ± 0.10	0.31	1.12	0.17	-	µmol L^{-1} d^{-1}
CO_2 fixation (max., Arc915 cell-specific)	0.2 ± 0.06	-	-	-	-	fmol C $cell^{-1}$ d^{-1}
C-content $cell^{-1}$ (Arc915)	9.02 ± 0.46	-	-	-	-	fg C $cell^{-1}$
C-content $cell^{-1}$ (DAPI)	9.42 ± 0.67	42.99	13.28	13.04	-	fg C $cell^{-1}$
Generation time (Arc915)	4.47 ± 0.65	-	-	-	-	days
Generation time (DAPI)	5.20 ± 0.63	94.25	12.78	21.75	11.03	days
N oxidized per C incorporated	10.07 ± 0.81	16.86	11.03	41.25	-	ratio

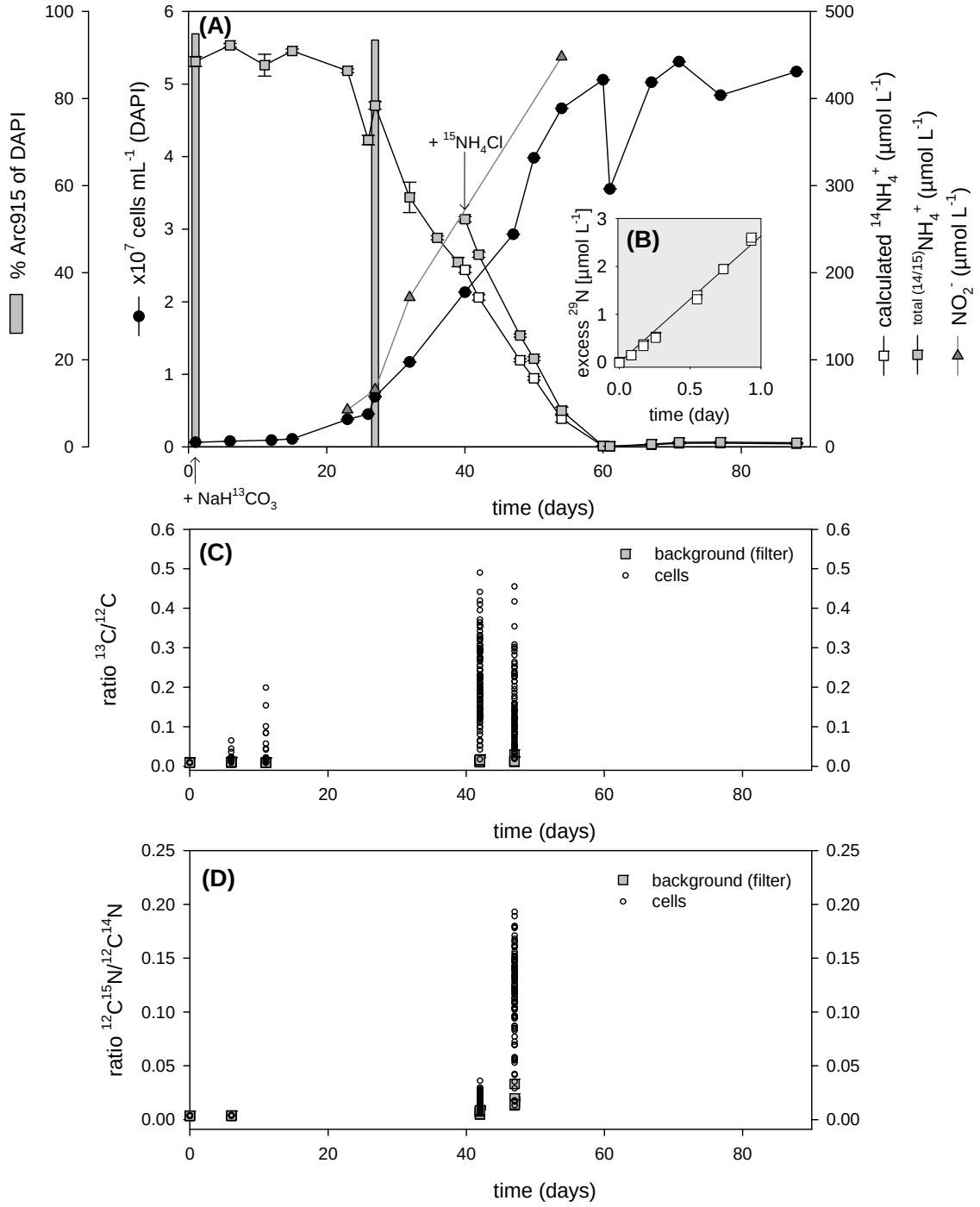

Figure 2.3.: (A) Growth curve of enrichment culture G, showing ammonium consumption, total cell numbers, and the fraction of archaeal cells. ^{15}N-labeled ammonium was added on day 40. The combined $^{14}NH_4^+$ and $^{15}NH_4^+$ concentration is plotted together with the calculated concentration of $^{14}NH_4^+$ based on the percentage of labeling. (B) Conversion of NH_4Cl to NO_x^- during a 24-h period within the exponential growth phase. Ratios of ^{13}C vs. ^{12}C (C) and ^{15}N vs. ^{14}N (D) enrichment in single cells was determined using NanoSIMS. Error bars show the standard deviation among triplicate samples. The data point of day 0 corresponds to unlabeled cells from enrichment E.

2.3.2 CO_2 fixation

CO_2 fixation rates in cultures A, B, and C reached 161 nmol L^{-1} d^{-1} (Figure 2.2B) during the lag phase and, together with cell numbers and ammonium consumption, increased substantially with the onset of the exponential growth phase. Bulk rates of up to 1585–2073 nmol C L^{-1} d^{-1} were determined at early exponential phase, declining to 648–926 nmol C L^{-1} d^{-1} during early stationary phase. Calculated archaeal-cell-specific CO_2 fixation rates were highest on day 23, at 0.2 ± 0.06 fmol C $cell^{-1}$ (Table 2.1 and Figure 2.4). Determination of the cumulative amount of CO_2 fixed over time showed that the total amount of incorporated C correlated with the increase in Arc915-hybridized cell counts (e.g., culture A: $r^2 = 0.992$, $p = 2.4 \times 10^{-5}$; Figure A.7). Based on a comparison of CO_2 fixation and ammonium oxidation rates during exponential growth, one atom C was fixed per ten atoms N oxidized (Table 2.1).

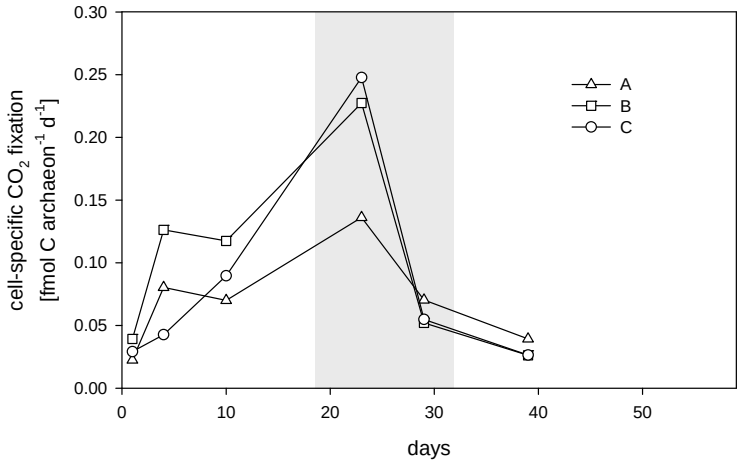

Figure 2.4.: Cell-specific CO_2 fixation rates calculated from archaeal cell numbers and bulk CO_2 fixation rates during the growth of enrichment cultures A, B, and C. The exponential phase is shown in gray.

2.3.3 Cellular uptake of ^{13}C-bicarbonate and $^{15}NH_4Cl$

Enrichment culture G, used exclusively for NanoSIMS analysis, was amended after inoculation with 2 mmol of ^{13}C-labeled bicarbonate L^{-1} (Figure 2.3A), corresponding to 50% ^{13}C-labeled bicarbonate, in addition to an ambient concentration of 2 mmol L^{-1} bicarbonate in the seawater-based medium. During the lag phase, the enrichment of ^{13}C in individual cells inspected via NanoSIMS increased above the natural ratio of 0.011 (Nier, 1950; International Atomic Energy Agency, IAEA) to 0.2 (Figure 2.3C and Figure 2.5).

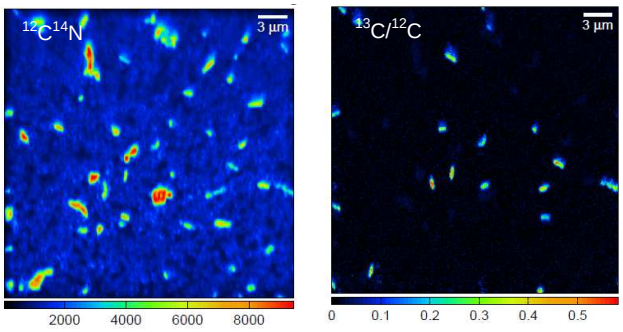

Figure 2.5.: Nano-scale secondary ion mass spectrometry (NanoSIMS) images of ^{13}C-enriched cells sampled 11 days after inoculation and amendment with 2 mmol ^{13}C-bicarbonate L^{-1}. Left: $^{12}C^{14}N^-$ counts representing organic material, right: $^{13}C^{12}C$ ratio representation derived from pixel by pixel calculations from the $^{12}C^-$ and $^{13}C^-$ signal counts.

During exponential growth, on days 42 and 47, the ratio of $^{13}C/^{12}C$ increased up to 0.5. Among all cells investigated (n=268) the ratios varied; on days 42 and 47, mean ^{13}C enrichment was 0.22 ± 0.09 and 0.14 ± 0.09, respectively. NanoSIMS image analysis showed that the labeled cells were analogous in size and morphology to the Arc915-hybridized cells detected via epifluorescence microscopy (Figure 2.1). Nearly all of the investigated cells were ^{13}C-enriched, with enrichment levels above the background values of the polycarbonate filters, the unlabeled cells of the control, and the natural $^{13}C/^{12}C$ ratio.

On day 40, ^{15}N-labeled ammonium was added, corresponding to 22% ^{15}N labeling of the ammonium pool on that day. Subsequently, the ratio of ^{15}N vs. ^{14}N in the cells was 0.04 on day 42 and as high as 0.19 on day 47, with means of 0.02 ± 0.006 and 0.12 ± 0.04, respectively (Figure 2.3D and Figure 2.6). These ratios were considerably higher than the natural ratio of 0.004 (Nier, 1950).

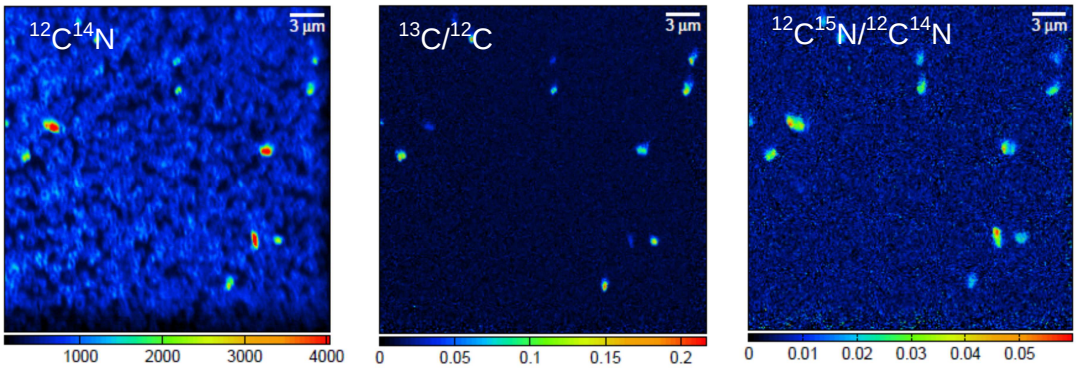

Figure 2.6.: NanoSIMS images of ^{13}C- and ^{15}N-enriched cells sampled on day 42. Left panel: Biomass signal represented by $^{12}C^{14}N$ counts. Middle: ^{13}C enrichment as determined from the ratio $^{13}C/^{12}C$. Right: ^{15}N enrichment as determined from the ratio $^{12}C^{15}N/^{12}C^{14}N$.

2.3.4 Phylogenetic affiliation

Amplification of the bacterial and archaeal 16S rRNA genes from DNA extracts of the enrichment cultures yielded products only for Archaea. All 16S rRNA gene sequences (n=19) thus obtained fell within the *Nitrosopumilus* cluster and were closely related to each other. The closest phylogenetic relative was *Ca.* Nitrosoarchaeum limnia SFB1 (`NZ_CM001158.1`), with 98.8–99.9% 16S rRNA gene sequence identity (Figure 2.7A). No beta- or gammaproteobacterial *amoA* gene sequences were amplified, whereas all archaeal *amoA* gene sequences (n=50) were affiliated with a putative low-salinity group (Figure 2.7B; Blainey *et al.*, 2011). With respect to their *amoA* sequences, the enrichment had 99.4–99.7% sequence identity with *Ca.* N. limnia SFB1 (`NZ_CM001158.1`).

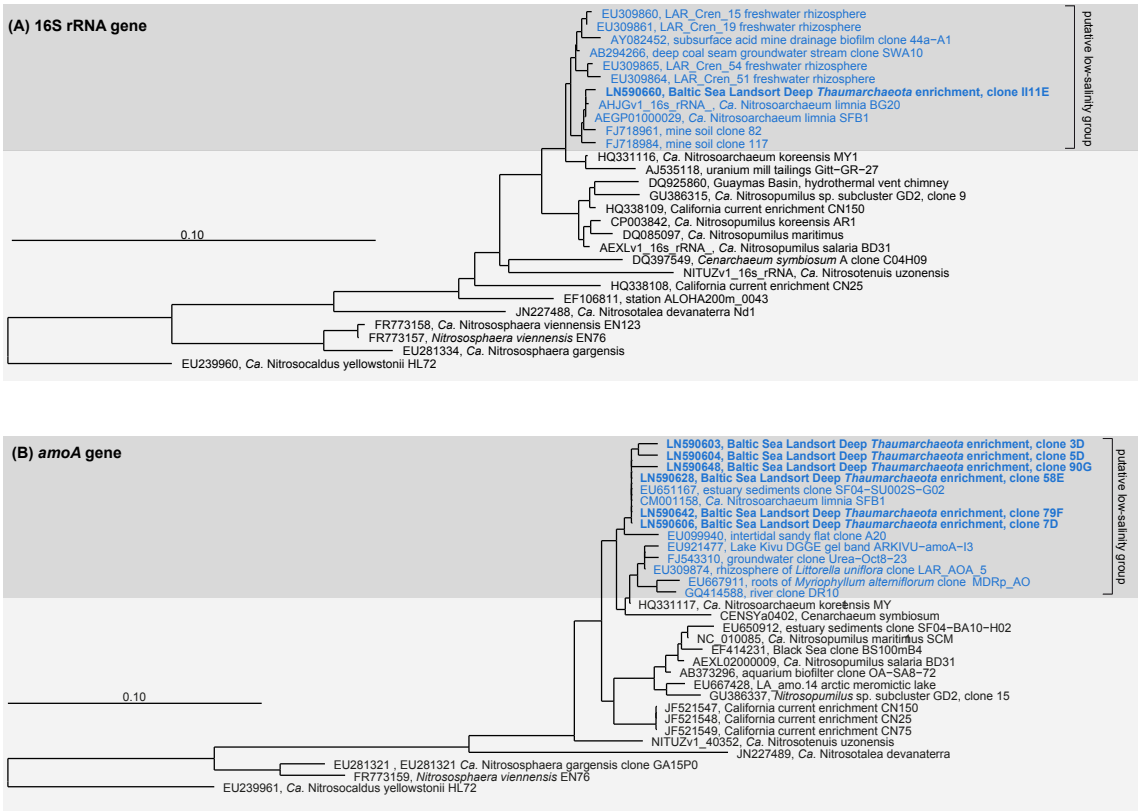

Figure 2.7.: Neighbor-joining trees showing the phylogenetic placement of the enrichment based on the cloned, nearly full-length 16S rRNA (A) and *amoA* (B) gene sequences. The scale bar represents 10 iterations per 100 nucleotides (A) or amino acids (B).

2.4 Discussion

Ammonia-oxidizing Thaumarchaeota may be among the most relevant chemolithoautotrophs in aquatic habitats. Our enrichment of AOA (up to 97% purity, Figure 2.1 and Figure 2.2) of the genus *Nitrosoarchaeum* showed that in seawater-based medium inorganic carbon fixation was sufficient to generate all cellular carbon. Ammonium utilization was ten-fold higher than dark carbon fixation, providing a relationship between these two processes carried out by most AOA. Phylogenetically, the enrichment was determined to fall within a putative low-salinity and freshwater group, concurrent with its geographic origin and the intermediate salinities of Baltic Sea redox gradients.

2.4.1 Autotrophy and calculated carbon content per cell

Growth of the AOA enrichment was accompanied by CO_2 fixation activity, which substantially increased with the onset of the exponential growth phase (Figure 2.2). By relating the amount of incorporated inorganic carbon to the increase in archaeal cell numbers during exponential phase we calculated an average of 9.02 fg of chemoautotrophy-derived carbon per newly produced cell (Table 2.1). This amount is comparable to the 8.39 fg C $cell^{-1}$ reported for autotrophic archaea in the deep Atlantic Ocean (Herndl *et al.*, 2005). By contrast, the mean carbon content of planktonic prokaryotes is about 20 fg C $cell^{-1}$ (Lee *et al.*, 1987). However, since AOA cells are at the lower end of the range of cell sizes, the estimated 9 fg C $cell^{-1}$ seems reasonable. Moreover, it suggests that CO_2 fixation alone generates enough carbon for the production of an archaeal cell. The maximal mean cell-specific CO_2 fixation rate of 0.2 ± 0.06 fmol C $cell^{-1}$ day^{-1} (Figure 2.4) is higher than the rate calculated for marine archaea in the North Atlantic by Herndl *et al.* (2005) or Varela *et al.* (2011), who reported maximum rates of 0.014 and 0.1 fmol C $cell^{-1}$ day^{-1}, respectively. These differences may reflect the distinctive physicochemical parameters of those natural environments compared to the better growth conditions of the enrichment cultures. Ideally, our calculations would be complemented by measurements of the particulate organic carbon (POC) content in the enrichment cultures, but the low cell concentration and the small cell size did not yield sufficient biomass to allow conventional POC measurements. Attempts to filter the cells onto glass-fiber GF/F filters were not successful because most of the cells passed through them. However, the amount of incorporated

carbon that accumulated, based on CO_2 fixation rates (Figure A.7), correlated with the increase in archaeal cell counts during batch growth, likewise suggesting that growth is mainly based on chemoautotrophy. Additionally, NanoSIMS analyses of single cells (Figure 2.3C, D) revealed that, until the exponential phase, up to 50% of the cellular ^{13}C carbon originated from labeled bicarbonate, which represents the fraction of ^{13}C-labeled bicarbonate present in the medium. Although the cells analyzed by NanoSIMS were not first hybridized and then re-identified, the dominance of archaea in the enrichment culture (Figure 2.3A) implies a high probability that the investigated cells were AOA. The enrichment cultures were also susceptible to the archaea-specific biosynthesis inhibitor N^1-guanyl-1,7-diaminoheptane (GC_7) (Jansson *et al.*, 2000), which led to an 81% decrease in CO_2 fixation activity (Berg *et al.*, in press). Taken together, our data show that the generation of the major portion of archaeal biomass in the Nitrosoarchaeum enrichment relied on chemoautotrophy. Yet, our approach does not exclude the incorporation of small amounts of organic compounds, since natural seawater is not free of dissolved organic carbon. For example, N. viennensis and the mixotrophic strains HCA1 and PS0, which are related to *Ca.* N. maritimus SCM1, require pyruvate (Tourna *et al.*, 2011) and α-ketoglutaric acid (Qin *et al.*, 2014), respectively, to achieve high cell numbers. Nonetheless, our results underline the potential role of AOA in the carbon cycle, and their presence may imply preceding contributions to primary production via chemoautotrophy, especially considering the worldwide distribution of AOA (Francis *et al.*, 2005), presumably dominating the large fraction of pelagic archaea in the dark ocean (Karner *et al.*, 2001).

The shortest generation time in our enrichment was 4.5 days (Table 2.1), which is substantially longer than the 21–26 h (at 28 °C) reported for *Ca.* Nitrosopumilus maritimus SCM1 (Könneke *et al.*, 2005; Martens-Habbena *et al.*, 2009) or the 45 h (at 37 °C) of *Nitrososphaera viennensis* (Tourna *et al.*, 2011) but comparable to the 4–4.6 days (at 22 °C) determined in AOA enrichment cultures of the California Current that were grown in natural seawater-based medium (Santoro and Casciotti, 2011) and somewhat slower than the 3.4 days of the closest relative, *Ca.* Nitrosoarchaeum limnia SFB1, grown at 22 °C (Mosier *et al.*, 2012). These differences may be the result of variations in media composition and cultivation temperatures, with faster growth promoted by warmer conditions. Clearly, the conditions used to obtain the enrichment cultures were not the same as those of the natural environment of these cells, i.e., the Baltic Sea redox gradients, where temperatures in the suboxic zone are 5–7 °C. In the latter setting, growth is expected to be slower and may be limited by substrate availability, while maximum *in situ* ammonium oxidation rates are at least 15-fold lower (122–884 nmol N L^{-1} d^{-1}, Berg *et al.*, in press).

2.4.2 Coupling between ammonia oxidation and CO_2 fixation

In the coupling between nitrogen and carbon cycles, AOA play a crucial role. Their high substrate affinity for ammonia (Martens-Habbena *et al.*, 2009) may explain their occurrence in areas of low ammonium concentrations in the open ocean (reviewed by Erguder *et al.*, 2009) and thus their broad distribution. Therefore, the availability of ammonia likely determines primary production by AOA. In our study, ammonium oxidation and inorganic carbon fixation occurred at a ratio of 10 N oxidized per 1 C incorporated (Table 2.1), which is in line with the 10:1 ratio previously discussed for nitrifiers (Tijhuis *et al.*, 1993; Wuchter *et al.*, 2006; Middelburg, 2011). This ratio is also comparable to the nitrification and CO_2 fixation rates determined in the central Baltic Sea (Berg *et al.*, in press): In the pelagic redox zone, where the gradients of oxygen and ammonium overlap and Thaumarchaeota are present in high numbers, nitrification rates (122–884 nmol N L^{-1} d^{-1}) are approximately one order of magnitude higher than those of CO_2 fixation (19–58 nmol C L^{-1} d^{-1}). This suggests that CO_2 fixation in oxygen-deficient waters of the Baltic Sea is largely mediated by AOA, since other chemoautotrophic microorganisms, such as the gammaproteobacterial SUP05 (Glaubitz *et al.*, 2013) and epsilonproteobacterial *Sulfurimonas* sp., reside and fix CO_2 in deeper waters of the Baltic redox gradients, mainly around the oxic-anoxic interface and below (Grote *et al.*, 2008).

2.4.3 Phylogenetic affiliation with a putative low-salinity group

Based on both 16S rRNA and *amoA* gene sequences, our Baltic Sea enrichment affiliates with *Ca.* Nitrosoarchaeum limnia (Figure 2.7). Many Thaumarchaeota sequences recovered from similar habitats cluster in specific groups, indicating that niche partitioning is also reflected in *amoA* sequence diversity. A putative "low-salinity group" comprising sequences collected from streams, estuaries, and groundwater habitats was proposed by Blainey *et al.* (2011) and by Biller *et al.* (2012). The salinities characteristic of brackish pelagic redox gradients in the central Baltic Sea are in the range of 6–11 (Labrenz *et al.*, 2007). Sequences recovered from our enrichment culture had 98.8–99.9% 16S rRNA sequence identity with *Ca.* Nitrosoarchaeum limnia SFB1 (Blainey *et al.*, 2011), which originates from low-salinity (7.9) sediments of San Francisco Bay (Mosier *et al.*, 2012). Although the two low-salinity habitats are geographically far apart, the sequence identity

between *Ca.* N. limnia SFB1 and our enrichment is remarkably high for both the 16S rRNA and the *amoA* genes. Bouskill *et al.* (2012) argued that the geochemical properties of a habitat strongly determine the distribution of phylogenetic groups of ammonia oxidizers. This conclusion gained support from a comprehensive analysis of *amoA* sequences from aquatic habitats, in which Biller *et al.* (2012) found that salinity, among other parameters, determined the distribution of niche-specific *amoA* sequence types. Genome sequencing of the enrichment may reveal physiological differences with *Ca.* N. limnia SFB1, as even closely related AOA can inhabit strikingly different ecological niches (Qin *et al.*, 2014).

Yet, the ecological relevance of the enriched *Nitrosoarchaeum* relative in Baltic Sea pelagic redox gradients may be limited because it was not detected in previous archaeal clone libraries. The latter were dominated by a *Nitrosopumilus* sp. subcluster (Labrenz *et al.*, 2010) with 94.1–98.0% 16S rRNA and 89.7–90.1% *amoA* sequence identity to our *Nitrosoarchaeum* sp. enrichment. Our growth experiment with a Baltic Sea AOA enrichment culture extends current knowledge on chemoautotrophic AOA by providing direct evidence that the biomass needed for cell growth is largely generated by the fixation of inorganic carbon. Furthermore, we were able to relate ammonium oxidation to CO_2 fixation, which has implications in the AOA-mediated coupling of N and C cycles in the environment and may contribute to the modeling of carbon and nitrogen cycles in AOA-dominated habitats.

2.5 Acknowledgment

This study was financed by the German Science Foundation (DFG) and European Science Foundation (EFG) within the EuroEEFG program and the project Microbial Oceanography of ChemolithoAutotrophic planktonic Communities (MOCA), grant JU 367/12-1. The SIMS instrument was funded by the German Federal Ministry of Education and Research (BMBF), grant identifier 03F0626A. Martin Könneke of MARUM is thanked for sharing his experience in enrichment procedures. Daniel P. R. Herlemann's useful help with ARB is highly appreciated. We thank Bo Thamdrup, of the University of Southern Denmark, for providing us with the opportunity to measure $^{29}N_2$ via GC-IRMS, and Volkmar Senz, of the University of Rostock, for his assistance in preparing the gold-sputtered filters. The support of both the chief scientist of the *R/V Heincke*, Martin Schmidt, and its crew and captain is highly appreciated.

Chapter three

Metatranscriptomic profiling of Thaumarchaeota within a chemoautotrophic community in a Baltic Sea pelagic redox gradient

3

METATRANSCRIPTOMIC PROFILING OF THAUMARCHAEOTA WITHIN A CHEMOAUTOTROPHIC COMMUNITY IN A BALTIC SEA PELAGIC REDOX GRADIENT

Abstract

Marine oxygen-depletion due to excess respiration of organic material and reduced circulation can cause pronounced, chemically stratified gradients of distinct redox conditions in the water-columns of the world oceans and alike systems. Here, chemolithoautotrophic microorganisms perform ecosystem-relevant biogeochemical transformations that impact e.g. the nitrogen, carbon and sulfur cycles. Investigations of the associated microorganisms emphasized their ecological significance but insights into taxa-specific activities at distinct chemical niches within a natural microbial community setting are scarce. Thus, to reveal the underlying gene expression of abundant key microbes, we sampled a characteristic, chemically stratified redox-gradient that covered oxic to sulfidic conditions in the model system Baltic Sea. *In situ* sample fixation for unbiased metatranscriptomics was employed to obtain snapshots of mRNA levels reflecting the microbial community state at gradually different chemical conditions with emphasis on the activity of prevailing chemoautotrophs. Thaumarchaeota affiliated with the ammonia-oxidizing *Candidatus* Nitrosopumilus maritimus, gammaproteobacteria of the potentially denitrifying SUP05 cluster and epsilonproteobacteria related to the denitrifying, sulfur-oxidizing *Sulfurimonas gotlandica* - all of which are relevant to chemoautotrophic primary production - occurred at high abundances, together accounting for up to 69% of the prokaryotic cells. Different distribution patterns of group-specific cell counts suggested specific chemical niches of increased activity. Accordingly, transcript recruitment using reference genomes revealed niche partitioning at specific chemical conditions and zones of maximal transcription activities, defining "comfort zones" for each of the chemoautotrophs. Peaks in cellular abundances did not always co-occur with maximum transcript levels of genes for energy conservation or carbon fixation. Outside the comfort zones, transcript levels of some genes for e.g. chemotaxis, carbon-metabolism restructuring and differential expression of transcription

factors were elevated, providing insights into strategies of coping with unfavorable conditions. Our study illuminates the transcriptional backbone of the chemoautotrophy-driven biogeochemistry of an oxygen-depleted water column and reveals adaptations of important key chemoautotrophs to thrive in these systems.

3.1 Introduction

Although marine oxygen minimum zones (OMZ) embody only 1–7% of the world's oceans volume (Wright *et al.*, 2012*b*), up to 50% of the global nitrogen removal occurs in these areas (Kuypers *et al.*, 2005). Nitrogen loss is achieved mainly via the concerted activities of different guilds of chemolithoautotrophic microorganisms, which conserve energy via reactions between oxidized and reduced inorganic compounds and use the energy for growth by fixation of carbon dioxide. Generating elevated abundances, they interconnect e.g. the nitrogen (N), carbon (C) and sulfur (S) cycles through their specific lifestyles. Various studies report prevalence of chemolithoautotrophs linked to e.g. sulfur-oxidation, nitrification, denitrification, dissimilatory nitrate reduction or anaerobic ammonium oxidation in OMZ areas and periodic anoxic waters (Lam *et al.*, 2007; Grote *et al.*, 2008; Lavik *et al.*, 2009; Walsh *et al.*, 2009; Stewart *et al.*, 2012; Yakimov *et al.*, 2011; Glaubitz *et al.*, 2013; Hawley *et al.*, 2014). In a Baltic redox-gradient, Grote *et al.* (2008) determined 12.2–29.0% of the cells to be active autotrophs, most of them sulfur-oxidizers affiliated with *Sulfurimonas* sp. In spatial proximity, Thaumarchaeota of the *Ca.* N. maritimus subcluster GD2 comprise up to 26% of all cells (Labrenz *et al.*, 2010), catalyzing up to 86–100% of ammonia oxidation (Berg *et al.*, in press) and are potentially living autotrophically, similar the closest relative, *Ca.* N. maritimus (Könneke *et al.*, 2005, 2014). These key organisms are common inhabitants of oxygen depleted zones (Stewart *et al.*, 2012; Ulloa *et al.*, 2012*a*; Schunck *et al.*, 2013), distributed worldwide and often phylogenetically closely related, which indicates versatile strategies to successfully adapt to the specific environmental conditions in OMZs. Enrichment, isolation and subsequent genome sequencing of specific organisms provided insights into their genetic inventory for energy conservation, carbon fixation and adaptations (e.g. Hallam *et al.*, 2006*a*; Walker *et al.*, 2010; Spang *et al.*, 2012). Thaumarchaeota are among the most abundant and ubiquitous planktonic groups in the dark ocean (Francis *et al.*, 2005). As revealed from studies with *Ca.* N. maritimus, the K_m of 133 nmol L^{-1} attests a high affinity for ammonia (Martens-Habbena *et al.*, 2009) and the thaumarchaeotal variant of the 3-hydroxypropionate/4-hydroxybutyrate cycle is

a very efficient carbon fixation pathway (Könneke *et al.*, 2014). These features presumably support the AOA-predominance. However, studies examining the functioning and regulation of these in a natural microbial community are scarce. Thaumarchaeota occur even in the anoxic, sulfidic water layers of the Baltic Sea water-columns (Labrenz *et al.*, 2010; Berg *et al.*, in press). Their role and strategies to survive in these waters remain yet to be clarified while recent investigations indicate a tolerance against periodic exposure of hydrogen sulfide (Berg *et al.*, in press).

Biogeochemical rate measurements are commonly performed to assess bulk microbial activities and showed high rates of nitrogen and carbon cycling in the Baltic (Jost *et al.*, 2008; Grote *et al.*, 2008; Hietanen *et al.*, 2012; Berg *et al.*, in press). However, these are limited in the number of processes that can be studied in parallel due to the relatively high number of samples to be handled. Additionally, assigning a process to a specific microbial group is complex. Detection of functional gene transcripts via quantitative PCR uses genes as proxies for biogeochemical processes but is selective as it requires previous information on the genes of interest. Employing metatranscriptomics instead, nearly all microbial gene transcripts can be captured at the same time. By this means, involvements of important key microorganisms in biogeochemical cycles were investigated by previous studies (Stewart *et al.*, 2012; Satinsky *et al.*, 2014). Transcript levels of key genes as proxies for particular biogeochemical processes can provide insights into potential gene-regulation in response to different environmental conditions. Thus, it is a powerful exploratory tool to analyze a multitude of gene sets simultaneously and to expose potential microbial interactions. Combined with an *in situ* fixation system (Feike *et al.*, 2012) that minimizes mRNA degradation during sampling, it is possible to obtain an unaltered transcriptional snapshot of the microbial community. Changes in microbial activities as inferred from transcript levels of specific genes may serve as indicators for biogeochemically performed processes along a gradient of different chemical conditions. Our study depicts the underlying gene expression of Thaumarchaeota within a redox gradient, that is as well governed by denitrifying, sulfur-oxidizing chemoautotrophs. The group-specific distribution of these three key organisms in terms of abundance versus activity along different chemical niches is unveiled and strategies of coping with unfavorable conditions are assessed.

3.2 Material and Methods

3.2.1 Sampling and physicochemical analyses

Samples were taken on board *R/V* Maria S. Merian during cruise MSM12/4b at Landsort Deep station 284 on September 14, 2009. The water was collected from six depths, covering the redox-gradient with an automatic flow injection sampler (AFIS, Feike *et al.*, 2012) attached to a conductivity, temperature and depth (CTD) probe. A volume of 1 L sample water was fixed with Carnoy solution (30% chloroform and 10% acetic acid in absolute ethanol, Wartman, 1960) as described in Feike *et al.* (2012) in the depth of sampling, directly *in situ* and prior to transfer onboard and filtration onto 0.2 µm PTFE filters. Additional free-flow water bottles served to obtain unfixed samples for cell quantifications and chemical analyses. Physico-chemical properties of the water-column as characterized by O_2, H_2S, PO_4^{3-}, NH_4^+, NO_3^- and NO_2^- were subsequently analyzed after Grasshoff *et al.* (1983) directly on board.

3.2.2 Quantification of specific phylogenetic groups by catalyzed reporter deposition fluorescence *in situ* hybridization (CARD-FISH)

From 100 mL of sample fixed for 6-12 hours with particle-free formaldehyde (2% final concentration) at 4 °C, volumes of 20–40 mL were filtrated onto 0.2 µm polycarbonate filters. The filters were stored at -20 or -80 °C until analysis. The collected filters were embedded in 0.1% agarose prior to digestion of the cells with lysozyme and achromopeptidase at 37 °C for 60 and 15 minutes, respectively. Hybridization with horseradish peroxidase labeled probes was carried out at 35 °C overnight with probe-specific concentrations of formamide and tyramide signal amplification with Alexa Fluor 488. The probes used were Cren679 targeting *Thaumarchaeota* of the *Ca.* Nitrosopumilus sp. subcluster GD2 (Labrenz *et al.*, 2010), SUL90 being specific for *Sulfurimonas* sp. subgroup GD17 (Grote *et al.*, 2007) and GSO1032 covering SUP05 *Gammaproteobacteria* (Glaubitz *et al.*, 2013). These probes were developed to specifically target the prevailing key microorganisms in Baltic Sea redox gradients and have been widely applied in previous studies. Hybridized filter sections were embedded in a mixture of Vectashield mounting medium containing DAPI (4',6-diamidin-2-phenylindol) for unspecific counter-staining of all cells. Prepared

filter sections were inspected using a Zeiss Axioskop 2 mot plus and 1,700–7,500 DAPI stained cells were quantified in 15 randomly selected microscopic fields.

3.2.3 RNA extraction and sequencing

Sample preparation was conducted according to the method described in Poretsky *et al.* (2009). Total RNA from the filters of each depth was extracted, the mRNA enriched by depletion of rRNA and then, the mRNA was amplified. Finally, the double-stranded cDNA was sequenced (100 bp paired end) on an Illumina HiSeq2000 system by LGC Genomics (Berlin, Germany). From each of the six sampled depths one metatranscriptomic library was generated.

3.2.4 MG-RAST

Concatenated files of forward and reverse sequence reads were uploaded to the MG-RAST system (Metagenomic Rapid Annotations using Subsystems Technology; Glass *et al.*, 2010) and automatically annotated. The system was used to explore the metatranscriptomic datasets and to deduce strategies for detailed analyses. The number of sequence reads for each dataset that matched a protein sequence in GenBank was determined using a maximum e-value of 0.0001, minimum identity of 60% and minimum alignment length of 15 amino acids.

3.2.5 Sequence recruitment using reference genomes

In order to recruit reads of mRNA transcripts covering a full genome, the reads were mapped based on the translated amino-acid sequences using the `promer`-function of MUMmer 3.22 (Kurtz *et al.*, 2004) against translated reference genomes of *Ca.* Nitrosopumilus maritimus (`NC_010085`, Walker *et al.*, 2010), *Sulfurimonas gotlandica* str. GD1 (`AFRZ00000000`, Grote *et al.*, 2012) or the draft genome of the SUP05 cluster (`ACSG00000000`, Walsh *et al.*, 2009).

Coordinates of the `promer` alignments were extracted with the `show-coords` function using the `-k` option. The resulting table was processed using BEDOPS (Neph *et al.*, 2012)

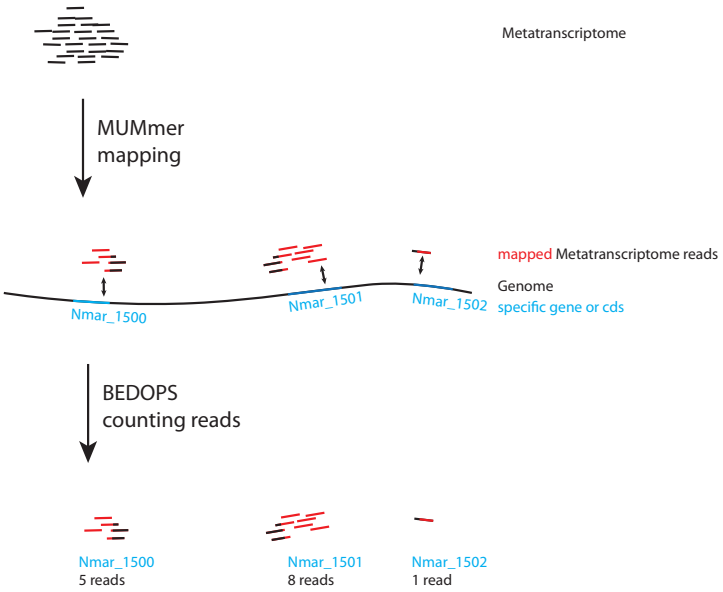

Figure 3.1.: Approach of the metatranscriptome analysis using MUMmer (Kurtz *et al.*, 2004) for mapping reads of the metatranscriptomic libraries to a reference genome. Subsequent assignment to gene loci and counting of reads assigned to a specific gene locus was conducted by BEDOPS (Neph *et al.*, 2012).

to recruit mapped reads and count the number of reads for each gene locus according to the reference genome (Figure 3.1). The different steps of the workflow were connected by customized Perl and Unix-shell scripts.

3.2.6 Alignments of specific genes via TBLASTN

Abundances of reads, i.e. transcript levels of specific genes of *Ca.* Nitrosopumilus maritimus, *Sulfurimonas gotlandica* or the SUP05 genome were assessed using a TBLASTN search of the amino acid query sequence against the respective metatranscriptome as subject with an e-value cutoff of 10^{-4}. Specific genes that were investigated in a TBLASTN search analysis are listed in Table A.2, Table A.3 and Table A.4 and were selected based on the annotations that indicated biogeochemically or physiologically relevant genes as provided by Walsh *et al.* (2009), Walker *et al.* (2010) and Grote *et al.* (2012).

3.2.7 Normalization of read counts

Depending on the specific question, either two different normalizations were applied (Table 3.1) on the number of transcript reads or the data are presented as not normalized, i.e. absolute and raw read counts.

Table 3.1.: Overview of the different types of normalization that were applied to the number of raw read counts obtained by MUMmer promer in relation to the specific questions of investigations.

Type	Parameters	Properties	Section
Relative normalization	Raw read counts, standard deviation and mean throughout depths	Facilitates comparison of gene transcript levels among different genes throughout different datasets, regardless the absolute number of raw reads	Section 3.2.7.1
Organism-specific normalization	Raw read counts, total counts assigned to specific reference genome	Analyze fraction of transcription dedicated to a specific gene by the target organism	Section 3.2.7.2

3.2.7.1 Cluster analysis

For each gene, the absolute number of reads was converted into a relative value based on the mean read count throughout the six depths and the standard deviation as explained by Equation 3.1. By this means, the change in relative transcript levels, ranging from –2 to +2, was compared between different genes, independent whether genes with high read counts were compared to those with low read counts.

$$\text{relative transcript level of specific gene} = \frac{\text{[(Value) - Mean(Row)]}}{\text{[Standard deviation(Row)]}} \tag{3.1}$$

As an exploratory means for finding patterns in different levels of gene transcripts throughout the redox gradient, a cluster analysis was conducted using the Multi Experiment Viewer (MeV) as part of the TM4 Microarray Software Suite (Saeed *et al.*, 2003, 2006) in order to determine depths of highest transcriptional activity for each gene of a target genome and to identify genes with correlating expression patterns. Gene expression patterns for the normalized relative transcript reads recruited by MUMmer `-promer` of the respective reference genomes were derived via K-Means Pearson correlation generating 10 clusters. Transcript reads of a specific gene were included in the analysis if at least in one of the sampled depths a minimum of 3 reads of a gene was counted.

3.2.7.2 Specific gene transcript levels in relation to total gene transcript levels of one organism

The relative portion of specific gene transcript levels in relation to the total gene transcript levels of a specific organism was determined via normalization according to Equation 3.2. The transcript level of the gene of interest was compared to the total number of transcripts mapped to this organism via MUMmer recruitment. The relative number is given as number of reads per 10,000 reads of that organism, providing information about how much transcription effort is assigned to a specific gene by the organism.

$$\text{relative portion} = \frac{\#\text{ of transcript reads of gene of interest}}{\text{sum of all transcript reads of one organism}} \times 10,000 \tag{3.2}$$

3.3 Results and Discussion

3.3.1 Redox gradient stratification and metatranscriptome properties

Oxygen-depleted zones like the redox gradients of the central Baltic Sea are hotspots for active chemoautotrophs, which impact the carbon, nitrogen and sulfur cycles. From this habitat, metatranscriptomic datasets were obtained from six depths within a chemically stratified redox-gradient by employment of an *in situ* fixation sampling system.

The physicochemical structure of the Landsort Deep redox gradient in September 2009 displayed a stable stratification as evidenced by gradually de- or increasing inorganic nutrient concentrations (Figure 3.2).

The sampled depths represented two different chemical regimes, a hypoxic zone (71, 75 and 82 m) with low oxygen levels of maximal 1.3 µmol L^{-1} and a subjacent sulfidic zone (88, 94 and 100 m) ranging from 5.2–13.9 µmol L^{-1} H_2S. In the hypoxic zone, only traces of sulfide below 0.2 µmol L^{-1} were measured while covering the lower part of a nitrate peak. Nitrite peaked with 0.12 µmol L^{-1} in the lower oxic part and then declined in the sulfidic. Ammonium was present throughout the profile with gradually increasing concentrations towards the sulfidic, ranging from 0.3–4.3 µmol L^{-1}. Phosphate was detected at a constant level of 3.7 µmol L^{-1} within the sulfidic zone, but in the hypoxic, concentrations were lower, with a minimum of 1.8 µmol L^{-1} in 75 m.

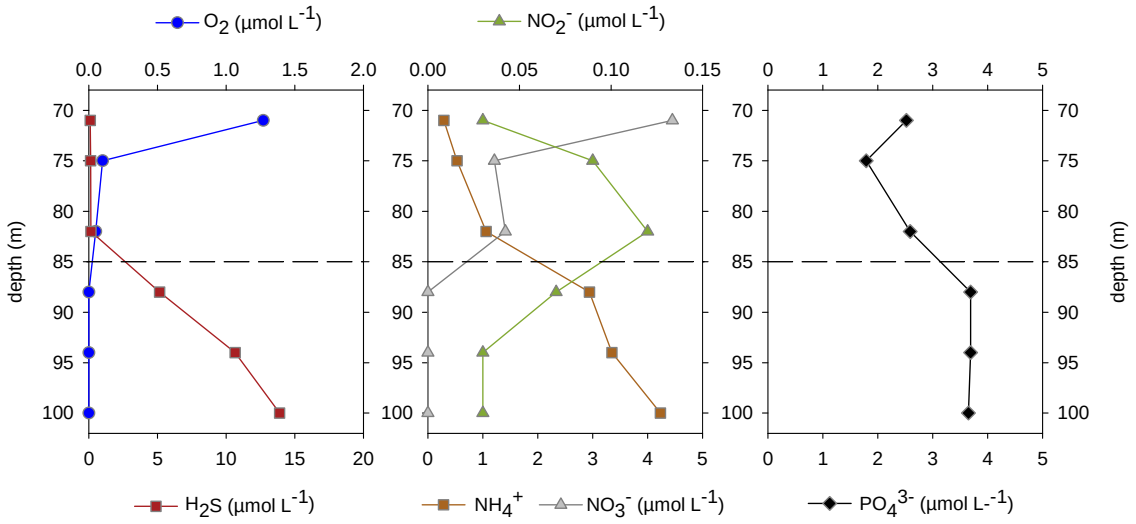

Figure 3.2.: Chemical profile displaying the distribution of inorganic nutrients throughout the sampled pelagic redox gradient at the Landsort Deep station 284 in September 2009, covering 6 depths from oxic to sulfidic conditions. The dashed horizontal line separates the hypoxic from the lower sulfidic depths.

The abundance of GD2 Thaumarchaeota was lowest in the most oxic (71 m) and most sulfidic (100 m) depths; in between, elevated numbers of 1.9–2.4 $\times$ 10^5 cells mL^{-1} were determined, representing up to 30.2% of total cell counts in 75 m (Figure 3.3), which is accordant to previous studies in the Baltic Deeps (Labrenz *et al.*, 2010; Berg *et al.*, in press). Abundance of SUP05 cells was minimal in 71 m, and sharply increased to 5.5 $\times$ 10^5 cells mL^{-1} in 75 m, followed by a gradual decline with depth until 1 $\times$ 10^5 cells mL^{-1} in 100 m. The largest relative portion of SUP05 cells was detected in 82 m, where these accounted for 34.5% of the total cell counts, comparable to what was determined by Glaubitz *et al.* (2013) at this site also in September 2009. Cells of *Sulfurimonas* sp. subgroup GD17 were generally less abundant than those of GD2 Thaumarchaeota or SUP05, while exhibiting an increase towards the sulfidic zone with maximum numbers of 1.5 $\times$ 10^5 cells mL^{-1} in 88 m, which represents 17.0% of the total cell counts in that depth (Figure 3.3). Altogether, the relative abundances of the three key chemoautotrophs showed that these dominated the microbial community around the oxic-anoxic interface, as together they were accounting for up to 69% of total cell numbers in 82 m. The individual contributions of the different chemoautotrophs to the total cell numbers within the redox gradient are in line with previous studies at the Baltic Deeps (Grote *et al.*, 2007; Labrenz *et al.*, 2010; Glaubitz *et al.*, 2013), which implies that the sampled depths cover a microbially representative Baltic redox gradient suitable for an in-depth analysis of *in situ* transcriptional activities of these chemoautotrophs.

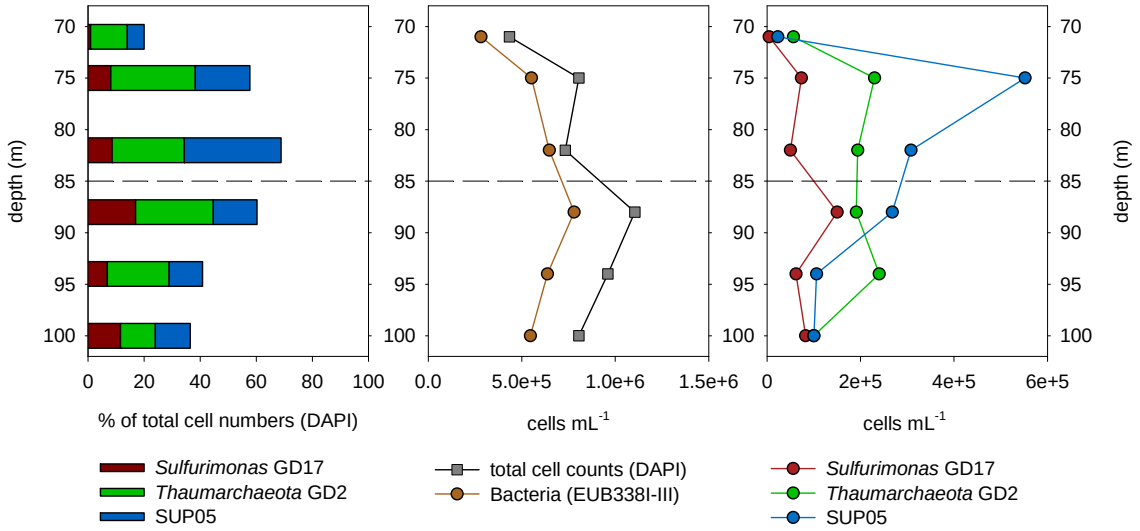

Figure 3.3.: Relative (left panel) and absolute cell counts (right) of the three chemoautotrophic key microorganisms and total cell numbers (middle) throughout the pelagic redox gradient of the Landsort Deep in September, 2009, based on group-specific cell counts by employment of CARD-FISH. The dashed horizontal line separates the hypoxic from the lower sulfidic depths.

The six metatranscriptomes yielded 2.7–4.1 $\times$ 10^7 raw reads with an average read length of 93–95 nt. After trimming and quality processing, 2.21–3.62 $\times$ 10^7 reads remained, containing 23.3–29.7% rRNA reads. 1.99–6.28 $\times$ 10^5 of the reads were identified as protein-coding reads with a functional annotation (Table 3.2) in the GenBank database using MG-RAST as annotation system (Glass *et al.*, 2010). Mapping of reads to reference genomes of *Ca.* N. maritimus, *S. gotlandica* and the SUP05 metagenome via MUMmer (Kurtz *et al.*, 2004) accounted for 0.46–5.99%, 5.17–69.87% and 0.45–1.94% of the protein coding reads, respectively, depending on depth (Table 3.2, Figure 3.4).

The relative distribution pattern of mapped reads followed partly the pattern of relative abundances of the respective organisms. The peaks in relative read and cell abundances coincided in the case of *Sulfurimonas gotlandica* and *Ca.* Nitrosopumilus maritimus but were located at different depths for SUP05 (Figure 3.4). Furthermore, cellular abundances of GD2 Thaumarchaeota remained stable throughout the gradient including the sulfidic zone while the relative read abundances assigned to Thaumarchaeota decreased significantly within the transition from the oxic to the sulfidic zone. This apparent discrepancy between cellular abundances and cellular activities raises the question whether thaumarchaeotal cells are dead in the sulfidic zone or if they can adapt to these conditions and remain viable.

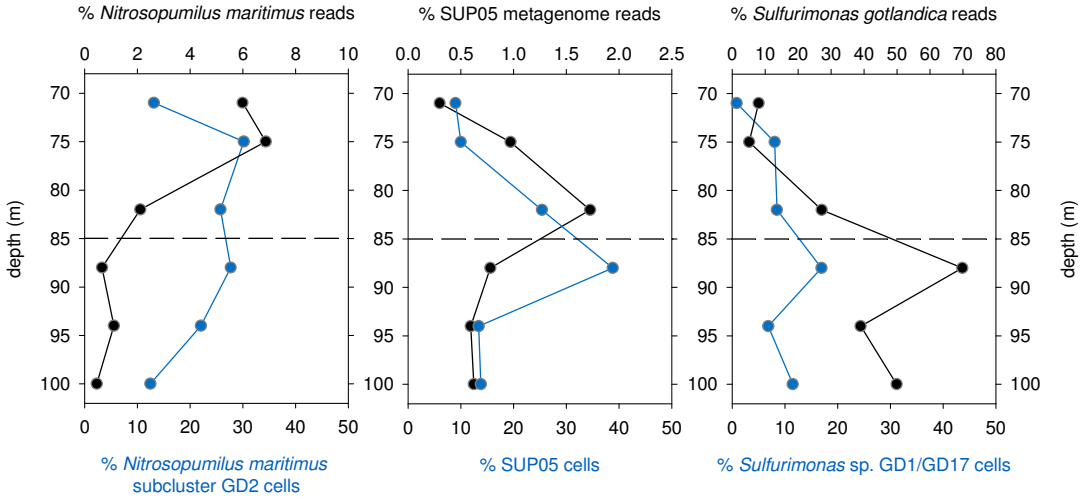

Figure 3.4.: Relative contributions of the three investigated chemoautotrophic key microorganisms in terms of read abundances (black lines) as mapped via MUMmer (see also Table 3.2) to the respective reference genome and cellular abundances (blue lines) in the pelagic redox gradient of Landsort Deep in September 2009. The dashed horizontal line separates the hypoxic from the sulfidic zone.

Table 3.2.: Sequencing, quality and recruitment parameters of the six metatranscriptomic datasets obtained from the Landsort Deep redox gradient in September 2009.

depth	71 m	75 m	82 m	88 m	94 m	100 m
Raw reads ($\times 10^7$)	4.11	4.10	2.68	3.8	4.41	3.05
After quality processing, trimming						
Total reads ($\times 10^7$)	3.32	3.28	2.21	3.15	3.62	2.50
% rRNA	29.7	26.5	23.3	25.3	27.2	25.8
average read length (nt)	93	94	95	95	95	95
average Phread quality	34.5	34.5	34.8	34.7	34.6	34.6
Number of reads that matched a protein sequence in GenBank via MG-RAST*						
Reads ($\times 10^5$)	1.99	2.99	4.98	6.28	2.16	4.01
Number of reads recruited to reference genome and percentage matching a GenBank entry						
Ca. N. maritimus ($\times 10^4$)	1.19	2.05	1.05	0.42	0.24	0.19
%	5.99	6.87	2.11	0.66	1.11	0.46
S. gotlandica ($\times 10^4$)	16.0	15.45	13.56	43.9	8.43	20.0
%	8.05	5.17	27.21	69.87	39.01	49.93
SUP05 metagenome ($\times 10^3$)	0.89	1.49	6.31	12.2	1.44	2.75
%	0.45	0.50	1.27	1.94	0.67	0.69

*max e-value: 0.0001; min identity: 60%; min alignment length: 15 amino acids

3.3.2 "Comfort zones" of key chemoautotrophs

Based on the total number of reads that were assigned to either *Ca.* N. maritimus, *S. gotlandica* or SUP05 via mapping to reference genomes, maximal transcript levels occurred in specific and different depths for these prokaryotes (Table 3.2, Figure 3.5).

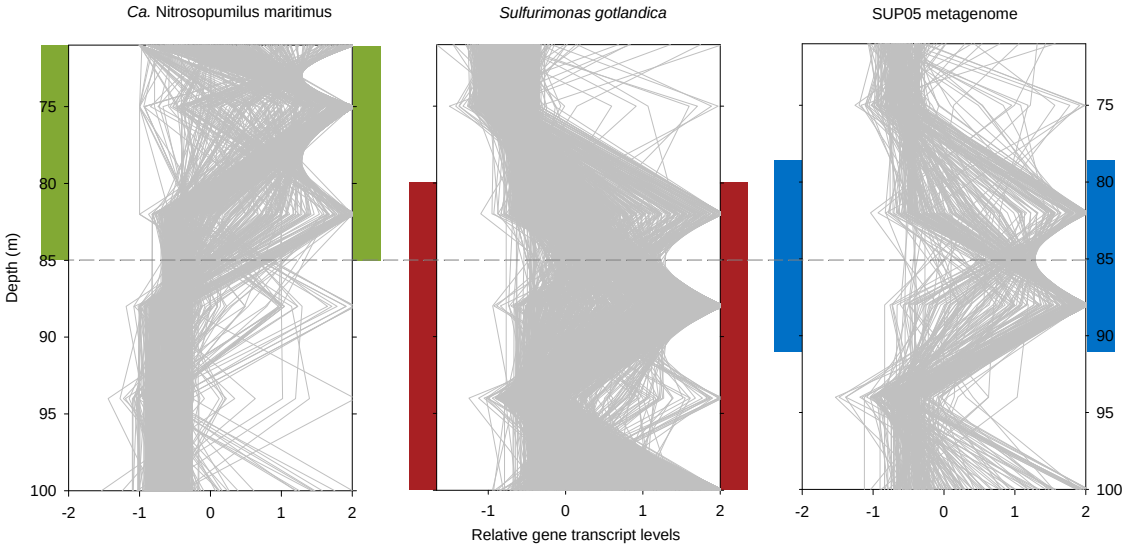

Figure 3.5.: Relative gene transcript levels of the three key chemoautotrophs as mapped via MUMmer in the Landsort Deep redox gradient in Septmeber 2009. The dashed horizontal line separates the hypoxic from the lower sulfidic depths. Approximate locations of the "comfort zones" are marked in green for transcript levels assigned to *Ca.* N. maritimus, in red for *S. gotlandica* and in blue for the SUP05 metagenome.

Ca. N. maritimus was most active in the upper two hypoxic depths while *S. gotlandica* and SUP05 were most active in the upper sulfidic depths below the oxic-anoxic interface layer. To further disentangle the general gene expression, a cluster analysis was used to categorize genes with similar transcript level patterns based on the read count data, which was obtained from mapping read counts to a specific reference genome. Considering the 10 clusters that were generated, most genes of *Ca.* N. maritimus showed higher transcript levels in the oxic depths than in the sulfidic (Figure 3.6). Only few genes showed a contrasting expression pattern, that is, having higher transcript levels in the sulfidic waters than in the oxic. Similar observations resulted for transcript levels of *S. gotlandica*, which were highest around the oxic-anoxic interface and in the sulfidic zone but were lower for the majority of genes in the oxic part of the redox gradient. Transcript levels of SUP05 were highest around the oxic-anoxic interface layer and low in the most oxic and most sulfidic depths. These differential patterns of gene transcripts revealed depths of overall increased activities (Figure 3.5) and suggest specific chemical niches that fulfill the requirements for energy conservation and growth.

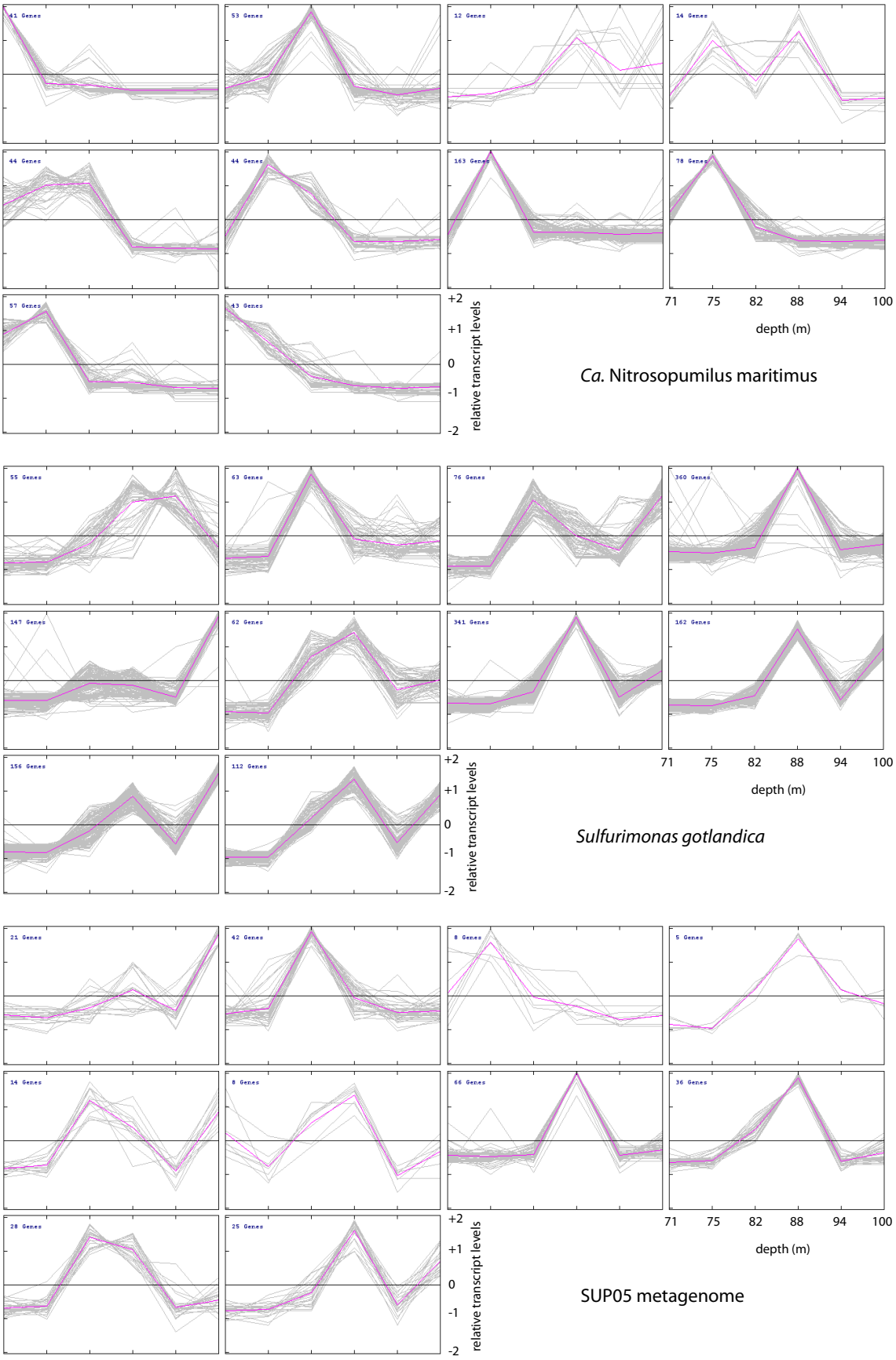

Figure 3.6.: Gene transcript levels normalized to relative values of reads mapped to the reference genomes of *Ca.* N. maritimus (top), *Sulfurimonas gotlandica* (middle) or the SUP05 metagenome (bottom) via MUMmer and for each sorted into 10 clusters of similar expression patterns based on correlating changes in transcript levels. One gray line represents the relative transcript level pattern of one gene. Each gene above a threshold of at least three reads in at least one depth is plotted in the graphs.

3.3.3 Adaptations outside the comfort zones

3.3.3.1 Transcription factors of *Ca.* Nitrosopumilus maritimus

The genome of *Ca.* N. maritimus comprises a minimum of eight genes that code for transcription factor B (TFB), as reported by Walker *et al.* (2010). The authors acknowledged that this is the largest number of transcription factors among currently known archaeal genomes, potentially enabling Thaumarchaeota to respond efficiently to environmentally fluctuating conditions. The TFB were reported to play a major role in archaeal niche adaptation (Turkarslan *et al.*, 2011). This may be achieved by duplications of target genes or transcription factor genes, accompanied by subtle sequence changes that facilitate reprogramming of gene regulatory networks, as emphasized by Turkarslan *et al.* (2011).

In the analyzed metatranscriptomics dataset, 7 out of the 8 TFB genes as well as transcription factor E (TFE), and the two TATA-box binding protein genes (TBP) of *Ca.* N. maritimus were detected active at significant transcript levels (Figure 3.7). The various transcription factors showed differential transcript level patterns throughout the redox gradient. Of these, TFB7 comprised the highest number of raw reads and was only active in the oxic depths (Figure 3.7). In contrast, transcript levels of TFB5 increased towards the transition from oxic to sulfidic depths and exhibited stable transcript levels in 88 and 94 m and then declined in 100 m depth. The observed differential and TFB-specific patterns support the hypothesis raised by Turkarslan *et al.* (2011) and may indeed play an important role for the transcription of genes that are required to adapt to the different chemical conditions.

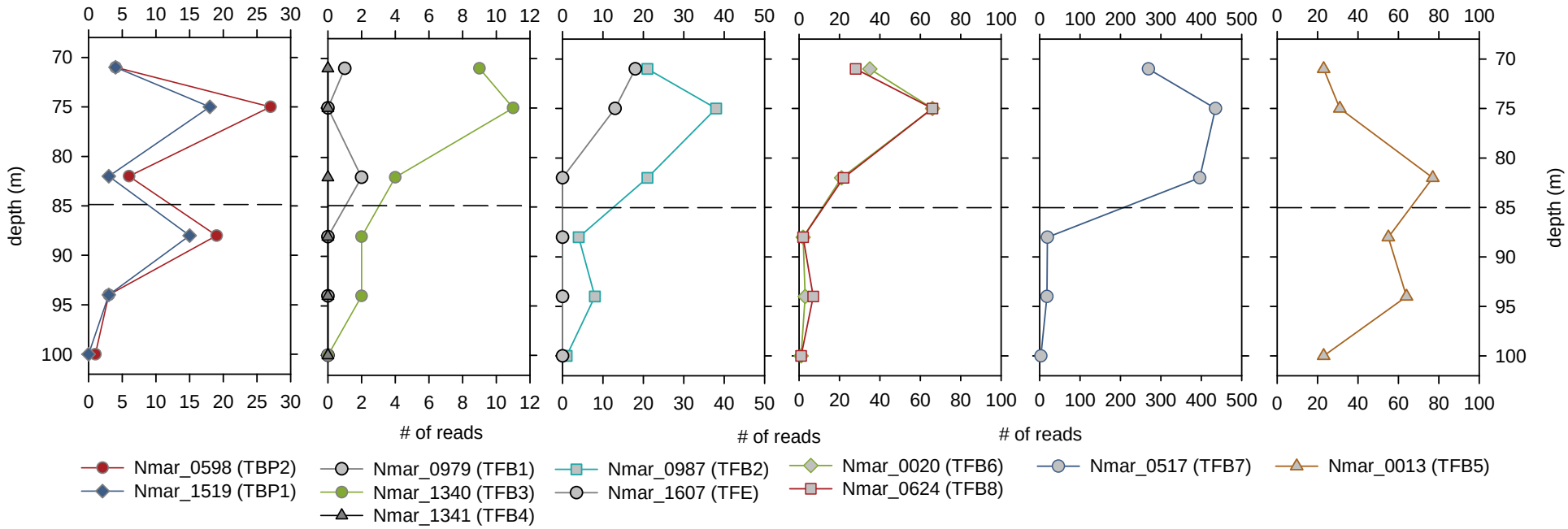

Figure 3.7.: Transcript levels of genes coding for transcription factor B (TFB1-TFB8), transcription factor E (TFE) and transcription binding proteins (TBP1 and TBP2) in the genome of *Ca.* Nitrosopumilus maritimus along the chemically stratified redox gradient based on a TBLASTN search (e-value cutoff: 10^{-4}). Note the different scaling of the x-axes. Raw read counts, not normalized.

3.3.3.2 Potential changes in carbon metabolism by Thaumarchaeota

Although the highest abundance of Thaumarchaeota is co-located with the presumed nitrification zone, a notable discrepancy between abundance and transcriptional activity is seen, mainly within the sulfidic zone where cell numbers are high while overall transcript levels were reduced (Figure 3.4). Here, abundance remains rather stable as previously reported (Labrenz *et al.*, 2010; Berg *et al.*, in press) and may be sustained by the expression of selected genes to ensure survival in the sulfidic zone. Since energy conservation is limited in these depths, changes in cellular metabolism may occur. One of the few genes that showed a contrasting transcription pattern to that of most other genes is *pckA* (`Nmar_0392`) encoding for phosphoenolpyruvate carboxykinase (PEPCK) in the genome of *Ca.* N. maritimus (Walker *et al.*, 2010). Transcript levels of *pckA* were significantly elevated in and increased towards the sulfidic zone (Figure 3.15). For bacteria it has been shown that *pckA* expression is dependent on the carbon-source and that intensified *pckA*-transcription might indicate a shift in the carbon metabolism towards the gluconeogenic pathway (Sauer and Eikmanns, 2005). As in the sulfidic zone, aerobic ammonia oxidation is not possible, CO_2-fixation may be reduced due to the lack of energy. PEP-carboxykinase may link the C_4 and C_3 carbon pools in *Ca.* N. maritimus by converting oxaloacetate to phosphoenolpyruvate (Könneke *et al.*, 2014). Studies with *Escherichia coli* showed that the activity of PEPCK is allosterically regulated as high levels of ATP or PEP repressed PEPCK activity (Krebs and Bridger, 1980). Whether this regulation functions similar in *Ca.* N. maritimus and is also reflected on the transcription level remains to be tested. Investigations on the functioning of PEPCK in *Ca.* N. maritimus or other Thaumarchaeota under energy-stress appear a worthwhile task, especially in the light of recent findings that emphasized the role of small organic carbon compounds and mixotrophy for close relatives of *Ca.* N. maritimus (Qin *et al.*, 2014) and the requirement of pyruvate for efficient growth by e.g. *Nitrososphaera viennensis* (Tourna *et al.*, 2011).

3.3.3.3 Importance of the thaumarchaeotal surface layer

Transcript levels of `Nmar_1201` and `Nmar_1547`, corresponding to the genes *slp1* and *slp2*, respectively, which potentially code for the surface layer (S-layer) proteins of *Ca.* N. maritimus (Hollibaugh *et al.*, 2011; Nakagawa and Stahl, 2013) were elevated in all depths. S-layer genes belong to the most strongly expressed genes in archaea (Sára *et al.*, 2000; Keller *et al.*, 2013) and a large portion of transcription activity may be dedicated to the

S-layer genes. The extent of transcription activity for *slp1* and *slp2* in relation to all transcribed genes by *Ca.* N. maritimus varied throughout the redox gradient and was increasing towards the sulfidic depths (Figure 3.8).

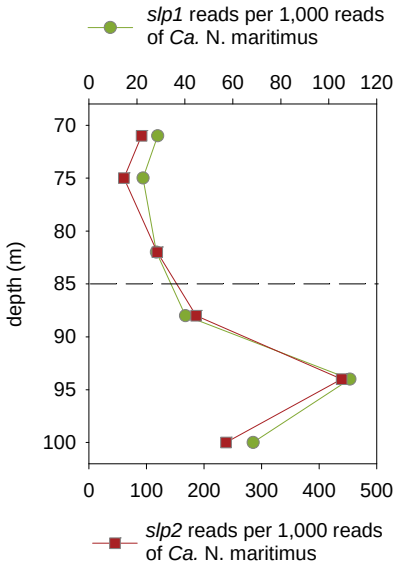

Figure 3.8.: Organism-specific normalization of S-layer gene (*slp*) transcript levels relative to total transcript levels of *Ca.* N. maritimus throughout the redox gradient. The dashed horizontal line separates the hypoxic from the lower sulfidic depths.

This suggests that a sufficient supply with surface layer proteins, which are essential for the archaeal cell envelope, is important outside the thaumarchaeotal activity zone to ensure survival under both anoxic and sulfidic conditions. This may also explain the relatively stable thaumarchaeotal cell abundances in moderately sulfidic waters as reported by Labrenz *et al.* (2010) and Berg *et al.* (in press) and as quantified within the redox-gradient of Landsort Deep, 2009, in this study.

3.3.3.4 Chemotaxis by *Sulfurimonas* sp. subgroup GD17

Figure 3.5 displays the activities of the investigated prokaryotes throughout the gradient. Relating these patterns to cellular abundances shows a discrepancy between abundance and activities in some depths located outside the major activity zones (Figure 3.4).

The optimal conditions for members of the *Sulfurimonas* sp. subgroup GD17 are characterized by the availability of both nitrate and reduced sulfur compounds, which may be ensured around the oxic-anoxic interface but in deeper sulfidic depths the availability of nitrate may be limited as nitrate appears predominantly in non-sulfidic waters. Autecological studies with *Sulfurimonas gotlandica* str. GD1 have shown that this strain may tolerate low amounts of oxygen (Grote *et al.*, 2012; Farnelid *et al.*, 2013; Labrenz

et al., 2013) albeit there was no indication that O_2 is utilized as an electron acceptor. Additionally, *S. gotlandica* str. GD1 possesses the genomic capacity for chemotaxis as well as for flagella, which was supported by electron micrographs that showed the cells with a monopolar flagellum and through experiments demonstrating chemotactic response to nitrate (Grote *et al.*, 2012). Within the investigated redox gradient metatranscriptomes, the genes for chemotaxis and flagella assembly (Table A.4) showed significant transcript levels (Figure 3.9, Figure A.9). *S. gotlandica* attributes a much higher part of transcription to the expression of chemotaxis (Figure 3.9) when compared to overall transcription activity, which declined in these depths. Supporting, flagella related genes are less active within the comfort zones (Figure A.9) in which the supply with electron donors and acceptors may not necessitate migration of the bacteria to higher concentrations of such.

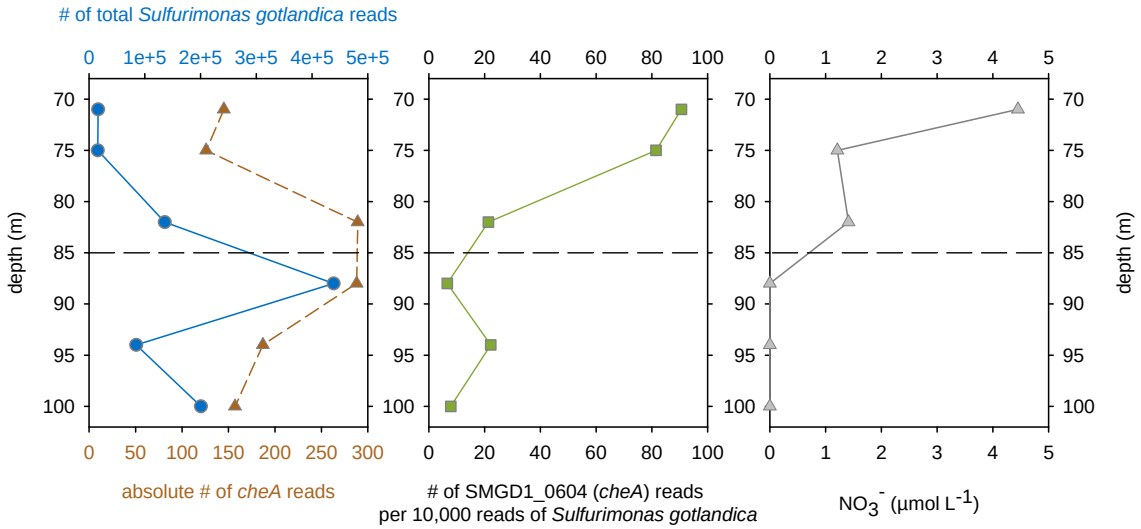

Figure 3.9.: Not normalized raw read counts (left panel) and organism-specific normalization (middle) of read counts of *cheA*, involved in chemotaxis. Reads per 10,000 *Sulfurimonas gotlandica* reads in relation to nitrate concentrations (right panel).

3.3.4 Transcriptional proxies for biogeochemical activities

The presence of biogeochemical processes was indicated by significant transcript levels of genes that are associated with ammonia oxidation, sulfur oxidation, denitrification or CO_2 fixation. The vertical allocation of e.g. *amo*, *nap*, *cbb* or *oor* transcripts reflects zones, which were previously recognized for active nitrification or CO_2 fixation activities, respectively (Hietanen *et al.*, 2012; Jost *et al.*, 2008; Grote *et al.*, 2008).

3.3.4.1 Archaeal ammonia oxidation

The *amoA* gene is typically used as a marker gene for ammonia oxidation (Rotthauwe *et al.*, 1997). Transcript levels of archaeal *amoA* and the subunits *BCX* were detected throughout the gradient, comprising particularly high levels within the hypoxic zone. This suggests high activities by Thaumarchaeota that oxidize ammonium (Figure 3.10) in the zone of overlapping ammonium and oxygen gradients, concurrent with previous observations of *amoA* transcript abundances in Baltic Sea redox gradients (Labrenz *et al.*, 2010; Feike *et al.*, 2012) and nitrification rate measurements (Hietanen *et al.*, 2012; Berg *et al.*, in press).

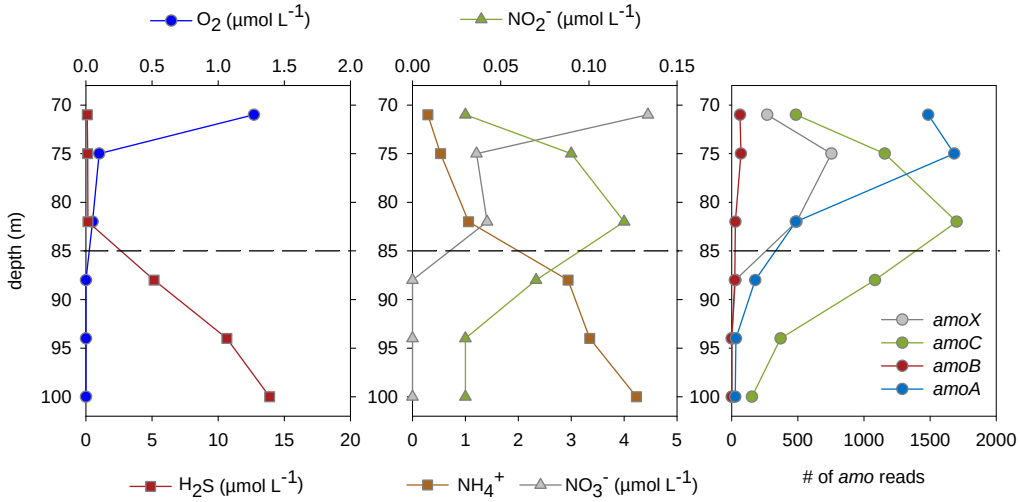

Figure 3.10.: Levels of gene transcripts (right panel) of the different *amo* subunits *A, B, C* and *X* of *Ca.* Nitrosopumilus maritimus along the pelagic redox gradient based on a TBLASTN analysis, e-value cutoff: 10^{-4}, raw read counts, not normalized.

Among all detected transcripts assigned to genes of the *Ca.* N. maritimus genome, the *amo* genes comprised, among others, high transcript levels throughout the gradient, emphasizing the importance of ammonia oxidation for this organism. Displaying the significance of assignment of the TBLASTN search in more detail for *amoA* of *Ca.* N. maritimus, it became evident that the majority of the alignments with the metatranscriptome reads showed a very low e-value and high sequence similarity (Figure 3.11), reflecting the phylogenetically close affiliation of the Baltic Sea thaumarchaeotal cluster (Labrenz *et al.*, 2010) to *Ca.* N. maritimus (2% distance based on 16S rRNA) also in terms of environmental *amoA* transcripts. It strengthens the finding by Labrenz *et al.* (2010) that the potential archaeal ammonia oxidizers in the Baltic Deeps are represented by only one archaeal phylogenetic group.

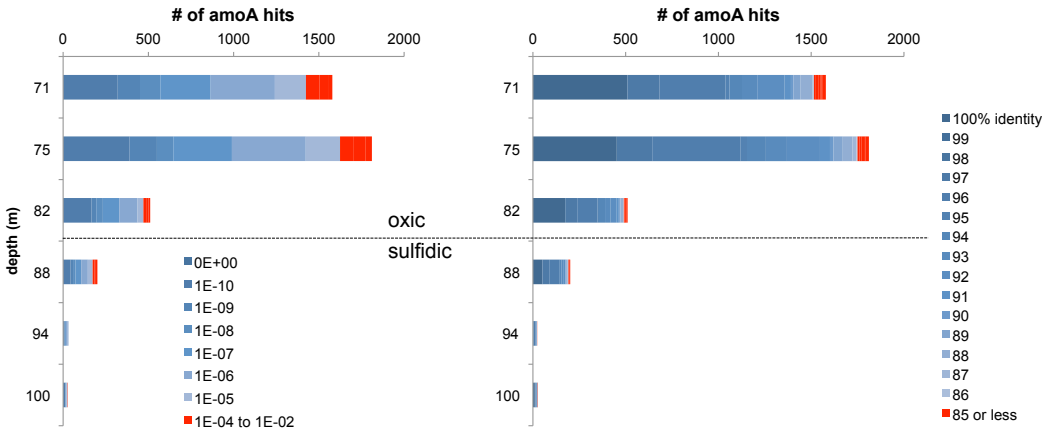

Figure 3.11.: Number of *amoA* gene transcripts along the pelagic redox gradient including information on the e-value (left panel) or % identity (right panel) of the subject (transcript read) to the query gene (`Nmar_1500`, *amoA*), based on a TBLASTN analysis. The dashed horizontal line separates the hypoxic from the lower sulfidic depths.

The lifestyle of Thaumarchaeota is largely determined by the environmental availability of ammonium as electron donor needed for energy conservation with oxygen. To ensure supply with sufficient concentrations of ammonium inside the cells, these can rely on passive diffusion if the environmental ammonium concentration is high or take up ammonium actively through transporters into the cell. The genome of *Ca.* N. maritimus harbors a variety of transporter genes (Offre *et al.*, 2014) of which two genes code for the ammonium transporters (Walker *et al.*, 2010), *amt1* (`Nmar_0588`) and *amt2* (`Nmar_1698`). Transcripts of these two *amt* genes were detected at different abundances throughout the gradient (Figure 3.12) with those of *amt2* correlating negatively with ammonium concentrations, being highest at ammonium concentrations below 1 µmol L^{-1}, which suggests that expression of *amt2* is coupled to very low concentrations of ammonium.

In contrast, *amt1* transcript levels were generally less pronounced but showed a peak in 82 m, the last oxic depth investigated before the transition into the sulfidic zone, while following the pattern of ammonium concentrations if considering only the hypoxic zone. In an elegant study, Nakagawa and Stahl (2013) determined abundances of *amt1* and *amt2* transcripts via quantitative PCR in dialysis bag cultures of *Ca.* N. maritimus that were exposed to minimal ammonium concentrations (<10 nmol L^{-1}) below its K_m (133 nmol L^{-1}, Martens-Habbena *et al.*, 2009). In their starvation experiment, *amt2* transcripts were about 10-fold more abundant than those of *amt1*, comparable to what we found in the Landsort Deep redox gradient. The authors suggested that the two Amt have different affinities, with Amt1 being the most affine of the two. However, inferring enzymatic affinities from quantitative PCR data or metatranscriptomic transcript levels may be limited.

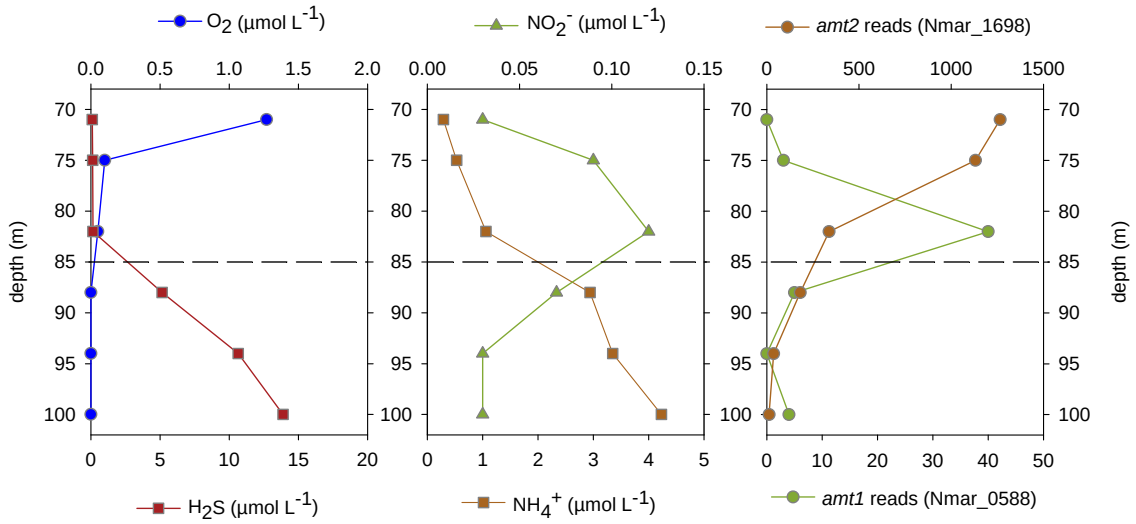

Figure 3.12.: Concentrations of oxygen, hydrogen sulfide, nitrite, ammonium and transcript levels of *amt1* and *amt2* throughout the redox gradient based on a TBLASTN search (not normalized, raw read counts). The dashed horizontal line separates the hypoxic from the lower sulfidic depths.

Nevertheless, the high transcript levels of *amt2* at low ammonium concentrations may result in increased translation of *amt2* mRNA and therefore in increased synthesis of the Amt2 ammonium transporter. The resulting cellular equipment with sufficient ammonium transporters may facilitate the efficient uptake of ammonium at low ambient concentrations.

3.3.4.2 Sulfur cycling and denitrification by *Sulfurimonas* and SUP05

In the genome of *Sulfurimonas gotlandica*, the *sox*-dependent sulfur oxidation pathway is encoded by two gene clusters of the *sox* operon, which comprise nine genes for the Sox multienzyme complex (Grote *et al.*, 2012). The *sqr* gene, coding for sulfide:quinone oxidoreductase, is present in 5 potential copies (Grote *et al.*, 2012). The transcript levels of the *sox* and *sqr* genes along the redox gradient (Figure 3.14) were relatively high in depths below 82 m, where sulfide was detected at concentrations between 0.15–13.9 µmol L^{-1}. The *oorDABC* genes, associated with CO_2 fixation by *Sulfurimonas* via 2-Oxoglutarate:ferredoxin oxidoreductase, were most active in 88 and 94 m, slightly below the oxic-anoxic interface. This is in line with biogeochemical measurements of dark CO_2 fixation rates in pelagic redox gradients by e.g. Jost *et al.* (2008) and Grote *et al.* (2008), who detected the CO_2 fixation maximum to be located below the onset of hydrogen sulfide, where the H_2S concentration gradient presumably allows for sufficient energy conservation with nitrate since in deeper depths nitrate is missing as electron acceptor.

The SUP05 metagenome (Walsh *et al.*, 2009) contains the genetic repertoire for sulfur oxidation, nitrate respiration and CO_2 fixation as represented by gene clusters for *sox*, *dsr*, *nar*, *nap* and *cbb*, respectively. These were also detected in the present redox gradient metatranscriptomic dataset at significant abundances of transcript reads around the intersection of hypoxic with sulfidic water masses. Comparing the depths in which *S. gotlandica* and SUP05 exhibit their highest transcript levels of genes that are relevant to the sulfur oxidation, denitrification and CO_2 fixation, both chemoautotrophs show overlapping ranges of respective transcript levels (Figure 3.13, Figure 3.14), with SUP05 being shifted towards more oxic and *Sulfurimonas* sp. towards sulfidic conditions, respectively. This strikingly similar niche-partitioning may indicate competition for reduced sulfur compounds as electron donors and oxidized nitrogen compounds as electron acceptors between both chemoautotrophs.

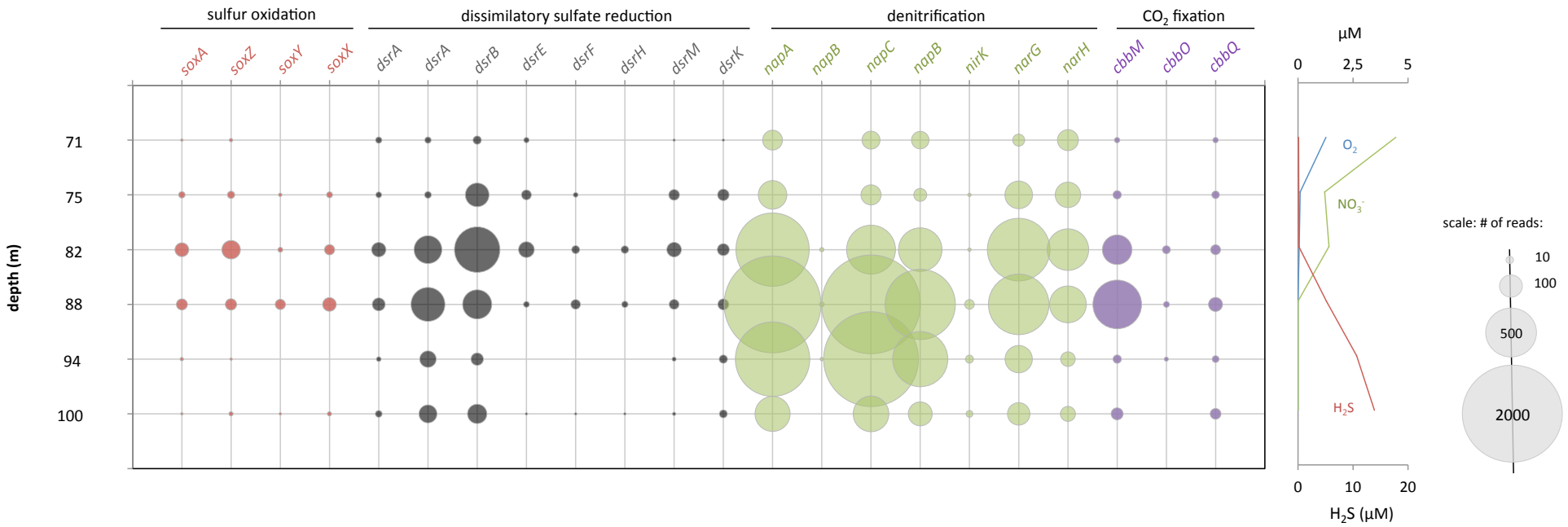

Figure 3.13.: Transcript levels of genes coding for biogeochemically relevant pathways of the SUP05 metagenome along the chemically stratified redox gradient based on a TBLASTN search (e-value cutoff: 10^{-4}). Raw read counts, not normalized.

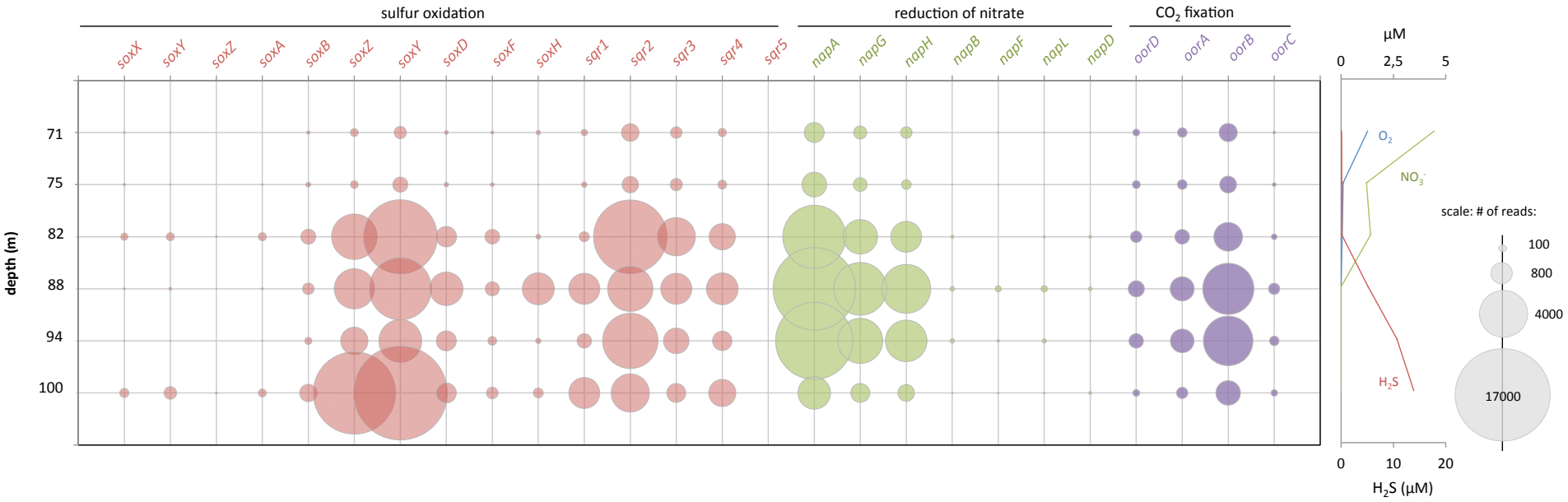

Figure 3.14.: Transcript levels of genes coding for biogeochemically relevant pathways of the genome of *Sulfurimonas gotlandica* along the chemically stratified redox gradient based on a TBLASTN search (e-value cutoff: 10^{-4}). Raw read counts, not normalized.

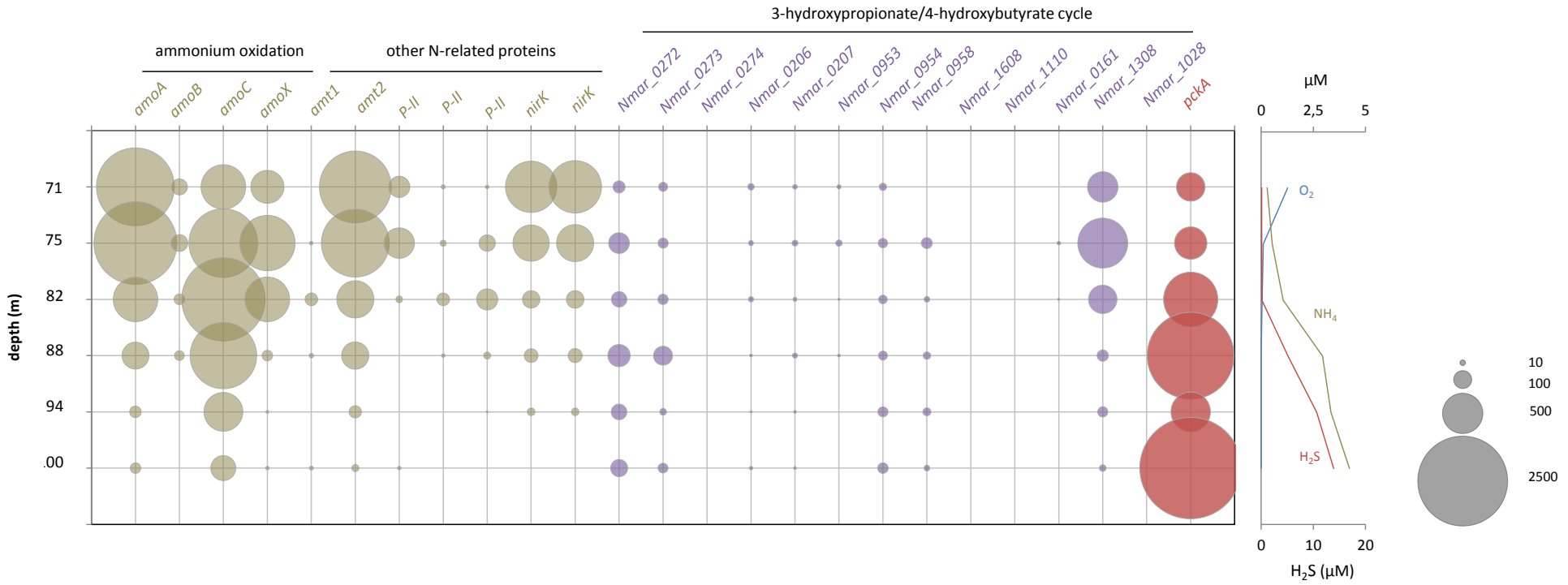

Figure 3.15.: Transcript levels of genes coding for biogeochemically relevant pathways of the genome of *Ca.* Nitrosopumilus maritimus along the chemically stratified redox gradient based on a TBLASTN search (e-value cutoff: 10^{-4}). Raw read counts, not normalized.

3.3.4.3 Fixation of inorganic carbon

Cumulatively adding up the transcript levels of genes that are associated with the respective CO_2 fixation pathways of *Ca.* N. maritimus, *Sulfurimonas gotlandica* and SUP05, revealed that transcriptiom related to inorganic carbon fixation is located in distinct and group-specific depths within the redox gradient (Figure 3.16). Thaumarchaeota exhibit their highest activities within the hyoxic zone, where they also display maximal *amo* transcript levels while *S. gotlandica* and SUP05 are most active in terms of CO_2 fixation in the upper sulfidic zone and around the oxic-anoxic interface layer, respectively. The *cbb* transcripts assigned to SUP05 display a sharp peak within the gradient, in depths of 82 and 88 m, which correspond to almost anoxic (0.05 µmol O_2 L^{-1}) and moderately sulfidic (5.2 µmol H_2S L^{-1}) conditions, respectively. In contrast, CO_2 fixation by *Sulfurimonas gotlandica* covers a broder range of depths including higher sulfide concentrations of 13.9 µmol H_2S L^{-1} in 100 m.

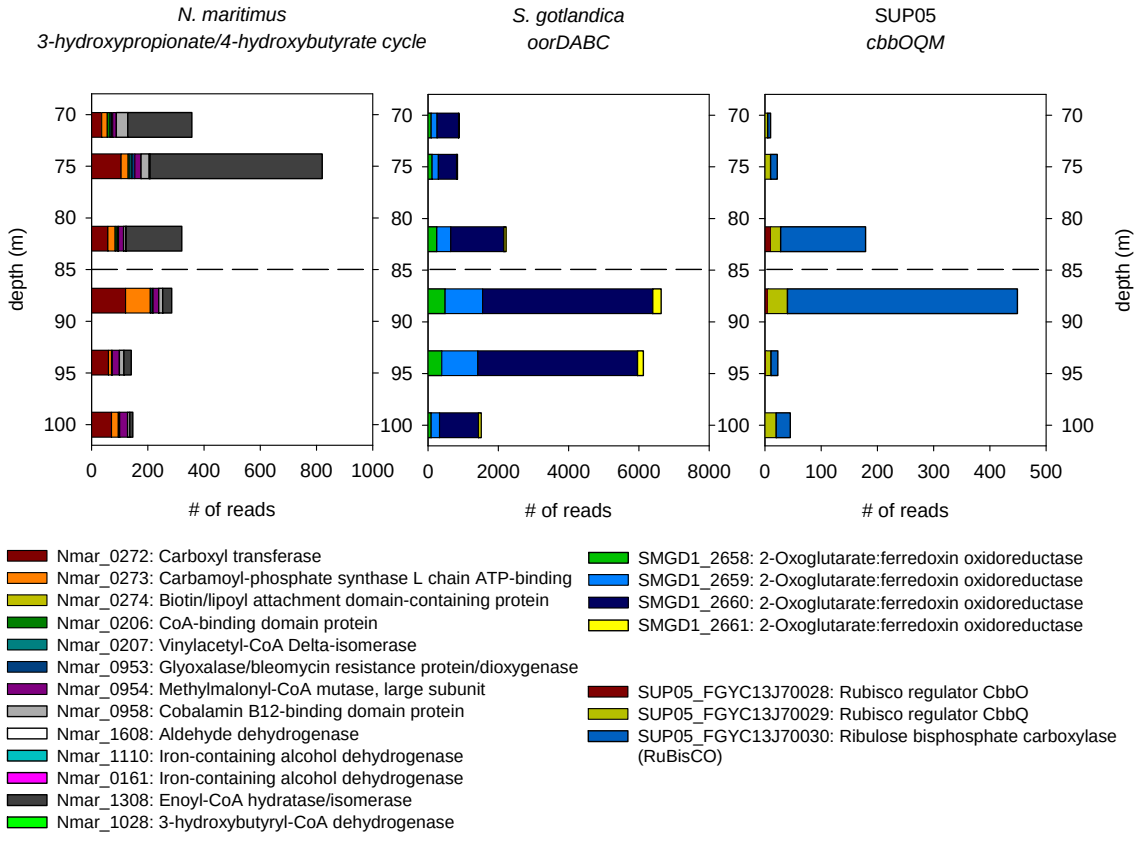

Figure 3.16.: Transcript levels of CO_2 fixation associated genes of the three chemoautotrophs. Raw read counts, not normalized. The e-value cutoff was set to 10^{-4}. The dashed horizontal line separates the hypoxic from the lower sulfidic depths.

3.4 Conclusions and implications

The current study illuminates the underlying gene expression of the dominating chemolithoautotrophs of Baltic Sea pelagic redox gradients as represented by one abundant thaumarchaeotal subcluster, the sulfur-oxidizing *Sulfurimonas* sp. subgroup GD17 and the potentially sulfur-oxidizing SUP05 cluster. The localization of discrete and group-specific "comfort zones" of elevated activities at specific chemical niches throughout the redox gradient of Landsort Deep revealed specific zones of highest activities and potential optimal energetic exploitation of redox-species. Outside these zones, where organism-specific transcript levels were decreased, the importance of particular genes was increased as evidenced by a higher portion of transcription activity attributed to genes coding for chemotaxis, flagella, surface layer proteins, transcription factors or carbon metabolism associated genes. These features provide first insights into strategies to cope with unfavorable conditions by Baltic Sea chemolithoautotrophs as they may be experienced at the boundaries of the redox gradients. The detected activities by Thaumarchaeota within the sulfidic zone imply that the abundant cells in this zone are viable and may perform changes in their carbon metabolism, that were previously unknown. Altogether, these results offer insights into the transcription and regulation of chemoautotrophs within a Baltic Sea pelagic redox gradient.

Synthesis and future perspectives

SYNTHESIS AND FUTURE PERSPECTIVES

The discoveries of ammonia oxidation within the archaeal domain came about one decade ago. Since then, astonishing findings were made with major implications for the fundamental understanding of the global nitrogen cycle. Nevertheless, the broad phylogenetic diversity with many different thaumarchaeotal physiologies still holds a magnitude of features and functions to uncover. In the meanwhile, ammonia-oxidizing Thaumarchaeota have been recognized as one of the most abundant and important prokaryotic groups that shape the functioning of the nitrogen cycle in many aquatic ecosystems.

Following up the study by Labrenz *et al.* (2010), the present thesis has set the focus on the contributions to nitrification and chemoautotrophy by archaeal ammonia oxidizers as well as on their adaptations to and niche-differentiation within pelagic redox gradients of the Baltic Sea deep basins. In the context of the results presented in this thesis it became evident that the occurrence and activities of Thaumarchaeota are not limited to episodic observations. In fact, ammonia-oxidizing Thaumarchaeota are enduring components of the Baltic Sea pelagic redox gradients and resemble ecologically important prokaryotes since ecosystem-relevant processes are dependent on the activities of these microorganisms.

Accomplishments

The occurrence of both Thaumarchaeota and nitrification were for the first time investigated simultaneously in Baltic Sea pelagic redox gradients and a direct link between this process and the activities of archaea was established via archaeal-specific inhibition experiments in environmental samples. Further insights were gained on the impact of sulfide on the activities of Baltic Sea nitrifying assemblages, which appear to be particularly well adapted to episodic exposure to sulfide since nitrification was detectable at significant rates after spiking of environmental samples with sulfide. Henceforth, the presence and biogeochemical involvement of ammonia-oxidizing Thaumarchaeota can be considered as enduring components of Baltic Sea pelagic redox gradients (Chapter 1).

As physiological features and growth parameters of specific prokaryotes are difficult to acquire from a mixed community, an ammonia-oxidizing thaumarchaeotal enrichment culture was established in the scope of this thesis, originating from the Landsort Deep redox gradient. This enrichment, phylogenetically falling into a low-salinity group and affiliated with *Ca.* Nitrosoarchaeum limnia was used for quantification of chemoautotrophy and its coupling to ammonia oxidation during batch growth. From this study it emerged that chemoautotrophy accounts for the major fraction of carbon uptake in natural seawater-based enrichments of this member of the Thaumarchaeota (Chapter 2).

The Baltic Sea thaumarchaeotal subcluster GD2 is embedded within a chemoautotrophic community, which also comprises members of the *Sulfurimonas* sp. subgroup GD17 and the SUP05 cluster. To examine the activities of Thaumarchaeota within this chemoautotrophic community and their enigmatic role in the sulfidic zone, a metatranscriptomic dataset was analyzed. Transcript recruitment to specific reference genomes of close relatives of the thaumarchaeotal subcluster GD2, *Sulfurimonas* sp. subgroup GD17 and the SUP05 cluster revealed group-specific patterns of elevated activities throughout the redox gradient, covering distinct "comfort zones". Outside these comfort zones, specific patterns of genes related to S-layer proteins, transcription factors, carbon metabolism, ammonium transporters (*Ca.* N. maritimus) or chemotaxis and flagella assembly (*Sulfurimonas* sp. subgroup GD17) were identified as being relevant for appropriate responses to chemically unfavorable conditions (Chapter 3).

Specifically, the following findings were made:

Chapter 1:

- Thaumarchaeota were found to be abundant at three sites with pelagic redox gradients, which were sampled throughout the years 2009 (Chapter 3) and 2011-2012 (Chapter 1) certifying an enduring chemoautotrophic group in Baltic Sea pelagic redox gradients
- Nitrification was substantially driven by ammonia-oxidizing archaea, being responsible for up to 86–100% of the rates
- Nitrification activities were found to be robust against *in-situ*-like concentrations of hydrogen sulfide, accompanied by the detection of a significant nitrification potential that accounted for 62 nmol L^{-1} d^{-1} in a sample from the sulfidic zone (3 µmol H_2S L^{-1})

Chapter 2:

- A thaumarchaeotal enrichment was established from the brackish Baltic Sea pelagic redox gradient at the Landsort Deep
- The enrichment was affiliated with *Ca.* Nitrosoarchaeum limnia and performed chemoautotrophy, which accounted for a substantial fraction (9 fg $cell^{-1}$) of cellular biomass
- During exponential growth phase of the AOA enrichment, 10 N were oxidized per 1 C fixed

Chapter 3:

- Each of the investigated chemoautotrophs displayed a specific zone of elevated activities of genes for CO_2 fixation, ammonia oxidation, sulfur oxidation or denitrification

  Thaumarchaeota:

- The zone of highest activities (based on all active genes) was localized within oxic conditions that allow for aerobic oxidation of ammonia
- Ammonium transporters *amt1* and *amt2* showed differential patterns of transcript levels and may be regulated by ambient ammonium concentrations. High transcript levels of *amt2* at low ammonium concentrations may explain the previously reported high substrate affinity through increased synthesis of ammonium transporter
- The fraction of transcript levels for S-layer proteins *slp1* and *slp2* increased towards sulfidic conditions suggesting increased importance of protection of the cells
- Nearly all (7) of the 8 transcription factors B (TFB) of *Ca.* N. maritimus were active throughout the redox gradients with differential patterns, suggesting a complex gene regulatory network to adapt to different chemical conditions
- Transcript reads of archaeal *amoA* were closely related to *Ca.* N. maritimus-like *amoA* sequences throughout the gradient, confirming that archaeal ammonia oxidation is almost exclusively performed by a single thaumarchaeotal subcluster in Baltic Sea redox gradients
- Transcript levels of *pckA* increased towards sulfidic depths indicating potential shifts in carbon metabolism

  Sulfurimonas sp. subgroup GD17 and SUP05:

- The patterns of total transcript levels by *Sulfurimonas gotlandica* and SUP05 occupied nearly identical zones within the redox gradient with SUP05 shifted rather towards the oxic and *Sulfurimonas gotlandica* towards the sulfidic conditions raising the question whether these two bacterial assemblages compete for the same reduced sulfur compounds and oxidized nitrogen compounds
- Transcription of genes related to chemotaxis and the assembly of flagella outside the activity zone of *Sulfurimonas* sp. subgroup GD17 may indicate active movements within microgradients for ensuring sufficient energy conservation

Future perspectives

The investigations of the present thesis advance our understanding of Baltic Sea Thaumarchaeota and add new aspects to the niche-determining factors that influence global distributions of AOA (Francis *et al.*, 2005; Erguder *et al.*, 2009) and their involvements in biogeochemical cycles of nitrogen and carbon. The fixation of inorganic carbon from CO_2, chemoautotrophy, has been a major focus of the conducted studies of the present thesis and was shown to be important for growth by certain members of the Thaumarchaeota as seen from enrichment cultures, expression of thaumarchaeotal CO_2 fixation genes or co-occurrence of CO_2 fixation activities with elevated Thaumarchaeota abundances in natural pelagic redox gradients. However, the uptake of additional organic compounds, which would comprise a mixotrophic lifestyle, has not been investigated in the scope of this thesis. Mixotrophy is a feature that has been debated for ammonia-oxidizing Thaumarchaeota since the beginning of their discoveries (Ingalls *et al.*, 2006). Only recently, the study by Qin *et al.* (2014) contributed with new details on obligate mixotrophy by marine AOA. The authors isolated two new maritime AOA strains, exhibiting 99% 16S rRNA gene sequence similarity with *Ca.* N. maritimus. By studying their physiological adaptations to salinity or pH and the utilization of organic compounds they found a strong ecotype variation, despite a close phylogenetic affiliation as well as an obligate requirement of α-ketoglutaric acid for sufficient growth. The obligate mixotrophy by these two novel strains and the dependance on pyruvate by *Nitrososphaera viennensis* (Tourna *et al.*, 2011) may indicate that mixotrophy is more widespread in Thaumarchaeota than currently known. Even if the contribution of organic substrates in relation to overall cellular carbon uptake is low, it may represent a significant additional carbon sink given the global distribution and abundance of Thaumarchaeota (Francis *et al.*, 2005). Despite the finding of the current thesis that the enriched *Nitrosoarchaeum* relative (Chapter 2) is mainly growing on inorganic carbon, further tests with a spectrum of organic compounds appear to be worthwhile as well as its isolation and transfer to a defined medium to enable controlled growth conditions. As the enrichment was cultivated on natural, cell-free seawater, which contains dissolved organic carbon, the additional uptake of organic carbon besides the fixation of inorganic carbon cannot be precluded.

The observations on thaumarchaeotal gene transcripts of *pckA* in sulfidic zone by metatranscriptomics further suggested, that the carbon metabolism is subject to changes under conditions that preclude energy conservation such as they are encountered in the

anoxic, sulfidic waters (Chapter 3). While thaumarchaeotal activity was decreased in the sulfidic zone, the gene for phosphoenol carboxykinase by *Ca.* N. maritimus displayed substantial and increasing transcript levels towards the sulfidic depths. This enzyme is the only link between C_4 and C_3 carbon compounds in *Ca.* N. maritimus (Könneke *et al.*, 2014). The importance of C_3 compounds such as pyruvate for Thaumarchaeota has been demonstrated previously (Tourna *et al.*, 2011) and may therefore play also a role in the Baltic Sea pelagic redox gradients. However, the role of *pckA* for e.g. growth and survival of Thaumarchaeota remains to be resolved.

Impact of lateral intrusions on nitrification activities

The studies of the present thesis were carried out at the redox gradients of the Bornholm Deep, Gotland Deep and the Landsort Deep, geographically near the deepest point of these deeps. The depths at which the redox gradients were located ranged between 70–130 m at Gotland Deep and Landsort Deep while at the Bornholm Deep, reduced compounds accumulated above the seafloor between 78–86 m. Given the hydrological properties of the Baltic Sea, which restrict inflow of North Sea water, the investigated redox gradients in the central Baltic Sea can be considered rather stable and as only rarely influenced by major lateral inflow events.

During the *R/V* Meteor research cruise M87-3b to the central Baltic in June 2012, a minor inflow event was observed at station TF260 at the southern border of the eastern Gotland Basin. The water column comprised a pronounced local maximum in oxygen concentrations directly above sulfidic waters and below oxygen-depleted waters (Figure 5). The upper and lower margins of the oxygenated waters were flanked by nitrite accumulation while nitrate co-occurred with oxygen. In the depths of nitrite accumulation, samples were taken and potential nitrification rates determined as described in Chapter 1. At both the upper and the lower margins of the inflow-water, the potential nitrification activities accounted for 178–324 nmol L^{-1} d^{-1}. Even in close proximity to sulfidic waters, the nitrification activities were substantial and comparable to the highest rates (122–884 nmol L^{-1} d^{-1}), which were measured in the deep basins (Chapter 1). This observation suggests that mixing of different water bodies has substantial effects also on nitrogen transformations, potentially sustained by well-adapted ammonia-oxidizing Thaumarchaeota, that are capable of active ammonia oxidation upon oxygenation.

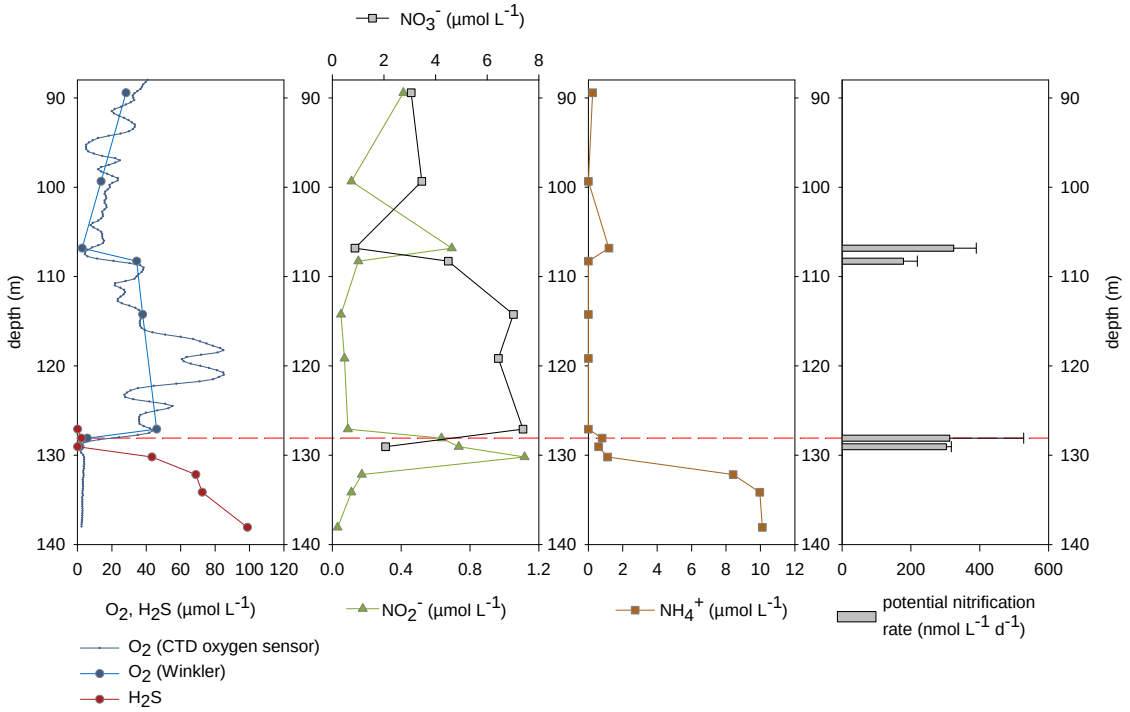

Figure 5.: Lateral intrusion of oxygenated water at station TF260 at the southern border of the Gotland Basin in June 2012. Measurements of the parameters were performed as described in Chapter 1. The dashed line represents accumulation of 2.3 µmol H_2S L^{-1} in 128 m depth.

Stimulation experiments focusing on activities by the denitrifying *Sulfurimonas* sp. subgroup GD17 demonstrated that high CO_2 fixation activities can be induced if substrates for energy conservation are made available (Labrenz *et al.*, 2005). Large- but also small-scale mixing may therefore play significant roles in the dynamics of biogeochemical cycling in the Baltic. The extrapolation of rate measurements made in stable waters may therefore lead to an under- or overestimation of stimulated or inhibited processes, respectively, if not regarding the variability in process rates caused from mixing. Future investigations on the effect of mixing water layers on biogeochemical activities of Thaumarchaeota may provide further insights into their ecological plasticity and adaptations.

Agogué, H., Brink, M., Dinasquet, J., and Herndl, G.J., Major gradients in putatively nitrifying and non-nitrifying Archaea in the deep North Atlantic. *Nature*, 456 (2008) (7223): 788–791. doi: 10.1038/nature07535 (Cited on page 18.)

Alonso-Sáez, L., Waller, A.S., Mende, D.R., Bakker, K., Farnelid, H., Yager, P.L., Lovejoy, C., Tremblay, J.E., Potvin, M., Heinrich, F., Estrada, M., Riemann, L., Bork, P., Pedrós-Alió, C., and Bertilsson, S., Role for urea in nitrification by polar marine Archaea. *Proceedings of the National Academy of Sciences of the United States of America*, 109 (2012) (44): 17989–17994. doi: 10.1073/pnas.1201914109 (Cited on pages 11 and 42.)

Alves, R.J.E., Wanek, W., Zappe, A., Richter, A., Svenning, M.M., Schleper, C., and Urich, T., Nitrification rates in Arctic soils are associated with functionally distinct populations of ammonia-oxidizing archaea. *The ISME Journal*, 7 (2013) (2): 1620–1631. doi: 10.1038/ismej.2013.35 (Cited on page 18.)

Amann, R.I., Krumholz, L., and Stahl, D.A., Fluorescent-oligonucleotide probing of whole cells for determinative, phylogenetic, and environmental studies in microbiology. *Journal of Bacteriology*, 172 (1990) (2): 762–770 (Cited on page 45.)

Amano-Sato, C., Akiyama, S., Uchida, M., Shimada, K., and Utsumi, M., Archaeal distribution and abundance in water masses of the Arctic Ocean, Pacific sector. *Aquatic Microbial Ecology*, 69 (2013) (2): 101–112. doi: 10.3354/ame01624 (Cited on page 18.)

Arp, D.J., Sayavedra-Soto, L.a., and Hommes, N.G., Molecular biology and biochemistry of ammonia oxidation by *Nitrosomonas europaea*. *Archives of microbiology*, 178 (2002) (4): 250–5. doi: 10.1007/s00203-002-0452-0 (Cited on page 10.)

Auguet, J.C. and Casamayor, E.O., Partitioning of Thaumarchaeota populations along environmental gradients in high mountain lakes. *FEMS microbiology ecology*, 84 (2013) (1): 154–64. doi: 10.1111/1574-6941.12047 (Cited on page 8.)

Auguet, J.C., Triadó-Margarit, X., Nomokonova, N., Camarero, L.L., Casamayor, E.O., and Triado-Margarit, X., Vertical segregation and phylogenetic characterization of ammonia-oxidizing Archaea in a deep oligotrophic lake. *The ISME Journal*, 6 (2012) (9): 1786–1797. doi: 10.1038/ismej.2012.33 (Cited on pages 8 and 18.)

Baker, B.J., Lesniewski, R.a., and Dick, G.J., Genome-enabled transcriptomics reveals archaeal populations that drive nitrification in a deep-sea hydrothermal plume. *The ISME Journal*, 6 (2012) (12): 2269–2279. doi: 10.1038/ismej.2012.64 (Cited on page 18.)

Bauer, S. (2003). Structure and function of nitrifying bacterial communities in the eastern Gotland Basin (central Baltic Sea). Ph.D. thesis, University of Rostock (Cited on pages 7, 8, and 9.)

Beman, J.M., Popp, B.N., and Francis, C.a., Molecular and biogeochemical evidence for ammonia oxidation by marine Crenarchaeota in the Gulf of California. *The ISME Journal*, 2 (2008) (4): 429–441. doi: 10.1038/ismej.2007.118 (Cited on pages 18 and 42.)

Berg, C., Beckmann, S., Jost, G., Labrenz, M., and Jürgens, K., Acetate-utilizing bacteria at an oxic-anoxic interface in the Baltic Sea. *FEMS microbiology ecology*, (2013). doi: 10.1111/1574-6941.12114

Berg, C., Listmann, L., Vandieken, V., Vogts, A., and Jürgens, K. (submitted). Chemoautotrophic growth of ammonia-oxidizing Thaumarchaeota enriched from hypoxic waters of the Baltic Sea (Cited on page 25.)

Berg, C., Vandieken, V., Thamdrup, B., and Jürgens, K. (in press). Significance of archaeal nitrification in hypoxic waters of the Baltic Sea (Cited on pages 42, 43, 44, 45, 46, 56, 57, 62, 63, 69, 76, 77, and 79.)

Berg, I.A., Kockelkorn, D., Buckel, W., and Fuchs, G., A 3-hydroxypropionate/4-hydroxybutyrate autotrophic carbon dioxide assimilation pathway in Archaea. *Science (New York, N.Y.)*, 318 (2007) (5857): 1782–6. doi: 10.1126/science.1149976 (Cited on pages 10 and 43.)

Berg, I.A., Kockelkorn, D., Ramos-Vera, W.H., Say, R.F., Zarzycki, J., Hügler, M., Alber, B.E., and Fuchs, G., Autotrophic carbon fixation in archaea. *Nature Reviews. Microbiology*, 8 (2010) (6): 447–60. doi: 10.1038/nrmicro2365 (Cited on page 10.)

Biller, S.J., Mosier, A.C., Wells, G.F., and Francis, C.A., Global biodiversity of aquatic ammonia-oxidizing archaea is partitioned by habitat. *Frontiers in Microbiology*, 3 (2012) (July): 252. doi: 10.3389/fmicb.2012.00252 (Cited on pages 18, 57, and 58.)

Blainey, P.C., Mosier, A.C., Potanina, A., Francis, C.a., and Quake, S.R., Genome of a low-salinity ammonia-oxidizing archaeon determined by single-cell and metagenomic analysis. *PloS one*, 6 (2011) (2): e16626. doi: 10.1371/journal.pone.0016626 (Cited on pages 42, 43, 54, and 57.)

Bouskill, N.J., Eveillard, D., Chien, D., Jayakumar, A., and Ward, B.B., Environmental factors determining ammonia-oxidizing organism distribution and diversity in marine environments. *Environmental Microbiology*, 14 (2012) (3): 714–29. doi: 10.1111/j.1462-2920.2011.02623.x (Cited on page 58.)

Brettar, I. and Rheinheimer, G., Denitrification in the Central Baltic: evidence for H2S-oxidation as motor of denitrification at the oxic-anoxic interface. *Marine Ecology Progress Series*, 77 (1991): 157–169 (Cited on pages 4 and 19.)

Brochier-Armanet, C., Boussau, B., Gribaldo, S., and Forterre, P., Mesophilic Crenarchaeota: proposal for a third archaeal phylum, the Thaumarchaeota. *Nature Reviews. Microbiology*, 6 (2008) (3): 245–252. doi: 10.1038/nrmicro1852 (Cited on pages 8, 18, and 42.)

Bruckner, C.G., Mammitzsch, K., Jost, G., Wendt, J., Labrenz, M., and Jürgens, K., Chemolithoautotrophic denitrification of epsilonproteobacteria in marine pelagic redox gradients. *Environmental Microbiology*, 15 (2013) (5): 1505–13. doi: 10.1111/j.1462-2920.2012.02880.x (Cited on pages 35 and 36.)

Caffrey, J.M., Bano, N., Kalanetra, K., and Hollibaugh, J.T., Ammonia oxidation and ammonia-oxidizing bacteria and archaea from estuaries with differing histories of hypoxia. *The ISME Journal*, 1 (2007) (7): 660–662. doi: 10.1038/ismej.2007.79 (Cited on pages 9, 18, 20, and 42.)

Carstensen, J., Andersen, J.H., Gustafsson, B.G., and Conley, D.J., Deoxygenation of the Baltic Sea during the last century. *Proceedings of the National Academy of Sciences*, (2014*a*) (16). doi: 10.1073/pnas.1323156111 (Cited on page 2.)

Carstensen, J., Conley, D.J., Bonsdorff, E., Gustafsson, B.G., Hietanen, S., Janas, U., Jilbert, T., Maximov, A., Norkko, A., Norkko, J., Reed, D.C., Slomp, C.P., Timmermann, K., and Voss, M., Hypoxia in the Baltic Sea: biogeochemical cycles, benthic fauna, and management. *Ambio*, 43 (2014*b*) (1): 26–36. doi: 10.1007/s13280-013-0474-7 (Cited on page 4.)

Carvajal-Arroyo, J.M., Sun, W., Sierra-Alvarez, R., and Field, J.a., Inhibition of anaerobic ammonium oxidizing (anammox) enrichment cultures by substrates, metabolites and common wastewater constituents. *Chemosphere*, 91 (2013) (1): 22–7. doi: 10.1016/j.chemosphere.2012.11.025 (Cited on page 19.)

Chain, P., Lamerdin, J., Larimer, F., Regala, W., Lao, V., Land, M., Hauser, L., Hooper, A., Klotz, M., Norton, J., Sayavedra-soto, L., Arciero, D., Hommes, N., Whittaker, M., and Arp, D., Complete genome sequence of the ammonia-oxidizing bacterium and obligate chemolithoautotroph *Nitrosomonas europaea*. *Journal of Bacteriology*, 185 (2003) (9): 2759–2773. doi: 10.1128/JB.185.9.2759 (Cited on page 43.)

Christner, B.C., Priscu, J.C., Achberger, A.M., Barbante, C., Carter, S.P., Christianson, K., Michaud, A.B., Mikucki, J.a., Mitchell, A.C., Skidmore, M.L., Vick-Majors, T.J., Adkins, W.P., Anandakrishnan, S., Barcheck, G., Beem, L., Behar, a., Beitch, M., Bolsey, R., Branecky, C., Edwards, R., Fisher, a., Fricker, H.a., Foley, N., Guthrie, B., Hodson, T., Jacobel, R., Kelley, S., Mankoff, K.D., McBryan, E., Powell, R., Purcell, a., Sampson, D., Scherer, R., Sherve, J., Siegfried, M., and Tulaczyk, S., A microbial ecosystem beneath the West Antarctic ice sheet. *Nature*, 512 (2014) (7514): 310–313. doi: 10.1038/nature13667 (Cited on page 9.)

Cline, J.D., Spectrophotometric determination of hydrogen sulfide in natural waters. *Limnology and Oceanography*, 14 (1969) (3): 454–458 (Cited on pages 21 and 24.)

Coolen, M.J.L., Abbas, B., van Bleijswijk, J., Hopmans, E.C., Kuypers, M.M.M., Wakeham, S.G., and Sinninghe Damsté, J.S., Putative ammonia-oxidizing Crenarchaeota in suboxic waters of the Black Sea: a basin-wide ecological study using 16S ribosomal and functional genes and membrane lipids. *Environmental Microbiology*, 9 (2007) (4): 1001–1016. doi: 10.1111/j.1462-2920.2006.01227.x (Cited on page 20.)

Daims, H., Brühl, A., Amann, R., Schleifer, K.H., and Wagner, M., The domain-specific probe EUB338 is insufficient for the detection of all Bacteria: development and evaluation of a more comprehensive probe set. *Systematic and Applied Microbiology*, 22 (1999) (3): 434–444. doi: 10.1016/S0723-2020(99)80053-8 (Cited on page 45.)

Dalsgaard, T., De Brabandere, L., and Hall, P.O., Denitrification in the water column of the central Baltic Sea. *Geochimica et Cosmochimica Acta*, 106 (2013): 247–260. doi: 10.1016/j.gca.2012.12.038 (Cited on page 19.)

De Brabandere, L., Thamdrup, B., Revsbech, N.P., and Foadi, R., A critical assessment of the occurrence and extend of oxygen contamination during anaerobic incubations utilizing commercially available vials. *Journal of microbiological methods*, 88 (2012) (1): 147–154. doi: 10.1016/j.mimet.2011.11.001 (Cited on page 35.)

De Corte, D., Yokokawa, T., Varela, M.M., Agogué, H., and Herndl, G.J., Spatial distribution of *Bacteria* and *Archaea* and *amoA* gene copy numbers throughout the water column of the Eastern Mediterranean Sea. *The ISME Journal*, 3 (2009) (2): 147–158. doi: 10.1038/ismej.2008.94 (Cited on page 18.)

DeLong, E.F., Archaea in coastal marine environments. *Proceedings of the National Academy of Sciences of the United States of America*, 89 (1992) (12): 5685–5689. doi: 10.1073/pnas.89.12.5685 (Cited on page 47.)

Erguder, T.H., Boon, N., Vlaeminck, S.E., and Verstraete, W., Partial nitrification achieved by pulse sulfide doses in a sequential batch reactor. *Environmental Science & Technology*, 42 (2008) (23): 8715–8720 (Cited on page 20.)

Erguder, T.H., Boon, N., Wittebolle, L., Marzorati, M., and Verstraete, W., Environmental factors shaping the ecological niches of ammonia-oxidizing archaea. *FEMS Microbiology Reviews*, 33 (2009) (5): 855–869. doi: 10.1111/j.1574-6976.2009.00179.x (Cited on pages 9, 11, 57, and 94.)

Farnelid, H., Bentzon-Tilia, M., Andersson, A.F., Bertilsson, S., Jost, G., Labrenz, M., Jürgens, K., and Riemann, L., Active nitrogen-fixing heterotrophic bacteria at and below the chemocline of the central Baltic Sea. *The ISME Journal*, 7 (2013): 1413–1423. doi: 10.1038/ismej.2013.26 (Cited on page 77.)

Feike, J., Jürgens, K., Hollibaugh, J.T., Krüger, S., Jost, G., Labrenz, M., and Kruger, S., Measuring unbiased metatranscriptomics in suboxic waters of the central Baltic Sea using a new in *in situ* fixation system. *The ISME Journal*, 6 (2012) (2): 461–470. doi: 10.1038/ismej.2011.94 (Cited on pages 18, 19, 63, 64, and 79.)

Francis, C.A., Beman, J.M., and Kuypers, M.M.M., New processes and players in the nitrogen cycle: the microbial ecology of anaerobic and archaeal ammonia oxidation. *The ISME Journal*, 1 (2007) (1): 19–27. doi: 10.1038/ismej.2007.8 (Cited on pages 5, 8, 19, and 42.)

Francis, C.A., Roberts, K.J., Beman, J.M., Santoro, A.E., and Oakley, B.B., Ubiquity and diversity of ammonia-oxidizing archaea in water columns and sediments of the ocean. *Proceedings of the National Academy of Sciences of the United States of America*, 102 (2005) (41): 14683–14688. doi: 10.1073/pnas.0506625102 (Cited on pages 8, 9, 18, 42, 47, 56, 62, and 94.)

French, E., Kozlowski, J.A., Mukherjee, M., Bullerjahn, G., and Bollmann, A., Enrichment and characterization of three ammonia-oxidizing Archaea from freshwater environments. *Applied and Environmental Microbiology*, 78 (2012) (June): 5773–5780. doi: 10.1128/AEM.00432-12 (Cited on pages 42 and 43.)

Friedrich, J., Janssen, F., Aleynik, D., Bange, H.W., Boltacheva, N., Çağatay, M.N., Dale, a.W., Etiope, G., Erdem, Z., Geraga, M., Gilli, A., Gomoiu, M.T., Hall, P.O.J., Hansson, D., He, Y., Holtappels, M., Kirf, M.K., Kononets, M., Konovalov, S., Lichtschlag, A., Livingstone, D.M., Marinaro, G., Mazlumyan, S., Naeher, S., North, R.P., Papatheodorou, G., Pfannkuche, O., Prien, R., Rehder, G., Schubert, C.J., Soltwedel, T., Sommer, S., Stahl, H., Stanev, E.V., Teaca, A., Tengberg, A., Waldmann, C., Wehrli, B., Wenzhöfer, F., and Çagatay, M.N., Investigating hypoxia in aquatic environments: diverse approaches to addressing a complex phenomenon. *Biogeosciences*, 11 (2014) (4): 1215–1259. doi: 10.5194/bg-11-1215-2014 (Cited on pages 5 and 20.)

Fuchsman, C.A., Murray, J.W., and Staley, J.T., Stimulation of autotrophic denitrification by intrusions of the bosporus plume into the anoxic black sea. *Frontiers in Microbiology*, 3 (2012) (July): 257. doi: 10.3389/fmicb.2012.00257 (Cited on page 20.)

Füssel, J., Lam, P., Lavik, G., Jensen, M.M., Holtappels, M., Günter, M., and Kuypers, M.M.M., Nitrite oxidation in the Namibian oxygen minimum zone. *The ISME Journal*, 6 (2011) (6): 1200–1209. doi: 10.1038/ismej.2011.178 (Cited on pages 23 and 46.)

Garcia, H.E., Locarnini, R.A., Boyer, T.P., Antonov, J.I., Baranova, O.K., Zweng, M.M., and Johnson, D.R. (2010). Dissolved oxygen, apparent oxygen utilization, and oxygen saturation. In S. Levitus, editor, World Ocean Atlas 2009, volume 3. U.S. Government Printing Office, Washington, D.C., noaa atlas edition (Cited on page 1.)

Glass, E.M., Wilkening, J., Wilke, A., Antonopoulos, D., and Meyer, F., Using the metagenomics RAST server (MG-RAST) for analyzing shotgun metagenomes. *Cold Spring Harbor Protocols*, 2010 (2010) (1): pdb.prot5368. doi: 10.1101/pdb.prot5368 (Cited on pages 65 and 70.)

Glaubitz, S., Kießlich, K., Meeske, C., Labrenz, M., and Jürgens, K., SUP05 dominates the gammaproteobacterial sulfur oxidizer assemblages in pelagic redoxclines of the central Baltic and Black Seas. *Applied and Environmental Microbiology*, 79 (2013) (8): 2767–2776. doi: 10.1128/AEM.03777-12 (Cited on pages 6, 7, 19, 20, 57, 62, 64, and 69.)

Glaubitz, S., Lueders, T., Abraham, W.R., Jost, G., Jürgens, K., and Labrenz, M., ^{13}C-isotope analyses reveal that chemolithoautotrophic *Gamma-* and *Epsilonproteobacteria* feed a microbial food web in a pelagic redoxcline of the central Baltic Sea. *Environmental Microbiology*, 11 (2009) (2): 326–337. doi: 10.1111/j.1462-2920.2008.01770.x (Cited on pages 7 and 35.)

Grasshoff, K., Ehrhardt, M., Kremling, K., and Anderson, L.G. (1983). Methods of seawater analysis. Verlag Chemie (VCH) Verlagsgesellschaft mbH (Cited on pages 21, 44, and 64.)

Grote, J., Jost, G., Labrenz, M., Herndl, G.J., and Jürgens, K., *Epsilonproteobacteria* represent the major portion of chemoautotrophic bacteria in sulfidic waters of pelagic redoxclines of the Baltic and Black Seas. *Applied and Environmental Microbiology*, 74 (2008) (24): 7546–7551. doi: 10.1128/AEM.01186-08 (Cited on pages 6, 19, 20, 34, 35, 45, 57, 62, 63, 78, and 81.)

Grote, J., Labrenz, M., Pfeiffer, B., Jost, G., and Jürgens, K., Quantitative distributions of *Epsilonproteobacteria* and a *Sulfurimonas* subgroup in pelagic redoxclines of the central Baltic Sea. *Applied and Environmental Microbiology*, 73 (2007) (22): 7155–7161. doi: 10.1128/AEM.00466-07 (Cited on pages 6, 22, 34, 35, 64, and 69.)

Grote, J., Schott, T., Bruckner, C.G., Glöckner, F.O., Jost, G., Teeling, H., Labrenz, M., and Jürgens, K., Genome and physiology of a model Epsilonproteobacterium responsible for sulfide detoxification in marine oxygen depletion zones. *Proceedings of the National Academy of Sciences of the United States of America*, 109 (2012) (2): 1–5. doi: 10.1073/pnas.1111262109 (Cited on pages 6, 7, 43, 65, 66, 77, 78, 81, XX, XXI, and XXII.)

Hallam, S.J., Konstantinidis, K.T., Putnam, N., Schleper, C., Watanabe, Y.I., Sugahara, J., Preston, C., de la Torre, J., Richardson, P.M., and DeLong, E.F., Genomic analysis of the uncultivated marine crenarchaeote *Cenarchaeum symbiosum*. *Proceedings of the National Academy of Sciences of the United States of America*, 103 (2006*a*) (48): 18296–18301. doi: 10.1073/pnas.0608549103 (Cited on pages 42 and 62.)

Hallam, S.J., Mincer, T.J., Schleper, C., Preston, C.M., Roberts, K., Richardson, P.M., and DeLong, E.F., Pathways of carbon assimilation and ammonia oxidation suggested by environmental genomic analyses of marine *Crenarchaeota*. *PLoS biology*, 4 (2006*b*) (4): e95. doi: 10.1371/journal.pbio.0040095 (Cited on page 42.)

Hammer, O.y., Harper, D.A.T., and Ryan, P.D., PAST : Paleontological statistics software package for education and data analysis. *Palaeontologica Electronica*, 4 (2001) (1): 4 (Cited on pages 26 and 46.)

Hannig, M., Lavik, G., Kuypers, M.M., Woebken, D., Martens-Habbena, W., and Jürgens, K., Shift from denitrification to anammox after inflow events in the central Baltic Sea. *Limnology and Oceanography*, 52 (2007) (4): 1336–1345 (Cited on pages 4, 5, 19, 33, and 35.)

Hatzenpichler, R., Diversity, physiology, and niche differentiation of ammonia-oxidizing archaea. *Applied and Environmental Microbiology*, 78 (2012) (21): 7501–7510. doi: 10.1128/AEM.01960-12 (Cited on page 43.)

Hatzenpichler, R., Lebedeva, E.V., Spieck, E., Stoecker, K., Richter, A., Daims, H., and Wagner, M., A moderately thermophilic ammonia-oxidizing crenarchaeote from a hot spring. *Proceedings of the National Academy of Sciences of the United States of America*, 105 (2008) (6): 2134–2139. doi: 10.1073/pnas.0708857105 (Cited on pages 8, 42, and 43.)

Hawley, a.K., Brewer, H.M., Norbeck, a.D., Paa-Toli, L., and Hallam, S.J., Metaproteomics reveals differential modes of metabolic coupling among ubiquitous oxygen minimum zone microbes. *Proceedings of the National Academy of Sciences*, (2014). doi: 10.1073/pnas.1322132111 (Cited on page 62.)

HELCOM (2003). The Baltic Marine Environment 1999–2002. Technical Report 87, HELCOM (Helsinki Commission) (Cited on page 2.)

Herndl, G.J., Reinthaler, T., Teira, E., Aken, H.V., Veth, C., Pernthaler, A., and Pernthaler, J., Contribution of archaea to total prokaryotic production in the deep atlantic ocean. *Applied and Environmental Microbiology*, 71 (2005) (5): 2303–2309. doi: 10.1128/AEM.71.5.2303 (Cited on pages 9, 19, and 55.)

Hietanen, S., Ja, H., Buizert, C., Ju, K., Labrenz, M., Voss, M., and Kuparinen, J., Hypoxia and nitrogen processing in the Baltic Sea water column. *Limnology and Oceanography*, 57 (2012) (1): 325–337. doi: 10.4319/lo.2012.57.1.0325 (Cited on pages 4, 6, 8, 11, 19, 33, 35, 36, 63, 78, and 79.)

Hollibaugh, J.T., Gifford, S., Sharma, S., Bano, N., and Moran, M.A., Metatranscriptomic analysis of ammonia-oxidizing organisms in an estuarine bacterioplankton assemblage. *The ISME Journal*, 5 (2011) (5): 866–78. doi: 10.1038/ismej.2010.172 (Cited on page 76.)

Holtappels, M., Lavik, G., Jensen, M.M., and Kuypers, M.M.M., ^{15}N-labeling experiments to dissect the contributions of heterotrophic denitrification and anammox to nitrogen removal in the OMZ waters of the ocean. *Methods in Enzymology*, 486 (2011): 223–51. doi: 10.1016/B978-0-12-381294-0.00010-9 (Cited on pages 22 and 46.)

Hoppe, H.G., Gocke, K., and Kuparinen, J., Effect of H_2S on heterotrophic substrate uptake, extracellular enzyme activity and growth of brackish water bacteria. *Marine Ecology Progress Series*, 64 (1990): 157–167 (Cited on page 20.)

Horak, R.E.A., Qin, W., Schauer, A.J., Armbrust, E.V., Ingalls, A.E., Moffett, J.W., Stahl, D.A., and Devol, A.H., Ammonia oxidation kinetics and temperature sensitivity of a natural marine community dominated by Archaea. *The ISME Journal*, (2013): 2023—2033. doi: 10.1038/ismej.2013.75 (Cited on page 33.)

Ingalls, A.E., Shah, S.R., Hansman, R.L., Aluwihare, L.I., Santos, G.M., Druffel, E.R.M., and Pearson, A., Quantifying archaeal community autotrophy in the mesopelagic ocean using natural radiocarbon. *Proceedings of the National Academy of Sciences of the United States of America*, 103 (2006) (17): 6442–6447. doi: 10.1073/pnas.0510157103 (Cited on pages 11, 19, and 94.)

Jakobsen, F. and Castejon, S., Calculation of the discharge through øresund at the drogden sill by measurements at two fixed stations. *Nordic hydrology*, 26 (1995) (3): 237–258 (Cited on page 3.)

Jansson, B.P., Malandrin, L., and Johansson, H.E., Cell cycle arrest in archaea by the hypusination inhibitor N^1-guanyl-1,7-diaminoheptane. *Journal of Bacteriology*, 182 (2000) (4): 1158–1161. doi: 10.1128/JB.182.4.1158-1161.2000 (Cited on pages 25, 34, and 56.)

Jensen, M.M., Petersen, J., Dalsgaard, T., and Thamdrup, B., Pathways, rates, and regulation of N_2 production in the chemocline of an anoxic basin, Mariager Fjord, Denmark. *Marine Chemistry*, 113 (2009) (1-2): 102–113. doi: 10.1016/j.marchem.2009.01.002 (Cited on page 4.)

Jin, R.C., Yang, G.F., Yu, J.J., and Zheng, P., The inhibition of the Anammox process: A review. *Chemical Engineering Journal*, 197 (2012): 67–79. doi: 10.1016/j.cej.2012.05.014 (Cited on page 19.)

Johnson, K.M., Wills, K.D., Butler, D.B., Johnson, W.K., and Wong, C.S., Coulometric total carbon dioxide analysis for marine studies : maximizing the performance of an automated gas extraction system and coulometric detector. *Marine Chemistry*, 44 (1993): 167–187 (Cited on page 25.)

Jones, M.N., Nitrate reduction by shaking with cadmium: Alternative to cadmium columns. *Water Research*, 18 (1984) (5): 8–11 (Cited on page 23.)

Jost, G., Martens-Habbena, W., Pollehne, F., Schnetger, B., and Labrenz, M., Anaerobic sulfur oxidation in the absence of nitrate dominates microbial chemoautotrophy beneath the pelagic chemocline of the

eastern Gotland Basin, Baltic Sea. *FEMS microbiology ecology*, 71 (2010) (2): 226–236. doi: 10.1111/j.1574-6941.2009.00798.x (Cited on page 24.)

Jost, G., Zubkov, M.V., Yakushev, E., Labrenz, M., and Jürgens, K., High abundance and dark CO_2 fixation of chemolithoautotrophic prokaryotes in anoxic waters of the Baltic Sea. *Limnology and Oceanography*, 53 (2008) (1): 14–22 (Cited on pages 6, 34, 63, 78, and 81.)

Joye, S.B. and Hollibaugh, J.T., Influence of Sulfide Inhibition of Nitrification on Nitrogen Regeneration in Sediments. *Science*, 270 (1995) (5236): 623–625. doi: 10.1126/science.270.5236.623 (Cited on pages 11, 20, and 33.)

Jung, M.Y., Park, S.J., Min, D., Kim, J.S., Rijpstra, W.I.C., Sinninghe Damsté, J.S., Kim, G.J., Madsen, E.L., and Rhee, S.K., Enrichment and characterization of an autotrophic ammonia-oxidizing archaeon of mesophilic crenarchaeal group I.1a from an agricultural soil. *Applied and Environmental Microbiology*, 77 (2011) (24): 8635–8647. doi: 10.1128/AEM.05787-11 (Cited on pages 42 and 43.)

Karner, M.B., DeLong, E.F., and Karl, D.M., Archaeal dominance in the mesopelagic zone of the Pacific Ocean. *Nature*, 409 (2001) (6819): 507–510. doi: 10.1038/35054051 (Cited on pages 8 and 56.)

Keller, M.W., Schut, G.J., Lipscomb, G.L., Menon, A.L., Iwuchukwu, I.J., and Adams, M.W.W., Exploiting microbial hyperthermophilicity to produce an industrial chemical , using hydrogen and carbon dioxide. (2013). doi: 10.1073/pnas.1222607110/-/DCSupplemental.www.pnas.org/cgi/doi/10.1073/pnas.1222607110 (Cited on page 76.)

Klotz, M.G., Arp, D.J., Chain, P.S.G., El-Sheikh, A.F., Hauser, L.J., Hommes, N.G., Larimer, F.W., Malfatti, S.a., Norton, J.M., Poret-Peterson, A.T., Vergez, L.M., and Ward, B.B., Complete genome sequence of the marine, chemolithoautotrophic, ammonia-oxidizing bacterium *Nitrosococcus oceani* ATCC 19707. *Applied and Environmental Microbiology*, 72 (2006) (9): 6299–6315. doi: 10.1128/AEM.00463-06 (Cited on page 43.)

Könneke, M., Bernhard, A.E., de la Torre, J.R., Walker, C.B., Waterbury, J.B., and Stahl, D.A., Isolation of an autotrophic ammonia-oxidizing marine archaeon. *Nature*, 437 (2005) (7058): 543–546. doi: 10.1038/nature03911 (Cited on pages 7, 8, 9, 18, 19, 42, 43, 44, 48, 56, and 62.)

Könneke, M., Schubert, D.M., Brown, P.C., Hügler, M., Standfest, S., Schwander, T., Schada von Borzyskowski, L., Erb, T.J., Stahl, D.A., and Berg, I.A., Ammonia-oxidizing archaea use the most energy-efficient aerobic pathway for CO_2 fixation. *Proceedings of the National Academy of Sciences of the United States of America*, (2014). doi: 10.1073/pnas.1402028111 (Cited on pages 8, 9, 10, 43, 62, 63, 76, and 95.)

Krebs, A. and Bridger, W.A., The kinetic properties of phosphoenolpyruvate carboxykinase of *Escherichia coli*. *Canadian Journal of Biochemistry*, 58 (1980) (4): 309–318 (Cited on page 76.)

Kurtz, S., Phillippy, A., Delcher, A.L., Smoot, M., Shumway, M., Antonescu, C., and Salzberg, S.L., Versatile and open software for comparing large genomes. *Genome biology*, 5 (2004) (2): R12. doi: 10.1186/gb-2004-5-2-r12 (Cited on pages 65, 66, and 70.)

Kuypers, M.M., Sliekers, A.O., Lavik, G., Schmid, M., Jørgensen, B.B., Kuenen, J.G., Damsté, J.S.S., Strous, M., and Jetten, M.S., Anaerobic ammonium oxidation by anammox bacteria in the black sea. *Nature*, 422 (2003) (6932): 608–611 (Cited on page 5.)

Kuypers, M.M.M., Lavik, G., Woebken, D., Schmid, M., Fuchs, B.M., Amann, R., Jørgensen, B.B., and Jetten, M.S.M., Massive nitrogen loss from the Benguela upwelling system through anaerobic ammonium oxidation. *Proceedings of the National Academy of Sciences of the United States of America*, 102 (2005) (18): 6478–6483. doi: 10.1073/pnas.0502088102 (Cited on pages 2 and 62.)

Kuzmina, N., Rudels, B., Stipa, T., and Zhurbas, V., The structure and driving mechanisms of the Baltic intrusions. *Journal of Physical Oceanography*, 35 (2005): 1120–1137. doi: 10.1175/JPO2749.1 (Cited on page 20.)

Labrenz, M., Grote, J., Mammitzsch, K., Boschker, H.T., Laue, M., Jost, G., Glaubitz, S., and Jürgens, K., *Sulfurimonas gotlandica* sp. nov., a chemoautotrophic and psychrotolerant epsilonproteobacterium isolated from a pelagic redoxcline, and an emended description of the genus *Sulfurimonas*. *International journal of systematic and evolutionary microbiology*, 63 (2013) (Pt 11): 4141–4148 (Cited on pages 6 and 77.)

Labrenz, M., Jost, G., and Jürgens, K., Distribution of abundant prokaryotic organisms in the water column of the central Baltic Sea with an oxic – anoxic interface. *Aquatic Microbial Ecology*, 46 (2007): 177–190. doi: 10.3354/ame046177 (Cited on pages 6, 35, and 57.)

Labrenz, M., Pohl, C., Beckmann, S., Martens-habbena, W., and Ju, K., Impact of Different In Vitro Electron Donor/Acceptor Conditions on Potential Chemolithoautotrophic Communities from Marine Pelagic Redoxclines. *Applied and Environmental Microbiology*, 71 (2005) (11): 6664–6672. doi: 10.1128/AEM.71.11.6664 (Cited on page 96.)

Labrenz, M., Sintes, E., Toetzke, F., Zumsteg, A., Herndl, G.J., Seidler, M., and Jürgens, K., Relevance of a crenarchaeotal subcluster related to *Candidatus* Nitrosopumilus maritimus to ammonia oxidation in the suboxic zone of the central Baltic Sea. *The ISME Journal*, 4 (2010) (12): 1496–1508. doi: 10.1038/ismej.2010.78 (Cited on pages 4, 6, 7, 8, 9, 11, 19, 20, 22, 32, 33, 34, 35, 43, 44, 58, 62, 63, 64, 69, 76, 77, 79, and 91.)

Lam, P., Jensen, M.M., Lavik, G., McGinnis, D.F., Müller, B., Schubert, C.J., Amann, R., Thamdrup, B., and Kuypers, M.M.M., Linking crenarchaeal and bacterial nitrification to anammox in the Black Sea. *Proceedings of the National Academy of Sciences of the United States of America*, 104 (2007) (17): 7104–7109. doi: 10.1073/pnas.0611081104 (Cited on pages 19, 33, and 62.)

Lam, P. and Kuypers, M.M., Microbial nitrogen cycling processes in oxygen minimum zones. *Annual Review of Marine Science*, 3 (2011) (1): 317–345. doi: 10.1146/annurev-marine-120709-142814 (Cited on pages 2 and 19.)

Lam, P., Lavik, G., Jensen, M.M., van de Vossenberg, J., Schmid, M., Woebken, D., Gutiérrez, D., Amann, R., Jetten, M.S.M., and Kuypers, M.M.M., Revising the nitrogen cycle in the Peruvian oxygen minimum zone. *Proceedings of the National Academy of Sciences of the United States of America*, 106 (2009) (12): 4752–4757. doi: 10.1073/pnas.0812444106 (Cited on pages 5, 8, and 42.)

Lane, D.J., 16S/23S rRNA sequencing. *Nucleic acid techniques in bacterial systematics*, (1991): 125–175 (Cited on page 47.)

Lavik, G., Stührmann, T., Brüchert, V., Van der Plas, A., Mohrholz, V., Lam, P., Mussmann, M., Fuchs, B.M., Amann, R., Lass, U., and Kuypers, M.M.M., Detoxification of sulphidic African shelf waters by blooming chemolithotrophs. *Nature*, 457 (2009) (7229): 581–584. doi: 10.1038/nature07588 (Cited on pages 7, 35, and 62.)

Lebedeva, E.V., Hatzenpichler, R., Pelletier, E., Schuster, N., Hauzmayer, S., Bulaev, A., Grigor'eva, N.V., Galushko, A., Schmid, M., Palatinszky, M., Le Paslier, D., Daims, H., and Wagner, M., Enrichment and genome sequence of the group I.1a ammonia-oxidizing archaeon "Ca. Nitrosotenuis uzonensis" representing a clade globally distributed in thermal habitats. *PLoS ONE*, 8 (2013) (11): e80835. doi: 10.1371/journal.pone.0080835 (Cited on page 42.)

Lee, S., Fuhrman, J.A., and Fuhrman, J.E.D.A., Relationships between biovolume and biomass of naturally derived marine bacterioplankton. *Applied and Environmental Microbiology*, 53 (1987) (6): 1298–1303 (Cited on pages 9 and 55.)

Lesniewski, R.A., Jain, S., Anantharaman, K., Schloss, P.D., and Dick, G.J., The metatranscriptome of a deep-sea hydrothermal plume is dominated by water column methanotrophs and lithotrophs. *The ISME Journal*, 6 (2012): 2257–2268. doi: 10.1038/ismej.2012.63 (Cited on page 18.)

Lin, X., Wakeham, S.G., Putnam, I.F., Astor, Y.M., Scranton, M.I., Chistoserdov, A.Y., Taylor, G.T., and Al, L.I.N.E.T., Comparison of vertical distributions of prokaryotic assemblages in the anoxic Cariaco Basin and Black Sea by use of fluorescence *in situ* hybridization. *Applied and Environmental Microbiology*, 72 (2006) (4): 2679–2690. doi: 10.1128/AEM.72.4.2679 (Cited on page 33.)

Lomas, M.W. and Lipschultz, F., Forming the primary nitrite maximum: Nitrifiers or phytoplankton? *Limnology and Oceanography*, 51 (2006) (5): 2453–2467. doi: 10.4319/lo.2006.51.5.2453 (Cited on page 18.)

Löscher, C., Kock, A., Könneke, M., LaRoche, J., Bange, H.W., and Schmitz, R., Production of oceanic nitrous oxide by ammonia-oxidizing archaea. *Biogeosciences*, 9 (2012) (7): 2419–2429 (Cited on pages 18, 20, and 25.)

Ludwig, W., Strunk, O., Westram, R., Richter, L., Meier, H., Yadhukumar, Buchner, A., Lai, T., Steppi, S., Jobb, G., Förster, W., Brettske, I., Gerber, S., Ginhart, A.W., Gross, O., Grumann, S., Hermann, S., Jost, R., König, A., Liss, T., Lüssmann, R., May, M., Nonhoff, B., Reichel, B., Strehlow, R., Stamatakis, A., Stuckmann, N., Vilbig, A., Lenke, M., Ludwig, T., Bode, A., and Schleifer, K.H., ARB: a software environment for sequence data. *Nucleic acids research*, 32 (2004) (4): 1363–1371. doi: 10.1093/nar/gkh293 (Cited on page 47.)

Martens-Habbena, W., Berube, P.M., Urakawa, H., de la Torre, J.R., Stahl, D.A., and Torre, R.D., Ammonia oxidation kinetics determine niche separation of nitrifying Archaea and Bacteria. *Nature*, 461 (2009) (7266): 976–979. doi: 10.1038/nature08465 (Cited on pages 9, 10, 56, 57, 62, and 80.)

Matsutani, N., Nakagawa, T., Nakamura, K., Takahashi, R., Yoshihara, K., and Tokuyama, T., Enrichment of a novel marine ammonia-oxidizing archaeon obtained from sand of an eelgrass zone. *Microbes and Environments*, 26 (2011) (1): 23–29. doi: 10.1264/jsme2.ME10156 (Cited on page 42.)

Matthäus, W. and Franck, H., Characteristics of major Baltic inflows - a statistical analysis. *Continental Shelf Research*, 12 (1992) (12): 1375–1400 (Cited on page 3.)

Middelburg, J.J., Chemoautotrophy in the ocean. *Geophysical Research Letters*, 38 (2011) (24): 94–97. doi: 10.1029/2011GL049725 (Cited on pages 34 and 57.)

Mincer, T.J., Church, M.J., Taylor, L.T., Preston, C., Karl, D.M., and DeLong, E.F., Quantitative distribution of presumptive archaeal and bacterial nitrifiers in Monterey Bay and the North Pacific Subtropical Gyre. *Environmental Microbiology*, 9 (2007) (5): 1162–1175. doi: 10.1111/j.1462-2920.2007.01239.x (Cited on page 18.)

Mosier, A.C., Lund, M.B., and Francis, C.A., Ecophysiology of an ammonia-oxidizing archaeon adapted to low-salinity habitats. *Microbial ecology*, 64 (2012) (4): 955–963. doi: 10.1007/s00248-012-0075-1 (Cited on pages 43, 56, and 57.)

Mußmann, M., Brito, I., Pitcher, A., Sinninghe Damste, J.S., Hatzenpichler, R., Richter, A., Nielsen, J.L., Nielsen, P.H., Muller, A., Daims, H., Wagner, M., Head, I.M., and Mussmann, M., Thaumarchaeotes abundant in refinery nitrifying sludges express *amoA* but are not obligate autotrophic ammonia oxidizers.

Proceedings of the National Academy of Sciences of the United States of America, 108 (2011) (40): 16771–6. doi: 10.1073/pnas.1106427108 (Cited on pages 18, 25, and 42.)

Musat, N., Foster, R., Vagner, T., Adam, B., and Kuypers, M.M.M., Detecting metabolic activities in single cells, with emphasis on nanoSIMS. *FEMS Microbiology Reviews*, 36 (2011) (2): 486–511. doi: 10.1111/j.1574-6976.2011.00303.x (Cited on page 46.)

Musat, N., Halm, H., Winterholler, B., Hoppe, P., Peduzzi, S., Hillion, F., Horreard, F., Amann, R., Jørgensen, B.B., and Kuypers, M.M.M., A single-cell view on the ecophysiology of anaerobic phototrophic bacteria. *Proceedings of the National Academy of Sciences of the United States of America*, 105 (2008) (46): 17861–17866. doi: 10.1073/pnas.0809329105 (Cited on page 19.)

Nakagawa, T. and Stahl, D.A., Transcriptional response of the archaeal ammonia oxidizer Nitrosopumilus maritimus to low and environmentally relevant ammonia concentrations. *Applied and Environmental Microbiology*, (2013) (August). doi: 10.1128/AEM.02028-13 (Cited on pages 76 and 80.)

Neph, S., Kuehn, M.S., Reynolds, A.P., Haugen, E., Thurman, R.E., Johnson, A.K., Rynes, E., Maurano, M.T., Vierstra, J., Thomas, S., Sandstrom, R., Humbert, R., and Stamatoyannopoulos, J.a., BEDOPS: high-performance genomic feature operations. *Bioinformatics (Oxford, England)*, 28 (2012) (14): 1919–20. doi: 10.1093/bioinformatics/bts277 (Cited on pages 65 and 66.)

Newell, S.E., Fawcett, S.E., and Ward, B.B., Depth distribution of ammonia oxidation rates and ammonia-oxidizer community composition in the Sargasso Sea. *Limnology and Oceanography*, 58 (2013) (4): 1491–1500. doi: 10.4319/lo.2013.58.4.1491 (Cited on page 18.)

Nier, A.O., A redetermination of the relative abundances of the isotopes of carbon, nitrogen, oxygen, argon and potassium. *Physical Review Letters*, 77 (1950) (6): 789–793. doi: 10.1103/PhysRev.77.789 (Cited on pages 52 and 53.)

Offre, P., Kerou, M., Spang, A., and Schleper, C., Variability of the transporter gene complement in ammonia-oxidizing archaea. *Trends in Microbiology*, (2014): 1–11. doi: 10.1016/j.tim.2014.07.007 (Cited on page 80.)

Offre, P., Spang, A., and Schleper, C., Archaea in biogeochemical cycles. *Annual review of microbiology*, 67 (2013) (June): 437–457. doi: 10.1146/annurev-micro-092412-155614 (Cited on pages 5, 8, and 18.)

Park, M.H., Wolff, E.C., Lee, Y.B., and Folk, J.E., Antiproliferative effects of inhibitors of deoxyhypusine synthase. *The Journal of Biological Chemistry*, 269 (1994) (45): 27827–27832 (Cited on page 34.)

Pelve, E.a., Lindå s, A.C., Martens-Habbena, W., de la Torre, J.R., Stahl, D.A., and Bernander, R., Cdv-based cell division and cell cycle organization in the thaumarchaeon Nitrosopumilus maritimus. *Molecular microbiology*, 82 (2011) (3): 555–66. doi: 10.1111/j.1365-2958.2011.07834.x (Cited on page 8.)

Pelve, E.A., Martens-Habbena, W., Stahl, D.A., and Bernander, R., Mapping of active replication origins in vivo in thaum- and euryarchaeal replicons. *Molecular microbiology*, (2013): 1–13. doi: 10.1111/mmi.12382 (Cited on page 8.)

Pernthaler, A., Pernthaler, J., and Amann, R., Fluorescence *in situ* hybridization and catalyzed reporter deposition for the identification of marine bacteria. *Applied and Environmental Microbiology*, 68 (2002) (6): 3094–3101. doi: 10.1128/AEM.68.6.3094 (Cited on pages 22 and 44.)

Pester, M., Rattei, T., Flechl, S., Gröngröft, A., Richter, A., Overmann, J., Reinhold-Hurek, B., Loy, A., and Wagner, M., *amoA*-based consensus phylogeny of ammonia-oxidizing archaea and deep sequencing of *amoA* genes from soils of four different geographic regions. *Environmental Microbiology*, (2012): no–no. doi: 10.1111/j.1462-2920.2011.02666.x (Cited on page 47.)

Polerecky, L., Adam, B., Milucka, J., Musat, N., Vagner, T., and Kuypers, M.M.M., Look@NanoSIMS - a tool for the analysis of nanoSIMS data in Environmental Microbiology. *Environmental Microbiology*, 14 (2012) (4): 1009–1023. doi: 10.1111/j.1462-2920.2011.02681.x (Cited on page 47.)

Poretsky, R.S., Hewson, I., Sun, S., Allen, A.E., Zehr, J.P., and Moran, M.A., Comparative day/night metatranscriptomic analysis of microbial communities in the North Pacific subtropical gyre. *Environmental Microbiology*, 11 (2009) (6): 1358–1375. doi: 10.1111/j.1462-2920.2008.01863.x (Cited on page 65.)

Pratscher, J., Dumont, M.G., and Conrad, R., Ammonia oxidation coupled to CO_2 fixation by archaea and bacteria in an agricultural soil. *Proceedings of the National Academy of Sciences of the United States of America*, 108 (2011) (10): 4170–4175. doi: 10.1073/pnas.1010981108 (Cited on page 18.)

Probst, A.J., Auerbach, A.K., and Moissl-Eichinger, C., Archaea on human skin. *PloS one*, 8 (2013) (6): e65388. doi: 10.1371/journal.pone.0065388 (Cited on page 9.)

Pruesse, E., Peplies, J., and Glöckner, F.O., SINA: accurate high-throughput multiple sequence alignment of ribosomal RNA genes. *Bioinformatics (Oxford, England)*, 28 (2012) (14): 1823–1829. doi: 10.1093/bioinformatics/bts252 (Cited on page 47.)

Purkhold, U., Pommerening-Röser, A., Juretschko, S., Schmid, M.C., Koops, H.P., and Wagner, M., Phylogeny of all recognized species of ammonia oxidizers based on comparative 16S rRNA and *amoA* sequence analysis: implications for molecular diversity surveys. *Applied and Environmental Microbiology*, 66 (2000) (12): 5368–5382. doi: 10.1128/AEM.66.12.5368-5382.2000 (Cited on page 47.)

Qin, W., Amin, S.A., Martens-Habbena, W., Walker, C.B., Urakawa, H., Devol, A.H., Ingalls, A.E., Moffett, J.W., Armbrust, E.V., and Stahl, D.A., Marine ammonia-oxidizing archaeal isolates display

obligate mixotrophy and wide ecotypic variation. *Proceedings of the National Academy of Sciences*, (2014). doi: 10.1073/pnas.1324115111 (Cited on pages 42, 43, 56, 58, 76, and 94.)

Quast, C., Pruesse, E., Yilmaz, P., Gerken, J., Schweer, T., Yarza, P., Peplies, J., and Glöckner, F.O., The SILVA ribosomal RNA gene database project: improved data processing and web-based tools. *Nucleic acids research*, 41 (2013) (Database issue): D590–6. doi: 10.1093/nar/gks1219 (Cited on page 47.)

Rotthauwe, J.H., Witzel, K.P., and Liesack, W., The ammonia monooxygenase structural gene *amoA* as a functional marker: molecular fine-scale analysis of natural ammonia-oxidizing populations. *Applied and Environmental Microbiology*, 63 (1997) (12): 4704–4712 (Cited on pages 18 and 79.)

Saeed, A., Sharov, V., J.White, J. Li, W.L., N.Bhagabati, Braisted, J., M.Klapa, Currier, T., Thia, M., Garajan, Sturn, A., Snuf-Fin, M., Rezantsev, A., Popov, D., Ryltsov, A., Kostukovich, E., Borisovsky, I., Liu, Z., A.Vinsavich, Trush, V., and Quackenbush, J., TM4: A free, open-source system for microarray data management and analysis. *BioTechniques*, 34 (2003) (2): 374–377 (Cited on page 67.)

Saeed, A.I., Bhagabati, N.K., Braisted, J.C., Liang, W., Sharov, V., Howe, E.A., Li, J., Thiagarajan, M., White, J.A., and Quackenbush, J., TM4 microarray software suite. *Methods in enzymology*, 411 (2006): 134–193. doi: 10.1016/S0076-6879(06)11009-5 (Cited on page 67.)

Santoro, A.E. and Casciotti, K.L., Enrichment and characterization of ammonia-oxidizing archaea from the open ocean: phylogeny, physiology and stable isotope fractionation. *The ISME Journal*, 5 (2011) (11): 1796–1808. doi: 10.1038/ismej.2011.58 (Cited on pages 42, 43, and 56.)

Santoro, A.E., Casciotti, K.L., and Francis, C.a., Activity, abundance and diversity of nitrifying archaea and bacteria in the central California Current. *Environmental Microbiology*, 12 (2010) (7): 1989–2006. doi: 10.1111/j.1462-2920.2010.02205.x (Cited on page 10.)

Sára, M., Sleytr, U.B., and Sa, M., S-Layer Proteins. *Journal of Bacteriology*, 182 (2000) (4): 859–868. doi: 10.1128/JB.182.4.859-868.2000.Updated (Cited on page 76.)

Satinsky, B.M., Crump, B.C., Smith, C.B., Sharma, S., Zielinski, B.L., Doherty, M., Meng, J., Sun, S., Medeiros, P.M., Paul, J.H., Coles, V.J., Yager, P.L., and Moran, M.a., Microspatial gene expression patterns in the Amazon River Plume. *Proceedings of the National Academy of Sciences*, 4 (2014) (15). doi: 10.1073/pnas.1402782111 (Cited on page 63.)

Sauder, L.A., Engel, K., Stearns, J.C., Masella, A.P., Pawliszyn, R., and Neufeld, J.D., Aquarium nitrification revisited: Thaumarchaeota are the dominant ammonia oxidizers in freshwater aquarium biofilters. *PLoS one*, 6 (2011) (8): e23281. doi: 10.1371/journal.pone.0023281 (Cited on page 18.)

Sauer, U. and Eikmanns, B.J., The PEP-pyruvate-oxaloacetate node as the switch point for carbon flux distribution in bacteria. *FEMS microbiology reviews*, 29 (2005) (4): 765–94. doi: 10.1016/j.femsre.2004.11.002 (Cited on page 76.)

Schleper, C., Ammonia oxidation: different niches for bacteria and archaea? *The ISME Journal*, 4 (2010) (9): 1092–1094. doi: 10.1038/ismej.2010.111 (Cited on page 18.)

Schneider, B., Nausch, G., and Pohl, C., Mineralization of organic matter and nitrogen transformations in the Gotland Sea deep water. *Marine Chemistry*, 119 (2010) (1-4): 153–161. doi: 10.1016/j.marchem.2010.02.004 (Cited on page 19.)

Schunck, H., Lavik, G., Desai, D.K., Groß kopf, T., Kalvelage, T., Löscher, C.R., Paulmier, A., Contreras, S., Siegel, H., Holtappels, M., Rosenstiel, P., Schilhabel, M.B., Graco, M., Schmitz, R.a., Kuypers, M.M.M., and Laroche, J., Giant hydrogen sulfide plume in the oxygen minimum zone off Peru supports chemolithoautotrophy. *PloS one*, 8 (2013) (8): e68661. doi: 10.1371/journal.pone.0068661 (Cited on pages 35 and 62.)

Sears, K., Alleman, J.E., Barnard, J.L., and Oleszkiewicz, J.A., Impacts of reduced sulfur components on active and resting ammonia oxidizers. *Journal of industrial microbiology & biotechnology*, 31 (2004) (8): 369–378. doi: 10.1007/s10295-004-0157-2 (Cited on page 20.)

Spang, A., Hatzenpichler, R., Brochier-Armanet, C., Rattei, T., Tischler, P., Spieck, E., Streit, W., Stahl, D.A., Wagner, M., and Schleper, C., Distinct gene set in two different lineages of ammonia-oxidizing archaea supports the phylum Thaumarchaeota. *Trends in microbiology*, 18 (2010) (8): 331–340. doi: 10.1016/j.tim.2010.06.003 (Cited on pages 8, 18, and 42.)

Spang, A., Poehlein, A., Offre, P., Zumbrägel, S., Haider, S., Rychlik, N., Nowka, B., Schmeisser, C., Lebedeva, E.V., Rattei, T., Böhm, C., Schmid, M., Galushko, A., Hatzenpichler, R., Weinmaier, T., Daniel, R., Schleper, C., Spieck, E., Streit, W., and Wagner, M., The genome of the ammonia-oxidizing *Candidatus* Nitrososphaera gargensis: insights into metabolic versatility and environmental adaptations. *Environmental Microbiology*, 14 (2012) (12): 3122–3145. doi: 10.1111/j.1462-2920.2012.02893.x (Cited on pages 42 and 62.)

Stahl, D. and Amann, R. (1991). Development and application of nucleic acid probes in bacterial systematics (Cited on page 45.)

Stahl, D.A. and de la Torre, J.R., Physiology and Diversity of Ammonia-Oxidizing Archaea. *Annual Review of Microbiology*, 66 (2012) (1): 83–101. doi: 10.1146/annurev-micro-092611-150128 (Cited on pages 9 and 11.)

Stewart, F.J., Ulloa, O., and Delong, E.F., Microbial metatranscriptomics in a permanent marine oxygen minimum zone. *Environmental Microbiology*, 14 (2012) (1): 23–40. doi: 10.1111/j.1462-2920.2010.02400.x (Cited on pages 18, 19, 62, and 63.)

Stieglmeier, M., Klingl, A., Alves, R.J.E., Rittmann, S.K.M.R., Melcher, M., Leisch, N., and Schleper, C., Nitrososphaera viennensis sp. nov., an aerobic and mesophilic ammonia-oxidizing archaeon from soil and member of the archaeal phylum Thaumarchaeota. *International journal of systematic and evolutionary microbiology*, 007536 (2014): 1–42. doi: 10.1099/ijs.0.063172-0 (Cited on pages 8 and 42.)

Stramma, L., Prince, E.D., Schmidtko, S., Luo, J., Hoolihan, J.P., Visbeck, M., Wallace, D.W., Brandt, P., and Körtzinger, A., Expansion of oxygen minimum zones may reduce available habitat for tropical pelagic fishes. *Nature Climate Change*, 2 (2012): 33–37. doi: 10.1038/nclimate1304 (Cited on page 1.)

Stramma, L., Schmidtko, S., Levin, L.A., and Johnson, G.C., Ocean oxygen minima expansions and their biological impacts. *Deep Sea Research Part I: Oceanographic Research Papers*, 57 (2010) (4): 587–595. doi: 10.1016/j.dsr.2010.01.005 (Cited on page 1.)

Sunamura, M., Higashi, Y., Miyako, C., Ishibashi, J.i., and Maruyama, A., Two bacteria phylotypes are predominant in the suiyo seamount hydrothermal plume. *Applied and Environmental Microbiology*, 70 (2004) (2): 1190–1198 (Cited on page 7.)

Teira, E., Burg, D., Aken, H.V., Veth, C., and Herndl, G.J., Archaeal uptake of enantiomeric amino acids in the meso- and bathypelagic waters of the North Atlantic. *Atlantic*, 51 (2006) (1): 60–69 (Cited on page 42.)

Thamdrup, B., New Pathways and Processes in the Global Nitrogen Cycle. *Annual Review of Ecology, Evolution, and Systematics*, 43 (2012) (1): 407–428. doi: 10.1146/annurev-ecolsys-102710-145048 (Cited on page 9.)

Thamdrup, B. and Dalsgaard, T., The fate of ammonium in anoxic manganese oxide-rich marine sediment. *Geochimica et Cosmochimica Acta*, 64 (2000) (24): 4157–4164 (Cited on page 23.)

Thureborn, P., Lundin, D., Plathan, J., Poole, A.M., Sjöberg, B.M., and Sjöling, S., A metagenomics transect into the deepest point of the Baltic Sea reveals clear stratification of microbial functional capacities. *PLoS ONE*, 8 (2013) (9): e74983. doi: 10.1371/journal.pone.0074983 (Cited on page 6.)

Tijhuis, L., Van Loosdrecht, M.C., and Heijnen, J.J., A thermodynamically based correlation for maintenance gibbs energy requirements in aerobic and anaerobic chemotrophic growth. *Biotechnology and bioengineering*, 42 (1993) (4): 509–519. doi: 10.1002/bit.260420415 (Cited on pages 34 and 57.)

Tourna, M., Stieglmeier, M., Spang, A., Könneke, M., Schintlmeister, A., and Urich, T., *Nitrososphaera viennensis*, an ammonia oxidizing archaeon from soil. *PNAS*, 108 (2011) (20): 8420–8425. doi: 10.1073/pnas.1013488108 (Cited on pages 8, 42, 43, 56, 76, 94, and 95.)

Treusch, A.H., Leininger, S., Kletzin, A., Schuster, S.C., Klenk, H.P., and Schleper, C., Novel genes for nitrite reductase and Amo-related proteins indicate a role of uncultivated mesophilic crenarchaeota in nitrogen cycling. *Environmental Microbiology*, 7 (2005) (12): 1985–1995. doi: 10.1111/j.1462-2920.2005.00906.x (Cited on pages 8, 18, and 42.)

Turkarslan, S., Reiss, D.J., Gibbins, G., Su, W.L., Pan, M., Bare, J.C., Plaisier, C.L., and Baliga, N.S., Niche adaptation by expansion and reprogramming of general transcription factors. *Molecular systems biology*, 7 (2011) (554): 554. doi: 10.1038/msb.2011.87 (Cited on page 74.)

Ulloa, O., Canfield, D.E., DeLong, E.F., Letelier, R.M., and Stewart, F.J., Microbial oceanography of anoxic oxygen minimum zones. *Proceedings of the National Academy of Sciences of the United States of America*, 109 (2012*a*) (40): 15996–16003. doi: 10.1073/pnas.1205009109 (Cited on pages 4 and 62.)

Ulloa, O., Canfield, D.E., DeLong, E.F., Letelier, R.M., and Stewart, F.J., Microbial oceanography of anoxic oxygen minimum zones. *Proceedings of the National Academy of Sciences of the United States of America*, 109 (2012*b*) (40): 15996–6003. doi: 10.1073/pnas.1205009109 (Cited on page 18.)

Vajrala, N., Martens-Habbena, W., Sayavedra-Soto, L.A., Schauer, A., Bottomley, P.J., Stahl, D.A., and Arp, D.J., Hydroxylamine as an intermediate in ammonia oxidation by globally abundant marine archaea. *Proceedings of the National Academy of Sciences of the United States of America*, 110 (2012) (3): 1006–1011. doi: 10.1073/pnas.1214272110 (Cited on page 10.)

Varela, M.M., van Aken, H.M., Sintes, E., Reinthaler, T., and Herndl, G.J., Contribution of Crenarchaeota and Bacteria to autotrophy in the North Atlantic interior. *Environmental Microbiology*, 13 (2011) (6): 1524–1533. doi: 10.1111/j.1462-2920.2011.02457.x (Cited on page 55.)

Venter, J.C., Remington, K., Heidelberg, J.F., Halpern, A.L., Rusch, D., Eisen, J.A., Wu, D., Paulsen, I., Nelson, K.E., Nelson, W., Fouts, D.E., Levy, S., Knap, A.H., Lomas, M.W., Nealson, K., White, O., Peterson, J., Hoffman, J., Parsons, R., Baden-tillson, H., Pfannkoch, C., Rogers, Y.H., and Smith, H.O., Environmental genome shotgun sequencing of the Sargasso Sea. *Science (New York, N.Y.)*, 304 (2004) (5667): 66–74. doi: 10.1126/science.1093857 (Cited on pages 8, 18, and 42.)

Veuger, B., Pitcher, a., Schouten, S., Sinninghe Damsté, J.S., and Middelburg, J.J., Nitrification and growth of autotrophic nitrifying bacteria and Thaumarchaeota in the coastal North Sea. *Biogeosciences*, 10 (2013) (3): 1775–1785. doi: 10.5194/bg-10-1775-2013 (Cited on page 11.)

Voss, M., Dippner, J.W., Humborg, C., Hürdler, J., Korth, F., Neumann, T., Schernewski, G., and Venohr, M., History and scenarios of future development of Baltic Sea eutrophication. *Estuarine, Coastal and Shelf Science*, 92 (2011) (3): 307–322. doi: 10.1016/j.ecss.2010.12.037 (Cited on pages 2 and 19.)

Walker, C.B., de la Torre, J.R., Klotz, M.G., Urakawa, H., Pinel, N., Arp, D.J., Brochier-Armanet, C., Chain, P.S.G., Chan, P.P., Gollabgir, A., Hemp, J., Hügler, M., Karr, E.a., Könneke, M., Shin, M., Lawton, T.J., Lowe, T., Martens-Habbena, W., Sayavedra-Soto, L.a., Lang, D., Sievert, S.M., Rosenzweig, a.C., Manning, G., and Stahl, D.A., Nitrosopumilus maritimus genome reveals unique mechanisms for nitrification and autotrophy in globally distributed marine crenarchaea. *Proceedings of the National Academy of Sciences of the United States of America*, 107 (2010) (19): 8818–8123. doi: 10.1073/pnas.0913533107 (Cited on pages 8, 42, 43, 62, 65, 66, 74, 76, 80, XX, and XXI.)

Walsh, D.a., Zaikova, E., Howes, C.G., Song, Y.C., Wright, J.J., Tringe, S.G., Tortell, P.D., and Hallam, S.J., Metagenome of a versatile chemolithoautotroph from expanding oceanic dead zones. *Science (New York, N.Y.)*, 326 (2009) (5952): 578–82. doi: 10.1126/science.1175309 (Cited on pages 7, 62, 65, 66, 82, XX, and XXI.)

Ward, B.B. and Kilpatrick, K.A. (1991). Nitrogen transformations in the oxic layer of permanent anoxic basins: the Black Sea and the Cariaco Trench. In Black Sea Oceanography, 111–124. Springer (Cited on page 33.)

Wartman, W.B., Leitfaden der Mikroskopischen Technik. *Arch Intern Med*, (1960) (106): 739 (Cited on page 64.)

Weinbauer, M.G., Fritz, I., Wenderoth, D.F., and Höfle, M.G., Simultaneous extraction from bacterioplankton of total RNA and DNA suitable for quantitative structure and function analyses. *Society*, 68 (2002) (3): 1082–1087. doi: 10.1128/AEM.68.3.1082 (Cited on page 47.)

Weiss, R.F., The solubility of nitrogen, oxygen and argon in water and seawater. *Deep Sea Research*, 17 (1970): 721–735 (Cited on page XII.)

Wieczorek, G., Hagen, E., and Umlauf, L., Eastern Gotland Basin case study of thermal variability in the wake of deep water intrusions. *Journal of Marine Systems*, 74 (2008): S65–S79. doi: 10.1016/j.jmarsys.2008.07.008 (Cited on pages 5 and 20.)

Wright, E.S., Yilmaz, L.S., and Noguera, D.R., DECIPHER, a search-based approach to chimera identification for 16S rRNA sequences. *Applied and Environmental Microbiology*, 78 (2012*a*) (3): 717–25. doi: 10.1128/AEM.06516-11 (Cited on page 47.)

Wright, J.J., Konwar, K.M., and Hallam, S.J., Microbial ecology of expanding oxygen minimum zones. *Nature Reviews. Microbiology*, 10 (2012*b*) (6): 381–94. doi: 10.1038/nrmicro2778 (Cited on pages 1, 2, 7, and 62.)

Wuchter, C., Abbas, B., Coolen, M.J.L., Herfort, L., van Bleijswijk, J., Timmers, P., Strous, M., Teira, E., Herndl, G.J., Middelburg, J.J., Schouten, S., and Sinninghe Damsté, J.S., Archaeal nitrification in the ocean. *Proceedings of the National Academy of Sciences of the United States of America*, 103 (2006) (33): 12317–12322. doi: 10.1073/pnas.0600756103 (Cited on pages 18, 43, and 57.)

Yakimov, M.M., Cono, V.L., Smedile, F., DeLuca, T.H., Juárez, S., Ciordia, S., Fernández, M., Albar, J.P., Ferrer, M., Golyshin, P.N., and Giuliano, L., Contribution of crenarchaeal autotrophic ammonia oxidizers to the dark primary production in Tyrrhenian deep waters (Central Mediterranean Sea). *The ISME Journal*, 5 (2011) (6): 945–961. doi: 10.1038/ismej.2010.197 (Cited on pages 11, 18, and 62.)

Yokokawa, T., Sintes, E., De Corte, D., Olbrich, K., and Herndl, G.J., Differentiating leucine incorporation of Archaea and Bacteria throughout the water column of the eastern Atlantic using metabolic inhibitors. *Aquatic Microbial Ecology*, 66 (2012) (3): 247–256. doi: 10.3354/ame01575 (Cited on pages 20 and 25.)

Zhang, L.M., Offre, P.R., He, J.Z., Verhamme, D.T., Nicol, G.W., and Prosser, J.I., Autotrophic ammonia oxidation by soil thaumarchaea. *Proceedings of the National Academy of Sciences of the United States of America*, 107 (2010) (40): 17240–17245. doi: 10.1073/pnas.1004947107 (Cited on page 18.)

APPENDIX

Supplementary material for Chapter 1

CO_2 fixation rates

The CO_2 fixation rates were calculated with the following formula:

$$CO_2\ fixation = \frac{\frac{dpm_f - dpm_d}{dpm_l} \times DIC}{t} \tag{A.1}$$

t: incubation time

dpm_f: filter disintegrations per minute

dpm_d: dpm-counts on filters of the dead control

dpm_l: dpm-counts in the liquid sample

DIC: ambient concentration of dissolved inorganic carbon

Nitrification rates

Nitrification rates were determined from the slope, α, of a linear regression of $^{15}NO_3^-$ + $^{15}NO_2^-$ concentration versus time and the ^{15}N-labeled fraction of NH_4^+, $F_{NH_4^+}$ as

$$nitrification\ rate = \frac{\mathrm{a}}{F_{NH_4^+}} \tag{A.2}$$

The concentration of $^{15}NO_3^-$ + $^{15}NO_2^-$ at a given time point, t_x, was determined after conversion to $^{15}N^{14}N$ ($^{29}N_2$) as excess $^{29}N_2$ derived from the change in the ratio of $^{29}N_2$ to $^{28}N_2$ relative to t_0:

$$excess\ ^{29}N_2 = [^{28}N_2]_{t_x}\left(\left(\frac{^{29}N_2}{^{28}N_2}\right)_{t_x} - \left(\frac{^{29}N_2}{^{28}N_2}\right)_{t_0}\right) \tag{A.3}$$

where $[^{28}N_2]$ represents the equivalent aqueous concentration of $^{28}N_2$ in the sample, derived from the amount, in µmol, of $^{28}N_2$ in the volume of headspace injected for mass spectrometry as calibrated by injection of known amounts of N_2 gas.

$$[^{28}N_2] = \frac{^{28}N_{2\ headspace}}{injected\ volume} \times \frac{headspace\ volume}{sample\ volume} \times \left(1 + B_{N2}\frac{sample\ volume}{headspace\ volume}\right) \times dilution \tag{A.4}$$

where B_{N_2} is the distribution coefficient of N_2 between water and air at room temperature and salinity 11 (Weiss, 1970), and the dilution arises during injection of helium into the headspace to replace the volume of gas removed.

Table A.1.: Data points that were not determined are represented by a dash (-); SE: standard error; SD: standard deviation; inorganic nutrients in µmol L^{-1}.

Site	(time)	Depth (m)	Nitrification (nmol L^{-1} d^{-1})	SE	CO_2 fixation (nmol L^{-1} d^{-1})	SD	Cren679 (cells mL^{-1})	DAPI (cells mL^{-1})	%Cren679 of DAPI	O_2	H_2S	NH_4^+	NO_2^-	NO_3^-	PO_4^{3-}	$^{15}NH_4^+$-labeling (%)
Bornholm Deep	(July 2011)	38	0	0	16.2	4.7	0.26	5.78	0.4	360.9	-	0.9	0.01	0.03	0.4	77.7
		48	0.5	0.2	9.2	3.5	0.15	2.6	0.6	250.1	-	2.0	0.02	0.8	0.6	69.2
		58	2.7	0.2	4.1	3.6	0.13	3.55	0.4	230.0	-	1.3	0.4	0.0	0.3	76.4
		68	4.8	0.3	5.7	5.0	0.93	5.71	1.6	114.8	-	1.3	0.2	0.0	0.6	78.0
		78	189.4	22.0	27.9	26.9	62.2	40.2	15.5	2.2	-	1.0	0.2	0.5	3.4	84.1
		87	177.8	35.6	289.8	221.3	47.7	16.9	28.2	1.8	0.06	1.8	1.5	1.2	3.7	73.9
Bornholm Deep	(Nov 2011)	38	0.4	2.1	13.4	1.2	0.41	8.75	0.5	337.2	-	0.3	0.03	8.9	2.1	93.2
		48	2.9	20.0	8.6	2.9	1.54	3.42	4.5	189.8	-	0.0	0.2	6.5	1.6	100
		58	6.3	7.2	3.9	3.4	1.51	3.15	4.8	134.0	-	0.0	0.03	0.2	1.2	100
		68	41.2	16.8	5.6	4.8	3.49	3.94	8.9	52.3	-	0.05	0.01	0.1	1.1	98.6
		78	883.8	85.2	27.2	24.2	42.5	16.9	25.1	16.5	0.2	0.34	0.01	0.1	1.2	92.9
		86	0.0	17.1	185.6	31.9	69.0	18.6	37.1	7.6	23.4	13.6	0.01	0.1	1.6	21.4
Bornholm Deep	(June 2012)	38	-	-	-	-	0.0	1.55	0	380.5	-	2.4	0.02	0.07	0.7	-
		48	-	-	-	-	0.14	1.28	1.1	357.3	-	1.5	0.04	0.05	0.7	-
		58	-	-	-	-	0.48	1.85	2.6	301.5	-	1.1	0.06	0.07	0.9	-
		68	-	-	-	-	0.58	2.48	2.3	143.4	-	0.5	0.4	3.7	1.5	-
		73	-	-	-	-	5.31	4.88	10.9	74.1	-	0.3	0.6	8.5	1.5	-
		78	-	-	-	-	6.47	6.16	10.5	85.3	-	0.1	0.3	9.9	1.5	-
		83	-	-	-	-	12.7	9.52	13.3	67.4	-	0.7	0.3	10.4	1.4	-
		86	-	-	-	-	16.3	9.58	17.0	62.5	0.0	0.7	0.3	11.0	1.3	-
Gotland Deep	(Feb 2011)	114	29.8	1.1	-	-	15.0	6.8	22.1	5.4	-	0.1	0.03	5.2	-	97.3
			26.6	1.0									0.03	5.3		97.3
		117	66.0	2.5	-	-	8.6	8.0	10.8	6.7	-	0.2	0.03	4.0	-	97.1
			47.8	10.7									0.04	3.9		97.1
		120	133.1	3.0	-	-	22.0	24.3	9.1	7.1	-	0.2	0.05	3.7	-	97.1
			130.8	5.7									0.06	3.8		97.1
		123	56.4	9.4	-	-	23.7	15.5	15.3	29.0	-	0.7	0.1	3.5	-	89.0
			57.5	11.5									0.1	3.5		89.0
Gotland Deep	(July 2011)	75	9.6	2.4	0.0	0.0	1.63	7.0	2.3	14.3	-	1.1	0.2	2.2	2.2	77.6
		90	18.1	2.4	5.3	3.9	6.76	4.91	13.8	10.3	-	0.03	0.3	4.9	2.5	99.3
		95	52.8	2.3	1.6	2.7	4.02	3.93	10.2	8.5	-	0.3	0.2	6.3	2.5	89.6
		100	37.4	1.7	2.7	0.1	0.94	4.49	2.1	8.0	-	0.1	0.3	5.4	2.5	97.4
		104	38.5	2.1	7.1	4.3	1.88	3.16	5.9	9.8	-	0.1	0.2	8.4	2.5	95.5
		109	122.3	2.8	19.6	4.5	6.76	5.01	13.5	3.6	-	0.2	0.4	5.1	2.6	95.5
		110	121.6	3.6	11.4	4.1	18.0	7.47	24.1	1.8	-	0.1	0.1	4.2	-	96.9
		114	79.1	1.3	16.7	5.7	7.62	4.97	15.3	4.9	0.06	0.2	0.3	5.0	2.5	94.6
		119	36.0	0.8	14.2	1.7	2.91	5.71	5.1	2.7	0.06	0.3	0.3	3.2	2.4	91.0
		124	61.5	2.6	340.6	57.4	-	-	-	3.0	1.2	0.1	0.0	2.5		73.6
		129	-	-	262.8	169.4	5.96	7.19	8.3	-	2.4	1.6	0.2	0.0	3.5	-
		134	-	-	380.9	140.5	-	-	-	15.4	5.3	0.2	-	4.3		-

Table A.1.: Data points that were not determined are represented by a dash (-); SE: standard error; SD: standard deviation; inorganic nutrients in µmol L^{-1}.

Site	(time)	Depth (m)	Nitrification (nmol L^{-1} d^{-1})	SE	CO_2 fixation (nmol L^{-1} d^{-1})	SD	Cren679 (cells mL^{-1})	DAPI (cells mL^{-1})	%Cren679 of DAPI	O_2	H_2S	NH_4^+	NO_2^-	NO_3^-	PO_4^{3-}	$^{15}NH_4^+$-labeling (%)
Gotland Deep	(Nov 2011)	94	115.7	7.3	219.1	126.5	23.6	14.5	16.3	1.8	-	1.4	0.3	0.3	-	74.7
		99	111.0	20.9	44.9	26.9	24.5	13.3	18.4	1.3	-	1.1	0.1	0.3	-	79.1
		104	114.2	37.4	25.8	25.3	14.9	7.0	21.3	2.2	-	0.2	0.5	4.2	-	94.7
		109	119.4	18.2	5.0	3.1	15.7	7.4	21.2	6.7	-	0.1	0.1	5.9	3.0	97.3
		114	63.1	36.8	5.4	2.7	21.6	7.2	30.0	7.2	-	0.2	0.1	5.3	2.7	93.8
		119	88.9	39.1	19.1	11.9	24.0	8.7	27.6	1.3	-	0.1	0.1	1.3	0.7	96.0
Gotland Deep	(June 2012)	70	-	-	-	-	0.15	2.0	0.8	304.5	-	0.7	0.1	-	0.8	-
		75	-	-	-	-	0.0	1.0	0.0	204.7	-	0.3	0.1	-	1.3	-
		77	-	-	-	-	0.0	2.7	0.0	137.7	-	0.3	0.2	-	1.6	-
		80	-	-	-	-	7.3	9.2	7.9	71.1	-	0.4	0.2	0.1	2.1	-
		82.1	0.2	0.4	-	-	0.5	4.6	1.1	31.8	-	0.6	0.3	0.5	2.3	84.3
		84.5	1.6	0.3	-	-	3.9	6.9	5.7	6.4	-	0.2	0.4	2.0	2.5	96.0
		87.0	4.3	3.2	-	-	14.8	19.6	7.6	2.2	-	1.1	0.3	0.0	2.0	74.9
		90	-	-	-	-	22.5	12.5	18.0	2.6	0.0	0.1	1.6	0.4	2.6	-
		92	-	-	-	-	19.1	13.7	13.9	4.3	0.0	0.6	0.2	-	2.3	-
		94	-	-	-	-	23.3	16.7	14.0	-	5.5	2.8	0.1	-	3.7	-
		99	-	-	-	-	23.0	12.0	19.2	2.4	0.0	1.1	0.4	-	3.7	-
		104	-	-	-	-	59.5	24.4	24.4	2.7	0.0	0.6	0.5	0.3	3.3	-
Landsort Deep	(Nov 2011)	80	38.5	12.2	30.4	5.3	14.6	15.6	9.4	20.5	-	1.91	0.1	1.0	3.1	71.3
		84	42.9	19.9	37.1	1.4	15.5	18.3	8.5	12.1	-	2.3	0.1	0.8	3.2	66.2
		88	79.9	16.2	40.4	8.3	16.2	20.3	8.0	27.2	-	2.4	0.1	0.7	3.2	63.8
		92	80.0	6.0	58.3	30.1	15.9	15.2	10.5	11.2	-	2.1	0.1	0.7	3.2	68.3
		95	81.4	5.4	-	-	13.4	14.3	9.4	12.1	-	2.4	0.1	0.6	3.3	64.2
		99	74.6	4.0	37.3	2.7	11.6	13.5	8.6	-	1.3	2.4	0.1	0.5	3.3	62.6
Landsort Deep	(June 2012)	74	110.5	2.0	7.0	1.4	4.69	3.46	13.6	21.5	-	0.1	0.2	4.6	2.9	97.7
		76	162.2	4.5	8.8	3.4	9.28	4.64	20.0	17.5	-	0.3	0.4	3.9	3.0	93.6
		78	288.7	25.9	5.4	1.3	14.9	5.86	25.4	7.6	0.1	0.5	1.0	3.1	2.9	89.4
		79.6	300.5	9.4	15.2	3.3	25.2	10.2	24.7	2.6	0.1	1.1	0.9	0.5	1.5	78.0
		81.0	321.0	9.3	25.8	11.6	34.1	12.1	28.2	2.8	0.1	1.1	0.9	1.1	2.2	83.2
		83	351.7	32.9	20.4	3.8	14.8	5.52	26.8	2.7	0.1	1.4	0.8	1.4	2.9	79.2

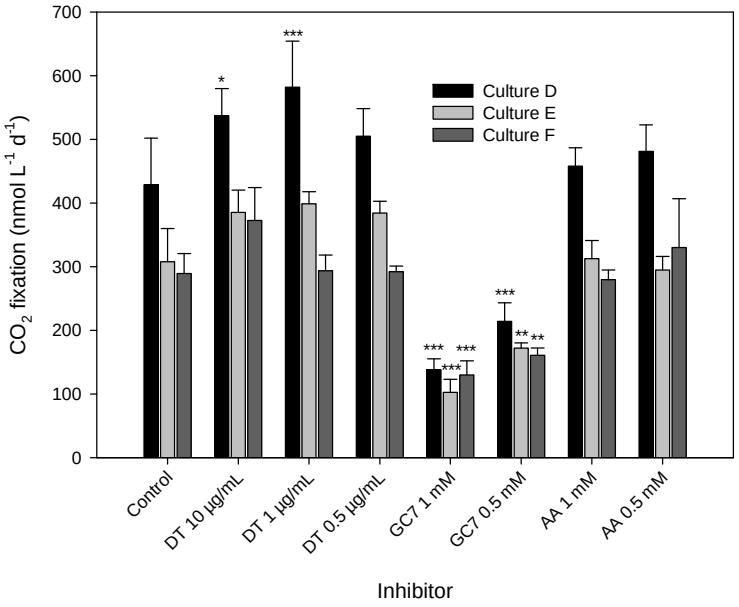

Figure A.1.: CO_2 fixation activities of three parallel enrichment cultures (D, E and F) of ammonia-oxidizing archaea treated with diphtheria toxin (DT) (0.5, 1 and 10 µg mL^{-1}), GC_7 (0.5 and 1 mmol L^{-1}) and acetic acid (AA), the solvent of GC_7 (0.5 and 1 mmol L^{-1}) compared to the control (no inhibitor). For each culture, CO_2 fixation measurements were conducted in quadruplicate subsamples from the respective culture; error bars show the standard deviation. Asterisks represent significant difference of the treatment compared to their respective control for each culture (one-way ANOVA and Tukey's pairwise comparison): * $p < 0.05$; ** $p < 0.005$; *** $p < 0.0005$.

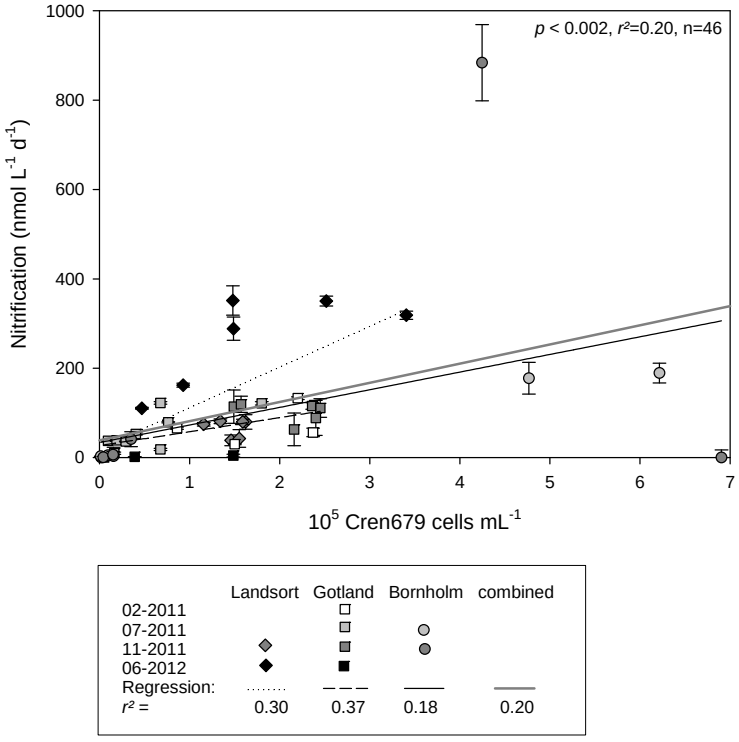

Figure A.2.: Relationship between Thaumarchaeota (Cren679-probe) cell abundances and potential nitrification rates during several samplings at Landsort Deep, Gotland Deep and Bornholm Deep from Feb 2011 until June 2012. Error bars show the standard error of the slope of excess ^{29}N, lines are regression lines for the respective stations, the gray diagonal line is the linear regression of all data points combined shown in the graph.

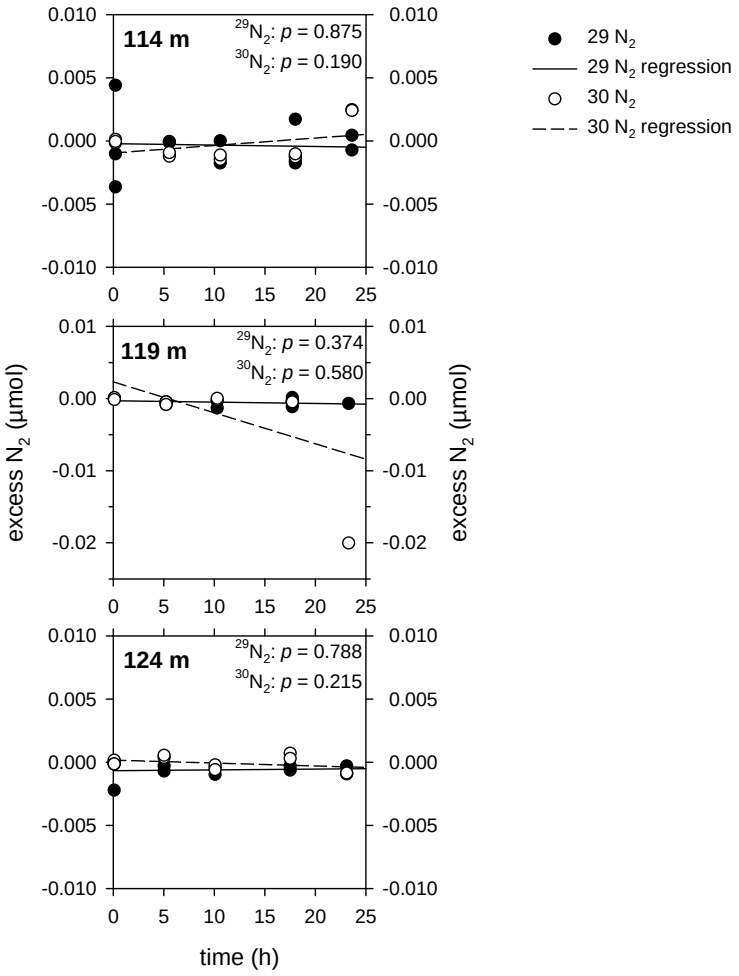

Figure A.3.: Concentrations of excess $^{29}N_2$ and $^{30}N_2$ during incubations targeting anaerobic ammonia oxidation (anammox) in 114, 119 and 124 m at Gotland Deep, July 2011.

Sampling:

Seawater was collected as described and distributed into exetainer vials with a headspace. After tracer amendment with 5 µmol $^{15}NH_4^+$ L^{-1} and 5 µmol $^{15}NO_2^-$ L^{-1}, the samples were degased for 10 min. with Helium/CO_2 to reduce background and eliminate oxygen. Incubations were stopped by freezing at -20 °C. Excess $^{29}N_2$ and $^{30}N_2$ was determined directly from the headspace via GC-IRMS as described.

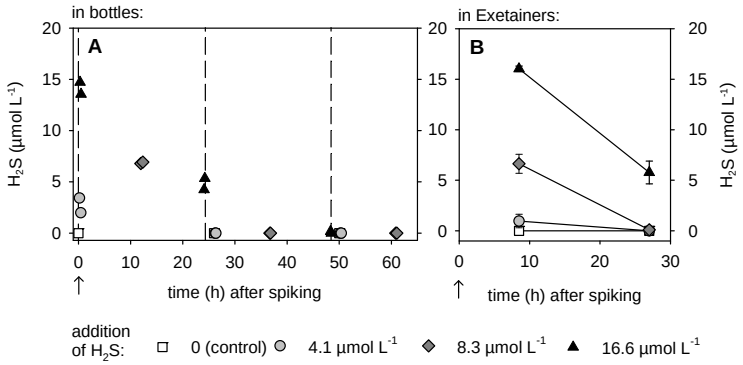

Figure A.4.: H_2S concentrations in (A) 0.5-L or 1-L bottles at different time points after spiking with different amounts of H_2S and prior to distribution of the samples into Exetainer vials and (B) after distribution into Exetainer vials and prior to the determination of nitrification rates. Vertical dashed lines mark the beginning of the intervals (0–24, 24–48, and 48–72 h) during which nitrification was determined. Error bars show the standard deviation of duplicate samples.

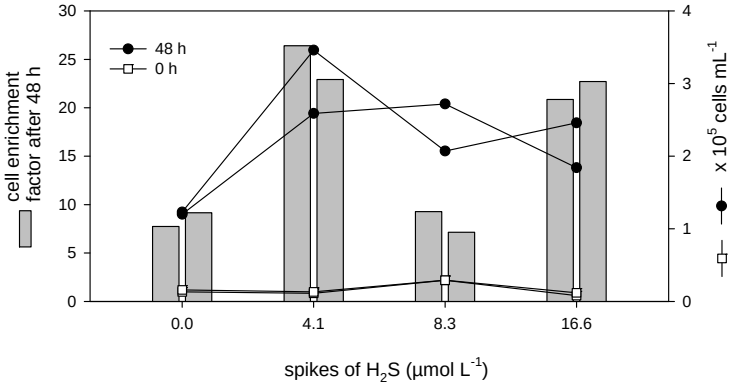

Figure A.5.: Absolute cell numbers (lines) and relative cell enrichment factor (final divided by initial cell numbers) (bars) of the epsilonproteobacterial *Sulfurimonas* sp. subgroup GD17 before and 48 h after spiking with different concentrations of H_2S.

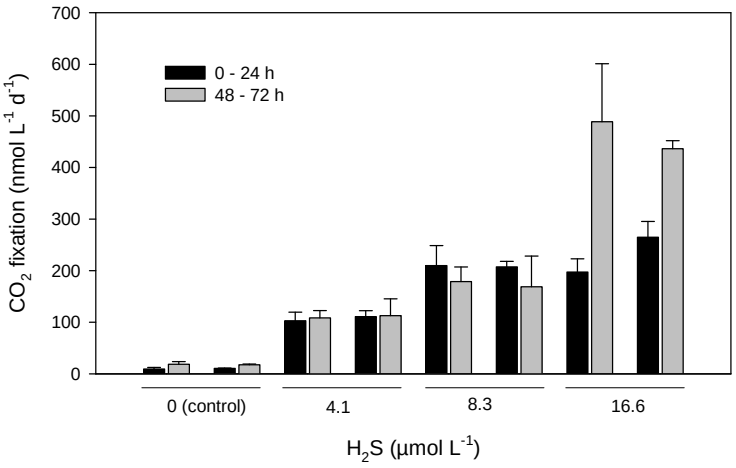

Figure A.6.: CO_2 fixation activities in parallel samples that were spiked with H_2S, determined immediately within the first 24 h or after 48 h. Error bars show the standard deviation of triplicate samples.

Supplementary material for Chapter 2

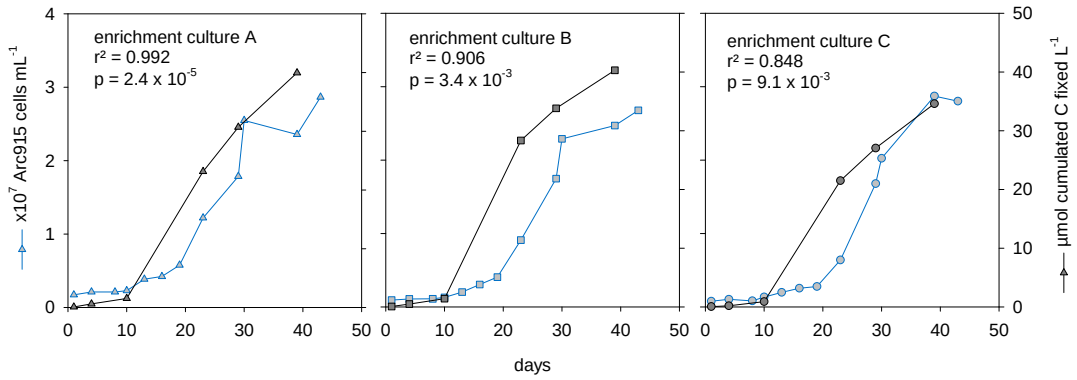

Figure A.7.: Total amount of carbon fixed over time in three parallel batch cultures (A–C) based on CO_2 fixation rates (see Figure 2.2B) versus the increase in archaeal cell numbers as determined using CARD-FISH and probe Arc915.

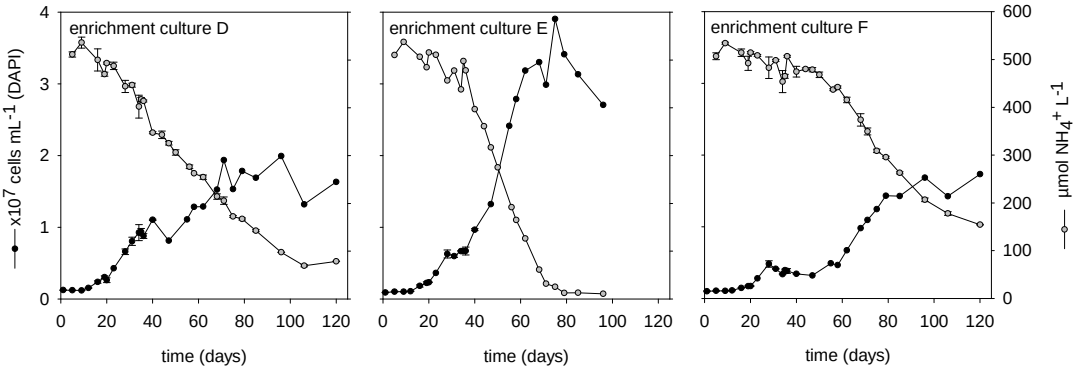

Figure A.8.: Ammonium consumption and total cell counts (DAPI) during the batch growth of cultures D, E, and F.

Supplementary material for Chapter 3

Table A.2.: List of investigated biogeochemically relevant genes present in the genomes of *N. maritimus* and *S. gotlandica* and in the SUP05 metagenome. Gene loci with the prefix `Nmar_` correspond to the genome of *N. maritimus* (Walker *et al.*, 2010), `Sup05_` corresponds to the SUP05 metagenome (Walsh *et al.*, 2009) and `SMGD1_` to *S. gotlandica* (Grote *et al.*, 2012). Table contents are composed from the named publications and annotations derived using The Universal Protein Resource (UniProt, http://www.uniprot.org/).

Gene	Gene locus	Function or protein
amoA	`Nmar_1500`	ammonia monooxygenase
amoB	`Nmar_1503`	ammonia monooxygenase
amoC	`Nmar_1502`	ammonia monooxygenase
amoX	`Nmar_1501`	ammonia monooxygenase
soxA	`Sup05_0516`	SoxAX cytochrome complex subunit A
soxZ	`Sup05_0517`	Sulfur oxidation protein SoxZ
soxY	`Sup05_0518`	Sulfur oxidation protein SoxY
soxX	`Sup05_0519`	Sulfur oxidation protein SoxX
	`Sup05_0682`	Sulfide-quinone reductase
dsrA	`Sup05_0722`	Intracellular sulfur oxidation protein DsrA
dsrA	`Sup05_0723`	Intracellular sulfur oxidation protein DsrA
dsrB	`Sup05_0724`	Intracellular sulfur oxidation protein DsrB
dsrE	`Sup05_0725`	Intracellular sulfur oxidation protein DsrE
dsrF	`Sup05_0726`	Intracellular sulfur oxidation protein DsrF
dsrH	`Sup05_0727`	DsrH family protein
dsrM	`Sup05_0729`	Intracellular sulfur oxidation protein DsrM
dsrK	`Sup05_0730`	Intracellular sulfur oxidation protein DsrK
soxX	`SMGD1_0062`	Sulfur oxidation protein SoxX
soxY	`SMGD1_0061`	Sulfur oxidation protein SoxY
soxZ	`SMGD1_0060`	Sulfur oxidation protein SoxZ
soxA	`SMGD1_0059`	Diheme cytochrome
soxB	`SMGD1_0058`	Sulfate thiol esterase
soxZ	`SMGD1_1162`	Sulfur oxidation protein
soxY	`SMGD1_1163`	Sulfur oxidation protein
soxC	`SMGD1_1165`	Sulfur oxidation protein
soxD	`SMGD1_1164`	Sulfur oxidation protein
soxF	`SMGD1_1158`	Sulfide dehydrogenase
soxH	`SMGD1_1160`	Putative sulfur oxidation protein
sorA	`SMGD1_1131`	Sulfite oxidoreductase
sorB	`SMGD1_1132`	Sulfite oxidoreductase
sqr1	`SMGD1_1402`	Sulfide-quinone oxidoreductase
sqr2	`SMGD1_2084`	Sulfide-quinone reductase
sqr3	`SMGD1_1224`	Sulfide-quinone oxidoreductase
sqr4	`SMGD1_1167`	Sulfide-quinone oxidoreductase
sqr5	`SMGD1_1602`	Putative sulfide-quinone oxidoreductase
napA	`Sup05_0420`	Periplasmic nitrate reductase subunit NapA
napB	`Sup05_0422`	Periplasmic nitrate reductase, electron transfer subunit
norC	`Sup05_1374`	Nitric oxide reductase subunit, NorC
norB	`Sup05_1373`	Nitric oxide reductase subunit, NorB
nirK	`Sup05_0208`	Dissimilatory nitrite reductase
narG	`Sup05_0393`	Nitrate reductase alpha subunit
narH	`Sup05_0394`	Nitrate reductase beta subunit

Table A.3.: Annotations for genes, which are involved in autotrophic carbon fixation pathways of *N. maritimus* (prefix `Nmar_`), *S. gotlandica* (`SMGD1_`) and of the SUP05 metagenome (`SUP05_`) according to Walker *et al.* (2010), Grote *et al.* (2012) and Walsh *et al.* (2009), respectively.

Gene locus	Annotation
Nmar_0272	Carboxyl transferase
Nmar_0273	Carbamoyl-phosphate synthase L chain ATP-binding
Nmar_0274	Biotin/lipoyl attachment domain-containing protein
Nmar_0206	CoA-binding domain protein
Nmar_0207	Vinylacetyl-CoA Delta-isomerase
Nmar_0953	Glyoxalase/bleomycin resistance protein/dioxygenase
Nmar_0954	Methylmalonyl-CoA mutase, large subunit
Nmar_0958	Cobalamin B12-binding domain protein
Nmar_1608	Aldehyde dehydrogenase
Nmar_1110	Iron-containing alcohol dehydrogenase
Nmar_0161	Iron-containing alcohol dehydrogenase
Nmar_1308	Enoyl-CoA hydratase/isomerase
Nmar_1028	3-hydroxybutyryl-CoA dehydrogenase
SMGD1_2658	2-Oxoglutarate:ferredoxin oxidoreductase
SMGD1_2659	2-Oxoglutarate:ferredoxin oxidoreductase
SMGD1_2660	2-Oxoglutarate:ferredoxin oxidoreductase
SMGD1_2661	2-Oxoglutarate:ferredoxin oxidoreductase
SUP05_FGYC13J70028	Rubisco regulator CbbO
SUP05_FGYC13J70029	Rubisco regulator CbbQ
SUP05_FGYC13J70030	Ribulose bisphosphate carboxylase/oxygenase (RuBisCO)

Table A.4.: List of genes, which are relevant to the assembly of the flagella according to the genome of *S. gotlandica* (Grote *et al.*, 2012).

Gene	Gene locus	Function or protein
flaB_2	SMGD1_1050	Flagellin (Minor flagellin subunit FlaB)
flaG	SMGD1_2307	Flagellar protein FlaG (Flagellar protein FlaG protein)
flgB	SMGD1_0880	Flagellar basal body rod protein FlgB
flgC	SMGD1_0881	Flagellar basal-body rod protein FlgC (Flagellar basal-body rod protein flgC)
flgE	SMGD1_1289	Flagellar hook protein FlgE (Flagellar hook protein flgE)
flgF	SMGD1_2731	Flagellar basal body rod protein (Flagellar basal-body rod protein flgF)
flgG	SMGD1_2730	Flagellar basal-body rod protein FlgG (Flagellar basal-body rod protein flgG)
flgH	SMGD1_0366	Flagellar L-ring protein (Basal body L-ring protein)
flgI	SMGD1_1930	Flagellar P-ring protein (Basal body P-ring protein)
flgK	SMGD1_1934	Flagellar hook-associated protein FlgK
flhA	SMGD1_0391	Flagellar biosynthesis protein A
flhB	SMGD1_2171	Flagellar biosynthesis protein FlhB (Flagellar biosynthetic protein FlhB)
flhf	SMGD1_1976	Flagellar biosynthesis protein FlhF (Uncharacterized protein)
flhF	SMGD1_2192	Flagellar biosynthesis regulator FlhF (GTP-binding signal recognition particle SRP54, G-domain)
fliC_3	SMGD1_0331	Flagellin (Flagellin domain)
fliE	SMGD1_0882	Flagellar hook-basal body complex protein FliE
fliF	SMGD1_0746	Flagellar M-ring protein
fliF2	SMGD1_1227	Flagellar protein export ATPase FliI (Flagellum-specific ATP synthase)
fliG	SMGD1_0745	Flagellar motor switch protein FliG
fliH	SMGD1_0744	Flagellar assembly protein
fliK	SMGD1_1286	Flagellar hook-length control protein
fliL_2	SMGD1_0176	Flagellar basal body-associated protein FliL
fliM	SMGD1_2196	Flagellar motor switch protein FliM
fliN	SMGD1_2197	Flagellar motor switch FliN (Flagellar motor switch protein FliN)
fliN2	SMGD1_2589	Flagellar motor switch protein FliN
fliP	SMGD1_2806	Flagellar biosynthesis protein FliP (Flagellar biosynthetic protein FliP)
fliQ	SMGD1_1361	Flagellar biosynthesis protein FliQ (Flagellar biosynthetic protein FliQ)
fliR	SMGD1_1718	Flagellar biosynthetic protein fliR
fliS	SMGD1_1035	Flagellar protein FliS
fliW	SMGD1_0814	Flagellar assembly factor FliW
motA	SMGD1_2808	Flagellar motor rotation protein A (MotA/TolQ/ExbB proton channel)
motB	SMGD1_2807	Flagellar motor protein MotB

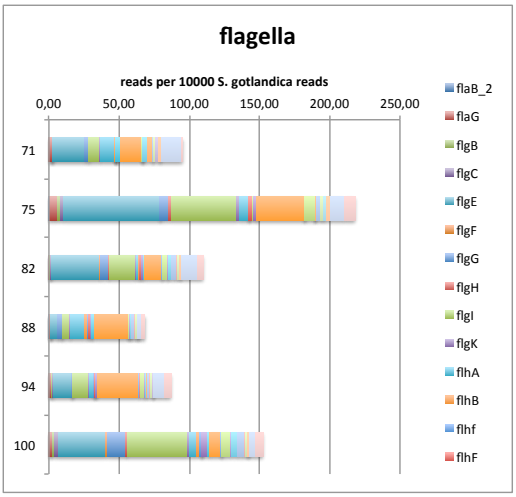

Figure A.9.: Organism-specific normalization of read counts. Number of reads per 10,000 *Sulfurimonas gotlandica* reads of genes associated with the flagella throughout the redox gradient.

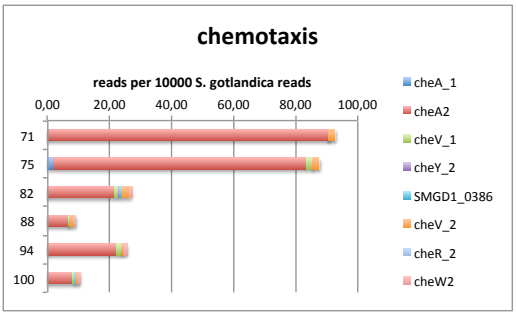

Figure A.10.: Organism-specific normalization of read counts. Number of reads per 10,000 *Sulfurimonas gotlandica* reads of genes associated with chemotaxis throughout the redox gradient.

LIST OF PUBLICATIONS

The contents of Chapter 1 have been accepted for publication in a peer-reviewed journal, those of Chapter 2 have been submitted for consideration of publication in a peer-reviewed journal. The manuscript of Chapter 3 is in preparation for publication. The specific contributions are outlined in the following.

Manuscripts

- Chapter 1: **Carlo Berg**, Verona Vandieken, Bo Thamdrup, Klaus Jürgens.
  Significance of archaeal nitrification in hypoxic waters of the Baltic Sea (*in press*). The ISME Journal.
  Contributions: **C.B.**, V.V. and K.J. designed the experiments. **C.B.** and V.V. performed sampling, analysis and data interpretation. V.V. and B.T. established the nitrification measurements. **C.B.** wrote the concept and first edition of the manuscript. V.V., B.T. and K.J. revised the manuscript.

- Chapter 2: **Carlo Berg**, Luisa Listmann, Verona Vandieken, Angela Vogts, Klaus Jürgens.
  Chemoautotrophic growth of ammonia-oxidizing Thaumarchaeota enriched from hypoxic waters of the Baltic Sea (*submitted*).
  Contributions: **C.B.** and V.V. initiated the enrichment cultures. **C.B.**, L.L. and K.J. designed the growth experiments. **C.B.** and L.L. performed experiments and analysis. A.V. performed measurements via NanoSIMS. **C.B.** wrote the concept and first edition of the manuscript. V.V., A.V., L.L. and K.J. revised the manuscript.

- Chapter 3: **Carlo Berg**, Janie Feike, Pierre Offre, Tim Urich, Christa Schleper, Matthias Labrenz, Klaus Jürgens.
  Metatranscriptomic profiling of Thaumarchaeota within a chemoautotrophic community at a Baltic Sea pelagic redox gradient (*in preparation*).
  Contributions: J.F., M.L. and K.J. designed and performed sampling. J.F. performed sample preparation, CARD-FISH was performed by Katja Becker. **C.B.** established the analysis workflow, performed analysis and data interpretation. P.O., T.U. and C.S. contributed with substantial ideas on data analysis, **C.B.** wrote the concept and first edition of the manuscript. K.J. revised the manuscript.

Conference contributions (Talks)

- **Carlo Berg**, Verona Vandieken, Luisa Listmann, Bo Thamdrup, Klaus Jürgens. Ecological significance and ecophysiological features of ammonia oxidizing *Thaumarchaeota* from hypoxic waters of the Baltic Sea. Symposium on Aquatic Microbial Ecology (SAME 13), Stresa, Italy, September 2013.

- **Carlo Berg**, Verona Vandieken, Bo Thamdrup, Klaus Jürgens. Significance of archaeal nitrification in hypoxic waters of the Baltic Sea. Jahrestagung der Vereinigung für Allgemeine und Angewandte Mikrobiologie (VAAM) 2013, Bremen, Germany, March 2013.

- **Carlo Berg**, Verona Vandieken, Bo Thamdrup, Klaus Jürgens. Significance of archaeal nitrification in hypoxic waters of the Baltic Sea. European Geosciences Union General Assembly (EGU) 2012, Vienna, Austria, April 2012.

Conference contributions (Poster)

- **Carlo Berg**, Luisa Listmann, Verona Vandieken, Klaus Jürgens. Ecophysiological features of ammonia oxidizing Thaumarchaeota from hypoxic waters of the Baltic Sea. ESF EuroEEFG Conference, Noordwijkerhout/Amsterdam, The Netherlands, May 2013.

- **Carlo Berg**, Verona Vandieken, Bo Thamdrup, Klaus Jürgens. Significance of archaeal nitrification in sulfide influenced hypoxic waters of the Baltic Sea. International Symposium on Microbial Ecology (ISME 14), Copenhagen, Denmark, August 2012.

Peer-reviewed publications, which are not part of this thesis

- **Carlo Berg**, Sabrina Beckmann, Günter Jost, Matthias Labrenz, and Klaus Jürgens. Acetate-utilizing bacteria at an oxic-anoxic interface in the Baltic Sea (2013). *FEMS Microbiology Ecology*, 85(2):251-61. doi: 10.1111/1574-6941.12114

CURRICULUM VITAE

Studies and work experience

09/2010 - 10/2014	Leibniz Institute for Baltic Sea Research (IOW), Germany
	PhD-Thesis
04/2013 - 07/2013	University of Vienna, Austria
	Visiting scientist
10/2004 - 08/2010	University of Rostock, Germany
	Diploma studies in Biology
01/2010 - 08/2010	Leibniz Institute for Baltic Sea Research (IOW), Germany
	Diploma-Thesis:
	"Identification of active microorganisms in pelagic redoxclines of the central Baltic Sea"
08/2008 - 04/2009	University of Umeå, Sweden
	ERASMUS study period

School

08/1997 - 06/2004	Christian-von-Dohm-Gymnasium, Goslar, Germany
01/2002 - 07/2002	J. A. Williams High School, Lac La Biche, Alberta, Canada

Grants, Scholarships, Awards

09/2013	Best student presentation at SAME13 conference, Stresa, Italy
04/2013 - 07/2013	FEMS Research Fellowship
08/2008 - 04/2009	ERASMUS Scholarship

ACKNOWLEDGMENTS

First of all, I would like to thank my supervisor Prof. Dr. Klaus Jürgens for giving me the opportunity to work on this topic about the little but important Thaumarchaeota at the Leibniz Institute for Baltic Sea Research. I am thankful to Klaus for numerous opportunities to conduct field samplings, attend conferences and for initiating my stay at the University of Vienna as well as for promoting my personal scientific progress through fruitful discussions and advice. I also want to thank PD Dr. Matthias Labrenz for letting me discover the world of microbial ecology when we were crawling through seawater cooling pipelines and taking samples and in this way my time at the IOW began.

Verona Vandieken was largely involved in sampling, analysis, establishing the nitrification measurements and enrichments, which were the basis of this work. I appreciate your careful and critical reading of manuscripts and valuable suggestions! Janie Feike, Angela Vogts and Bo Thamdrup are thanked for their support in sample retrievement, preparation or analysis as well as Luisa Listmann for great support on R/V *Meteor* and during the growth experiments. All the samples would have never been pulled out of the Baltic deeps without the highly professional efforts by the captains, crews and scientific parties of the research vessels *Alkor*, *Elisabeth-Mann-Borgese*, *Heincke*, *Maria S. Merian* and *Meteor*. I am grateful to everyone who was teaching me new methods, principles, viewpoints, explaining and helping me whenever I had questions or who helped with sampling on board, when patiently capping Exetainers or moving around all those "MOCA"-Boxes ;-). Thank you people also for a nice and enjoyable time at and around the IOW in every respect:

Katja Becker, Benjamin Bergen, Heike Benterbusch-Brockmöller, Bärbel Buuk, Christian Burmeister, Sabine Glaubitz, Anna Hagenmeier, Daniel Herlemann, Günter Jost, Julia Klier, Solveig Kühl, Christian Meeske, Markus von Scheibner, Dandan Shen, Christian Stolle, Juliane Unger, Felix Weber, Jana Woelk and Claudia Wylezich. At the Department of Ecogenomics and Systems Biology in Vienna, the home of *Nitrososphaera viennensis*, I want to thank Christa Schleper, Tim Urich and Pierre Offre for a nice and inspiring time in their group, made possible through the support of the VAAM and the Federation of European Microbiological Societies (FEMS) by granting me a research fellowship. The DFG and ESF funded the "Microbial Oceanography of ChemolithoAutotrophic planktonic communities" project "MOCA". Thanks also to André Miede who provided the LaTeXClassicThesis template for typesetting.

Above all, I want to thank my family and friends for support of any kind, for making my studies possible, your continued interest in my research, for letting me explain the big, the small and the tiny features of the Baltic Sea and for great times during studies!

DANKE! TACK! THANKS!

DECLARATION OF AUTHORSHIP - SELBSTÄNDIGKEITSERKLÄRUNG

Erklärung gemäß §4, Absatz 1, Buchstaben g und h der Promotionsordnung der Mathematisch-Naturwissenschaftlichen Fakultät der Universität Rostock

Ich gebe folgende Erklärung ab:

1. Die Gelegenheit zum vorliegenden Promotionsvorhaben ist mir nicht kommerziell vermittelt worden. Insbesondere habe ich keine Organisation eingeschaltet, die gegen Entgelt Betreuerinnen/Betreuer für die Anfertigung von Dissertationen sucht oder die mir obliegenden Pflichten hinsichtlich der Prüfungsleistungen für mich ganz oder teilweise erledigt.
2. Ich versichere hiermit an Eides statt, dass ich die vorliegende Arbeit selbstständig angefertigt und ohne fremde Hilfe verfasst habe. Dazu habe ich keine außer den von mir angegebenen Hilfsmitteln und Quellen verwendet und die den benutzten Werken inhaltlich und wörtlich entnommenen Stellen habe ich als solche kenntlich gemacht.

Rostock, den 24. Okt. 2014

Carlo Berg